# COMPARISON STUDY ON THE EFFECT OF DIAPHRAGM TYPES AND SLAB VOIDS ON PLANNER IRREGULAR ASYMMETRICAL STRUCTURES USING TIME HISTORY ANALYSIS

**AMIN AMMAR ALDADDOU**

**IŞIK UNIVERSITY**
**SEPTEMBER, 2022**

# COMPARISON STUDY ON THE EFFECT OF DIAPHRAGM TYPES AND SLAB VOIDS ON PLANNER IRREGULAR ASYMMETRICAL STRUCTURES USING TIME HISTORY ANALYSIS

AMIN AMMAR ALDADDOU
Isik University, School of Graduate Studies, Master of Science, 2022

Submitted to School of Graduate Studies
In partial fulfillment of the requirements for the degree of
Master of Science
in
Civil Engineering

IŞIK UNIVERSITY
SEPTEMBER, 2022

IŞIK UNIVERSITY
SCHOOL OF GRADUATE STUDIES
CIVIL ENGINEERING THESIS MASTER'S DEGREE PROGRAM

# COMPARISON STUDY ON THE EFFECT OF DIAPHRAGM TYPES AND SLAB VOIDS ON PLANNER IRREGULAR ASYMMETRICAL STRUCTURES USING TIME HISTORY ANALYSIS

AMIN AMMAR ALDADDOU

APPROVED BY:

Ass. Prof. Dr. Önder Umut (Işık Üniversitesi)
(Thesis Supervisor)

Ass Prof. Dr. Bora Akşar (Işık Üniversitesi)
(Member)

Ass Prof. Dr. Fatma İlknur Kara (Gebze Teknik Üniversitesi)
(Member)

APPROVAL DATE: 06/09/2022

# COMPARISON STUDY ON THE EFFECT OF DIAPHRAGM TYPES AND SLAB VOIDS ON PLANNER IRREGULAR ASYMMETRICAL STRUCTURES USING TIME HISTORY ANALYSIS

## ABSTRACT

In the past years plan-irregular structures with different diaphragm types have been limitedly studied regarding their seismic performance using nonlinear static procedures, which limited the application of those methods to existing irregular structures. In this study, the effect of gap existing and flexibility in the diaphragms on asymmetrical irregular structures is studied by free vibration analysis, equivalent lateral force method, and nonlinear time history analysis approach using 11 different earthquake records comparing two two-story similar steel structures, one with rigid diaphragm for both stories, and the other with flexible diaphragm in the second story and a large void in its second story slab. Both are irregular structures with re-entrant corner. It is found that the existence of the large void and diaphragm flexibility affect the period and natural frequency of the structures, increase the joint displacements and joint drifts, increase the base shear, increase the internal forces in beams and columns significantly specially in the critical places such as re-entrant corners. So overall, the study showed that irregular structures can be highly influenced and dramatically change its behavior when the existence of voids in the diaphragms, and when the diaphragms act as flexible diaphragm rather than rigid diaphragms.

**Keywords:** Nonlinear Time History Analysis, Structural Irregularities, Flexible Diaphragm, Rigid Diaphragm, Response Spectrum, Diaphragm Void, Seismic Performance, ETABS.

# PLANDA DÜZENSİZ YAPILARIN DİYAFRAM TİPLERİNİN VE BOŞLUK ORANLARININ ZAMAN TANIM ALANINDA ANALİZ YAPILARAK KIYASLANMASI

## ÖZET

Son yıllarda depremselliğin yüksek olduğu bölgelerde düzensiz binaların yapımı giderek artmaktadır. Estetik, farklılık arayışı gibi mimari nedenler ya da pratik sebepler bu durumun oluşmasının başlıca sebeplerindendir. Bu yapıların deprem etkisindeki davranışları hakkında çalışmalar olmakla birlikte araştırmaya açık bir konudur. Olağandışı şekle sahip bazı binaların döşemelerinde bulunan geniş açıklıklar veya boşluklar döşemeyi rijit diyafram olmak yerine yarı rijit ya da esnek hale getirebilir, bu da binaların deprem altındaki davranışını etkileyebilmektedir. Bu çalışmada, boşluklu döşemelerin ve rijit olmayan diyaframların, yapının sismik kuvvetler altındaki davranışı üzerindeki etkisi incelenmiştir. Buna ilaveten 11 farklı sismik kayıt kullanılarak zaman tanım alanında analizler yapılmış, binaların bazıları doğrusal, bazıları doğrusal olmayan yöntemlerle analiz edilmiştir boşlukların ve diyafram tipinin düzensiz yapıların davranışını büyük ölçüde etkilediği ve deprem etkisi altındaki davranışını olumsuz yönde değiştirdiği ortaya konmuştur. Sismik aktivenin yüksek olduğu bölgelerde inşa edilecek yapılarda büyük boşlukların yapının davranışı üzerindeki etkisi detaylı bir şekilde irdelenmelidir.

**Anahtar Kelimeler:** Doğrusal Olmayan Zaman Tanım Alanında Analiz, Yapı Düzensizlikleri, Rijit Olmayan Diyafram, Rijit Diyafram, Mukabele Spektrumu, Diyafram Boşluğu, Sismik Performans, ETABS.

## ACKNOWLEDGEMENTS

Upon the end of this research, my sincere gratitude to His Almighty God for granting me all the blessings to successfully complete this work.

I would like to express my gratefulness to IŞIK University, who facilitates my admission and joining this program.

Particular thanks to my supervisor Dr. Onder Umut who's direct and constant guidance made this work happened and to Prof. Dr. H. Faruk Karadogan who inspired me during this journey.

Furthermore, I am extremely thankful to all faculty members and all employees at the College of Civil Engineering. Also, special thanks to graduate studies faculty and employees, who were there for us and supported us among every corner and facilitated any difficulty.

At the end, my genuine thanks to my father Prof. Dr. Ammar Aldaddou my mother Mrs. Rehab Younso whose continuous encouragement and unconditional love and support inspired me to reach the end of this achievement.

Thanks to everyone who helped me to make my dreams come true.

Amin ALDADDOU

# TABLE OF CONTENT

# LIST OF TABLES

# LIST OF FIGURES

# LIST OF SYMBOLS

| | | |
|---|---|---|
| A | = | Area (m2) |
| C | = | Compression (KN) |
| C.M | = | Center of mass |
| C.S | = | Center of stiffness |
| C.V | = | Center of strength |
| Cd | = | Deflection amplification factor |
| CRS | = | Mapped value of the risk coefficient at short periods |
| Ct | = | Approximate fundamental period coefficient |
| Cvx | = | Vertical distribution factor for distribution of seismic forces |
| dmax | = | Maximum length of building dimensions |
| E | = | Modulus of elasticity (KN) |
| em | = | eccentricity of center of mass |
| es | = | eccentricity of center of stiffness |
| ev | = | eccentricity of center of strength |
| Dead | = | Dead load assigned including self-weight and superimposed. |
| Live | = | Live load assigned to the structural floor. |
| EQx ecc | = | Earthquake force in x-direction with 5% eccentricity |
| EQx eccM | = | Earthquake force in negative x-direction with 5% eccentricity |
| EQx | = | Earthquake force in x-direction |
| EQy ecc | = | Earthquake force in y-direction with 5% eccentricity |
| EQy eccM | = | Earthquake force in negative y-direction with 5% eccentricity |

| | | |
|---|---|---|
| EQy | = | Earthquake force in y-direction |
| Wind X | = | Wind force in x-direction |
| Wind Y | = | Wind force in x-direction |
| Fi | = | Floor lateral force (KN) |
| Fx | = | Lateral seismic force (KN) |
| Fa | = | Short-period site coefficient |
| Fv | = | Long-period site coefficient |
| G | = | Gust-Effect Factor |
| g | = | gravitational acceleration (m/sec2) |
| $I$ | = | Importance factor |
| K | = | Stiffness (KN-m) |
| Kd | = | Directionality Factor |
| Ke | = | Ground Elevation Factor |
| Kzt | = | Topographic Factor |
| M | = | Moment (KN m) |
| Ri | = | Re-entrant corner coefficient |
| $R$ | = | Response modification factor |
| Sa | = | Spectral response acceleration (g) |
| Ss | = | Short period spectral acceleration |
| $S_1$ | = | One-second periodic spectral response acceleration |
| $S_{D1}$ | = | Spectral response acceleration parameter at 1 second |
| $S_{DS}$ | = | Spectral response acceleration parameter at short periods |
| T | = | Tension (KN) |
| $T$ | = | Natural period of structure (sec) |
| TL | = | Long-period transition period (sec) |
| V | = | Base shear (KN) |
| W | = | Weight (KN) |
| α | = | Design philosophy factor (1.0 for LRFD) |
| Δ | = | Story drift |
| Ω | = | Over strength factor |
| $Cs$ | = | Seismic response coefficient |

# LIST OF ABBREVIATIONS

| | | |
|---|---|---|
| ACI | = | American Concrete Institute |
| AFAD | = | Disaster and Emergency Management Presidency in Turkey. |
| AISC | = | American Institute of Steel Construction |
| ASCE | = | American Society of Civil Engineering |
| ELF | = | Equivalent Lateral Force |
| FEM | = | Finite Element Method |
| FVA | = | Free Vibration Analysis |
| IBC | = | International Building Code |
| LRFD | = | Load Resistance Factor Design |
| LFRS | = | Lateral Force-Resisting System |
| MRF | = | Moment-Resisting Frame |
| NTHA | = | Nonlinear Time History Analysis |
| PEER | = | Ground Motion Database |
| PGA | = | Peak Ground Acceleration |
| SDC | = | Seismic Design Category |
| SMF | = | Special Moment Frame |
| THA | = | Time History Analysis |
| TEC | = | Turkish Earthquake Code |

# CHAPTER 1

# 1. INTRODUCTION

## 1.1 Overview

In recent years, a growing demand among architects and owners towards the irregularly shaped buildings seeking for aesthetics or distinguishment. Furthermore, gaps in these irregular structures may be present either for the same reasons above or for other practical reasons. Where these irregular structures are noticed to be present in a lot of areas including seismically active areas. Strong earthquakes motion and its effect on buildings have been studied throughout the years since it is one of the main forces that could cause failure to the structures, and the behavior of the buildings under these earthquake forces are usually dependent on the arrangement and configuration of the structural elements where geometry, shape, and size of the structure defines how the building will interact with the earthquake motion. When a structure is subjected to lateral earthquake forces, inertia forces within the structure are generated, the resultant of these inertia forces is assumed to be acting on a certain point in the structure called Center of Mass. And as a response, vertical members of the structures such as shear walls and columns act against these inertia forces, the resultant of these forces are assumed to be acting on certain point of the structure called Center of Stiffness. When these two points do not coincide, eccentricity in the structure happens causing the torsional actions to act on the structure. Irregularities in the structure could cause this phenomenon since in most irregular structures, Center of Mass and Center of Stiffness do not coincide. Irregularities have many types in both vertical and planner views, in this study, two structures consisted of two-stories, and plan-irregularities, like Asymmetrical plan shape, re-entrant corners, and irregular distribution of mass and diaphragm discontinuity along with flexibility in the diaphragm in one of them, are studied regarding their seismic performance to see how much the diaphragm types and void existence in slabs affects their seismic performance.

Structure 1 is a steel structure, designed under ultimate gravitational and lateral loads and the design is done by trial and error using ETABS software to assure safety, serviceability, and economical aspects. Structure 1 has its diaphragms as rigid for the first floor, and flexible on the second floor having a large gap in the second-floor slab, it has irregular plan with re-entrant corner as the structure shaped like an L shape. Structure 2 has exactly the same aspects of structure 1, with the same profile, same sections that assure safety for both structures, and same in other aspects. However, the difference is that structure 2 has its diaphragms as rigid diaphragms for both stories, with no existence of any void in the slabs. Both are located in Istanbul – Turkey

## 1.2 Methodology

The analysis of two the structures carried out using FEM base software, which is CSI ETABS 2019, where free vibration analysis, equivalent lateral force method, and mainly Time History Analysis are applied to both structures to obtain the difference in the behavior between the two. In free vibration analysis, the structure is to be displaced by a certain amount and released suddenly, where under the effect of the first excitation without any additional action of external force, the structure starts to vibrate back and forth. Free vibration analysis can be defined as the study of structural response when vibrating without external force effect, and it gives information about the natural periods, frequencies, and resonance of the structure for different mode shapes. Therefore, the free vibration analysis is applied to the two structures under the same circumstances where the periods, natural frequencies and joint drifts and displacements of the two structures are obtained and compared.

Regarding equivalent lateral force for the structures, both are located in Istanbul – Turkey, with site soil classification ZC which is described in the Turkish seismic code as “very tight layers of sand, gravel and hard clay or weathered, very cracked weak rocks”. Afterward, Turkish Hazard Map is used to determine the short and one-second periodic spectral accelerations Ss and S1 which are equal to 1.159s and 0.314s, respectively. Taking the response modification factor R equal to 4.5, and Importance factor I is 1. The period of the first mode shape for both structures are taken from the free vibration analysis rather than estimating it using the code procedure to obtain more accurate results. After applying the equivalent lateral force, the obtained outcomes are the equivalent static earthquake lateral forces on each story, and the base shear force on the base.

For the time history analysis, 11 different earthquakes are chosen for 6 different earthquakes obtained from PEER Ground Motion Database using NGA-West2 horizontal ground motion prediction equations (GMPEs) with 5% damped spectra of vertical ground motion. Spectral response acceleration parameters Sd1 and Sds obtained from equivalent lateral force method procedure are used to obtain the response spectrum for time history analysis. Then the response spectrum is used in the ETABS model. Using the Defined Response Spectrum, matching of every earthquake is done, then load cases are created including both components of the earthquake record to take into consideration the planner irregularity of the structure.

# CHAPTER 2

# 2. LITERATURE REVIEW

## 2.1 Structural Irregularities

When lateral loads due to seismic excitation act upon a structure, internal horizontal forces are generated within the structure acting as inertia forces, the resultant of these forces is assumed acting on a point of the structure called *center of mass CM*. And to resist these forces, the vertical members of the structure act against them making the total resultant of the whole force system to act on the *center of stiffness CS* point of the structure. Structural irregularities presence causes these two points of center of mass and center of stiffness to not coincide, and when such thing happens, eccentricities in the structure may happen causing the phenomenon of torsion coupling to occur due the interaction between lateral loads and resisting forces. Such torsion forces act upon the irregular structure causing severe damage. (Varadharajan et al., 2016). To avoid such damage, seismic design codes try to control the torsional behavior by applying design rules and limits that control irregularities in the structures in addition to control lateral stiffness, lateral torsion, and seismic inputs. (Giordano et al., 2008). It is safe to state that most of regular structures have rather predictable behavior when subjected to earthquake loading. However, the irregular structure may undergo unpredictable behavior when subjected to the same circumstances because of the torsion irregularities, local failure, mass irregular distribution etc.(Darshan & Shruthi, 2016). Different examples and types of irregularities are shown in Figure 1.

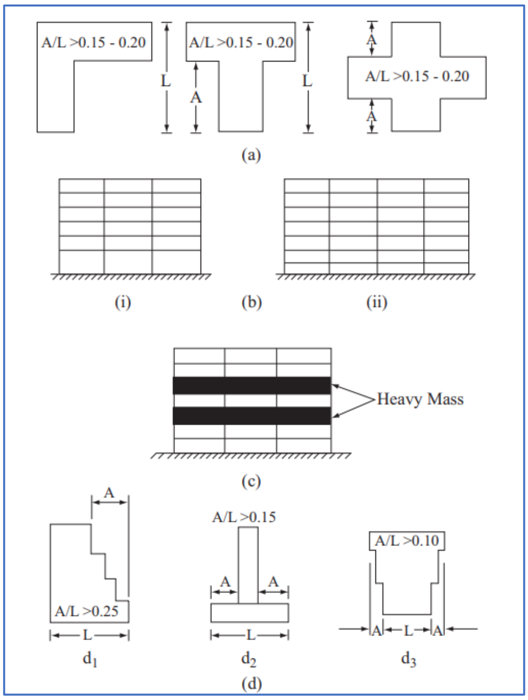


**Figure 1** Examples of structural irregularities. a) Re-entrant corners. b) Irregular stiffness distribution. c) Irregular mass distribution. d) Vertical setback irregularities.

### 2.1.1 Classification of Structural Irregularities:

Vertical Irregularity Types:

- Mass
- Stiffness (soft story)
- Strength (weak story)
- Setback (vertical geometrical irregularity).

Plan Irregularity Types:

- Asymmetrical Plan Shapes.
- Re-Entrant Corners.
- Diaphragm Discontinuity.
- Irregular Distribution of Mass, Strength, or Stiffness Along Plan.

To classify a structure as irregular structure, it needs to exceed the irregularities limits stated by different design codes, where the limits of horizontal and vertical irregularities stated by IBC 2003, Turkish Code TEC 2007, and ASCE7 – 5 are shown in Tables 1 and 2.

**Table 1** Limits of horizontal irregularities stated by IBC 2003, TEC 2018, and ASCE7-5.

| **Plan Irregularities** | | | |
|---|---|---|---|
| **Irregularity type** | **ASCE 7 -05** | **TEC 2018** | **IBC 2003** |
| **Re-entrant Corners** | $R_i \leq 15\%$ | $R_i \leq 20\%$ | - |
| **Torsional Irregularity** | $d_{max} \leq 1.2d_{avg}$<br>$d_{max} \leq 1.4d_{avg}$ | $d_{max} \leq 1.2d_{avg}$ | - |
| **Diaphragm Discontinuity** | $O_a > 50\%$ $S > 50\%$ | $O_a > 33\%$ | - |

**Table 2** Limits of vertical irregularities stated by IBC 2003, Turkish Code 2018, and ASCE7-5.

| **Vertical Irregularities** | | | |
|---|---|---|---|
| **Irregularity type** | **ASCE 7 -05** | **TEC 2018** | **IBC 2003** |
| **Mass** | Mi < 1.5 Ma | - | Mi < 1.5 Ma |
| **Stiffens** | $S_i < 0.7S_{i+1}$ Or<br>$S_i < 0.8\ (S_{i+1}+S_{i+2}+S_{i+3})$ | - | $S_i < 0.7S_{i+1}$ Or<br>$S_i < 0.8\ (S_{i+1}+S_{i+2}+S_{i+3})$ |
| **Soft Storey** | $S_i < 0.7S_{i+1}$ Or<br>$S_i < 0.8\ (S_{i+1}+S_{i+2}+S_{i+3})$ | $\frac{\eta ki = (\Delta i\ /\ hi)\ avr}{(\Delta i+1\ /\ hi+1)\ avr} > 2.0$ | $S_i < 0.7S_{i+1}$ Or<br>$S_i < 0.8\ (S_{i+1}+S_{i+2}+S_{i+3})$ |
| **Weak Storey** | $S_i < 0.6S_{i+1}$ Or<br>$S_i < 0.7\ (S_{i+1}+S_{i+2}+S_{i+3})$ | $\eta ci = (Ae)i\ / < 0.80$ | $S_i < S_{i+1}$ |
| **Setback Irregularity** | $SB_i < 1.3\ SB_a$ | - | $SB_i < 1.3\ SB_a$ |

Definitions of different types of eccentricities are shown in Figure 2 where a) mass eccentricity, b) stiffness eccentricity, and c) strength eccentricity. All of which are done by creating a distance between the positions of CM and CS As known these eccentricity leads to irregularities in the structure which leads to excessive unwanted torsion. According to (Tso & Bozorgnia, 1986), irregular distribution of stiffness and strength is one of the major casus of structural failure during seismic excitation.

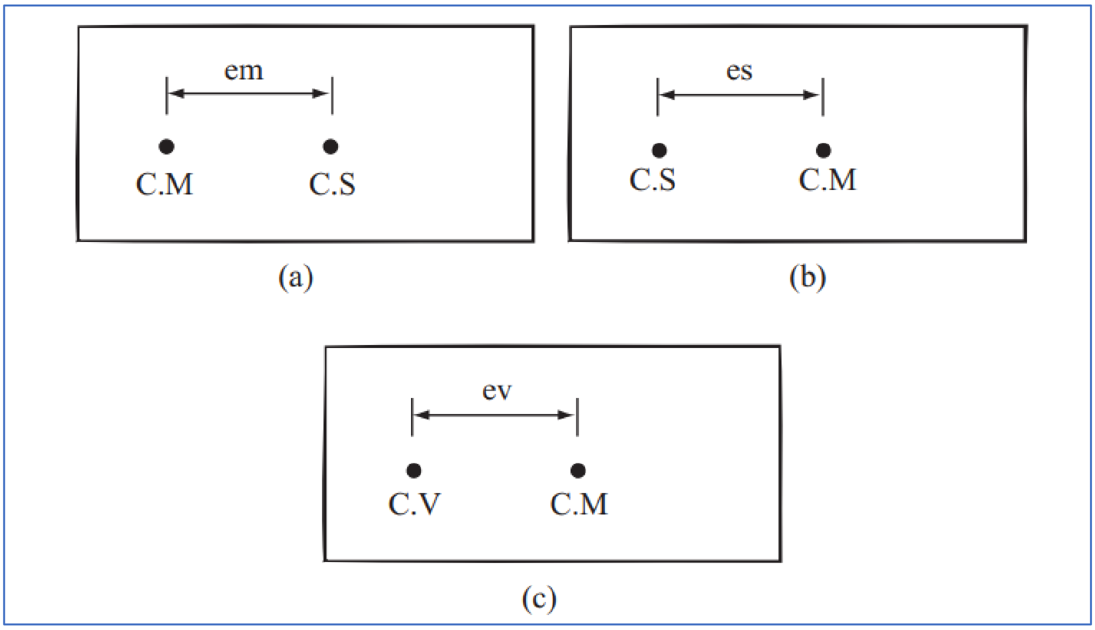


**Figure 2** Different types of eccentricity a) Mass b) Stiffness c) Strength.

### 2.1.2 Plan Irregularities in Structures:

Plan irregularity according to researchers is the irregular distribution of mass, stiffness, or strength along the plan of the structure (Darshan & Shruthi, 2016). Structural performance during earthquakes showed that one of the most important causes of seismic structural damage is plan irregularities. Where this plan irregularities as stated before can be occur due to several reasons including different mass distribution, different stiffness, or strength along the structural plan (Varadharajan et al., 2016). Most of early research studied the plan irregularities in buildings, adopted one-storey structures due to its simplicity and ease of application. These models have been studied to observe the torsional influence on the seismic response parameters where design methodologies are formulated. However, in the recent years multistorey models have been more studied despite their complexity due to their accurate and realistic torsional response representation. Researchers previously studied the one-storey irregularities focused on changing positions of CM and CS points along the plan of the structure generating that by playing with mass eccentricity, strength eccentricity, or other methods explained before. Common types of plan irregularities will be discussed next.

### 2.1.2.1 Asymmetrical Plan Shape:

Asymmetrical plan layout is common in modern structures due to different functional reasons and architectural requirements. This asymmetry is one of the most common causes of torsion forces within structure during earthquake excitation. Recent building codes tried to avoid such problem in torsion by restricting the irregularity in building layouts, also by taking into consideration the accidental eccentricity in the design process. The lateral-torsional coupling due to eccentricity between center of mass (CM) and center of rigidity (CR) in asymmetric building structures generates torsional vibration even under purely translational ground shaking. During seismic shaking of the structural systems, inertia force acts through the center of mass while the resistive force acts through the center of rigidity as shown in Figure 3 (Maske &

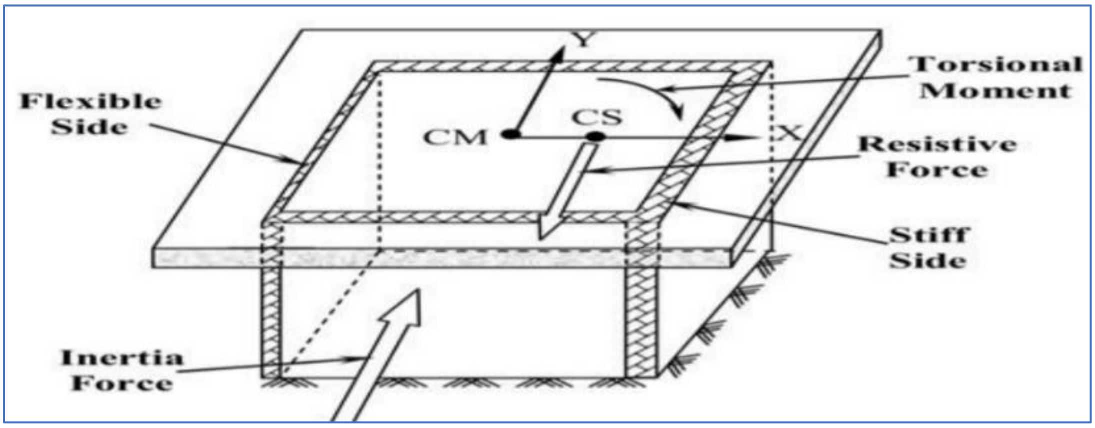


**Figure 3** Torsional moment generation under seismic excitation in asymmetric structures.

Pajgade, 2013).

### 2.1.2.2 Re-Entrant Corners.

Building with re-entrant corners are usually common in urban area when maximum land space is needed to be occupied. However, such buildings may undergo sever torsion when subjected to seismic excitation Since the structure in the study is corner shaped, it has re-entrant corner within it which may cause torsion within the structure when subjected to earthquake lateral loading. Different layouts of common building shapes with re-entrant corners are shown in Figure 4.

For the structural layout considered in the study, the dynamic response of a re-entrant configuration and potential floor diaphragm damage area is shown in Figure 5.

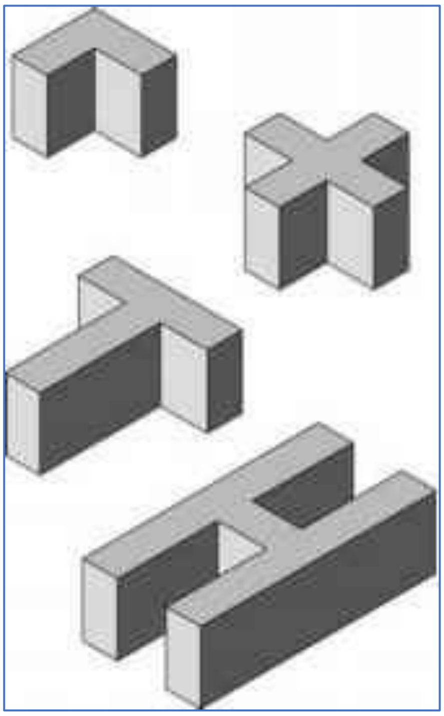

**Figure 4** Common shapes of re-entrant corners.

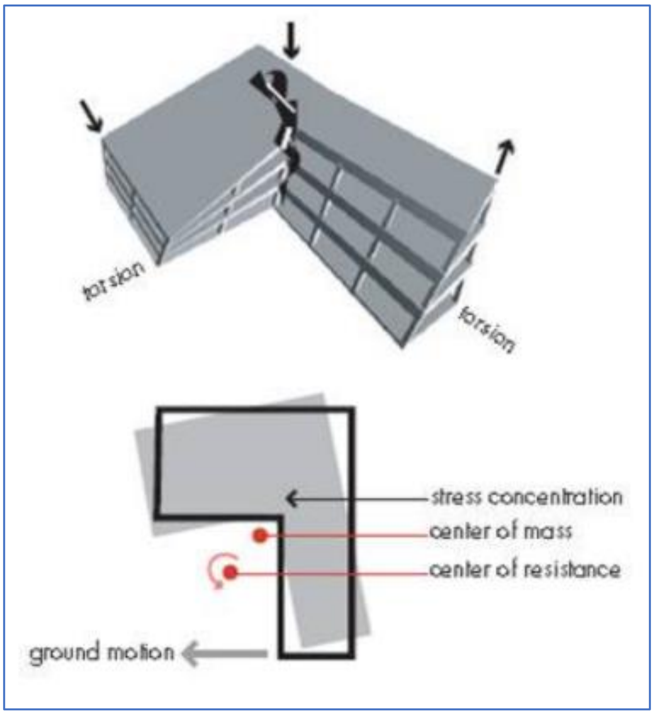


**Figure 5** Dynamic response of certain re-entrant configuration.

### 2.1.2.3 Diaphragm Discontinuity:

Diaphragm discontinuity is defined as discontinuities or variations in stiffness and mass in the form of slab openings and variation in slab thicknesses. The structure considered in the study has a slab opening on the second floor, which makes the structure diaphragm discontinued.

### 2.1.3 Vertical Irregularities in Structures:

Mass, stiffness, and strength irregularities along the elevation of the building can be classified as vertical irregularities (Darshan & Shruthi, 2016). And their effects are different from each other's regarding the seismic response (Varadharajan et al., 2016). Common types of vertical irregularities will be discussed next.

### 2.1.3.1 Mass Irregularity (Soft Story)

Mass irregularity as other irregularities can significantly affect the seismic response of a structure subjected to an earthquake load. It is considered to be existed in a certain structure if the effective weight of any storey is > 150% of its adjacent storey according to ASCE7 -5 and NBCC 2005. Mass irregularity effect vary from structure to another depending on multiple factors including the used model, location of the mass irregularity and the analysis method used.

#### 2.1.3.2 Stiffness Irregularity (Weak Story)

It is usually referred to as soft storey, and it happens when a storey has its lateral stiffness < 70% of any adjacent storey, or < 80% of the average lateral stiffness of the three stories above or below it as defined by ASCE7 -5, BNBC 1993 and NBCC 2005. Stiffness irregularity can be introduced by removing slab from certain floor or space frame in order to make it less stiffen (soft) comparing to other frames (Hasnat & Rahim, 2013).

#### 2.1.3.3 Strength Irregularity

It is also referred to as capacity discontinuity or weak storey. It happens when the storey shear strength of a certain storey is less than the storey shear strength of the storey above it. According to ASCE7 -5, it is considered to be there when a storey lateral strength is <80% of that in the storey above. Storey shear strength is the strength sum of all lateral resisting elements of the SFRS resisting the shear in the chosen direction (Tremblay, 2005).

#### 2.1.3.4 Setback Irregularity

It is a geometrical irregularity; it is in plan discontinuity in the lateral force resisting elements in vertical direction. According to ASCE7 -5 setback irregularity is defined to exists when in-plane offset of the lateral force-resisting elements is greater than the length of those elements or there exists a reduction in stiffness of the resisting element in the story below. Figure 6 shows different types of setbacks according to EC8.

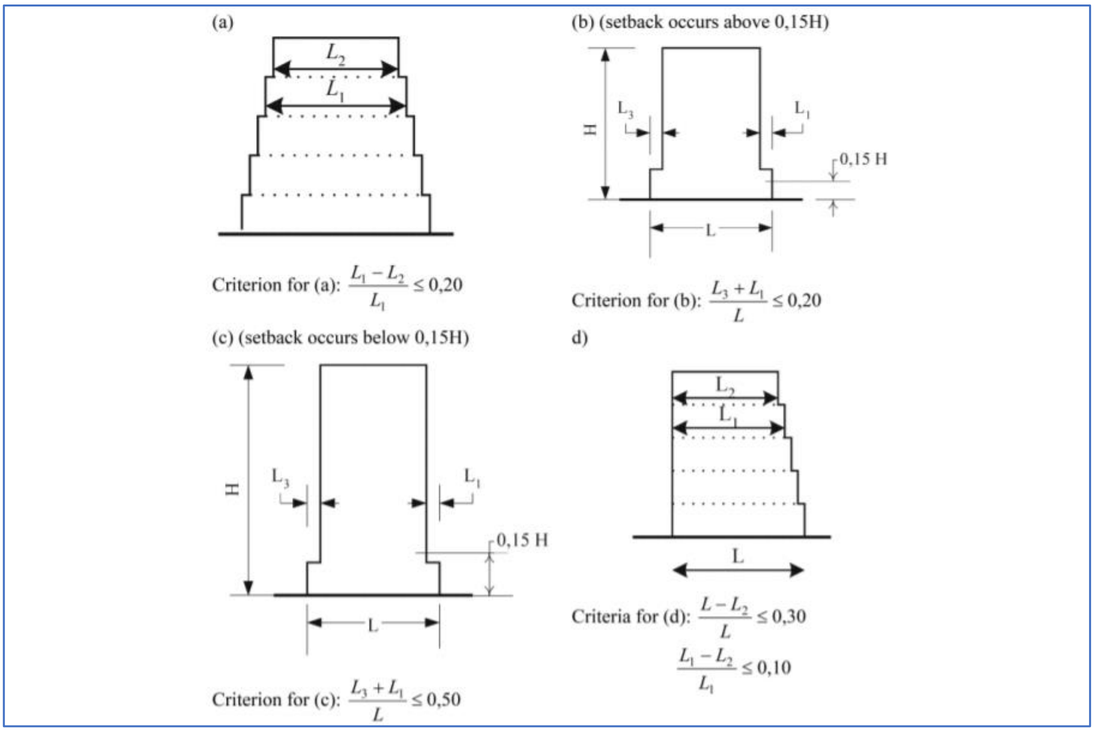


**Figure 6** Setback irregularity types.

Change in the seismic response depends on the structural irregularities, where the latter can be classified under two main categories vertical, and plan irregularities. Researcher stated that larger amount of research has been done on plan irregularities. Plan irregularities are studied as single and multi storey buildings (Varadharajan et al., 2016).“Most of the building models in recent years are multistorey building models, so the expressions for seismic response parameters and design philosophies formulated are not valid for multistorey building models. So, most of the design codes which use expressions are formulated on basis of single-storey models need to be revised”.

Torsion generated on structures due to seismic loads highly influenced by the locations of centers of the structure such as CM, CV, and CR with respect to each other. Optimum position of CV-CR is found to be highly depended of type and period of seismic excitation (Dutta & Das, 2002).

## 2.2 Diaphragm Actions

Diaphragm can be defined as the lateral resisting system that transmits lateral forces to the vertical resisting system to be carried safely to earth. It includes the roof, floors slabs and the bracing system in the horizontal plan. The floors and roofs in the building are designed to carry gravitational forces as their main task and are designed as diaphragm to distribute seismic forces to the main resisting system such frames and shear walls, and to tie the structure together to act as a single unit in case of earthquake, highly effecting the robustness and redundancy of the structure. Diaphragms have two main types which are rigid diaphragm and semi-rigid diaphragm (The Structural World, 2021). The former can rotate and translate but cannot deform nor it can report any associated force since it has infinite in-plane stiffness properties. While the latter can deform giving the structure the ability to behave its actual behavior since it simulates the actual in-plane properties and behavior. In rigid diaphragm, the lateral forces are distributed based on the relative stiffness of all the member forming the lateral force resisting system at each level. The semi-rigid diaphragms are mainly used against lateral wind loads. The results showed that rigid diaphragm resulted nearly identical results to semi-rigid diaphragms, when obtained from reinforced concrete slabs with sufficient thickness and similar slabs or decks having negligible deformation due to lateral loading, while taking the advantage of the simpler and faster calculations (Guzman, 2019; The Structural World, 2021). According to CSI (Guzman, 2019), the semi-rigid modeling should be used when significant in-plane deformation is present in the slab due to lateral loads (e.g., for weak in-plane slabs), or when required by code. The primary difference between the two diaphragm types that the formation time of rigid diaphragm is faster, so it consumes less time since its infinite in-plan stiffness components allow the matrix to be condensed. Another difference is in the eccentricity, where for rigid diaphragms the accidental eccentricity associated with automated seismic loading is taken at the center of mass CM, while for semi rigid, the accidental eccentricity should be taken at each node. Finally, in some software like ETABS and SAP2000, the reported force for in-plan axial chord forces, shear forces, and collector forces are only reported when semi-rigid diaphragm is used (Guzman, T., 2019). According to (Rahman, and Jamshetty, 2019), diaphragms can be classified into three main types which are rigid, semi-rigid, and flexible diaphragms.

### 2.2.1 Rigid Diaphragms

In this type of diaphragms, the lateral forces are distributed from horizontal to the vertical resisting system based on the relative stiffness, where the vertical resisting systems could be shear walls or moment resisting frames. In this model it is safe to consider that under the lateral load effect, the displacement (in-plan) is equal along the entire length of the diaphragm. A diaphragm is to be considered rigid when its midpoint displacement is < 200% of the average displacement at its ends when subjected to lateral loads (Rahman, and Jamshetty, 2019).

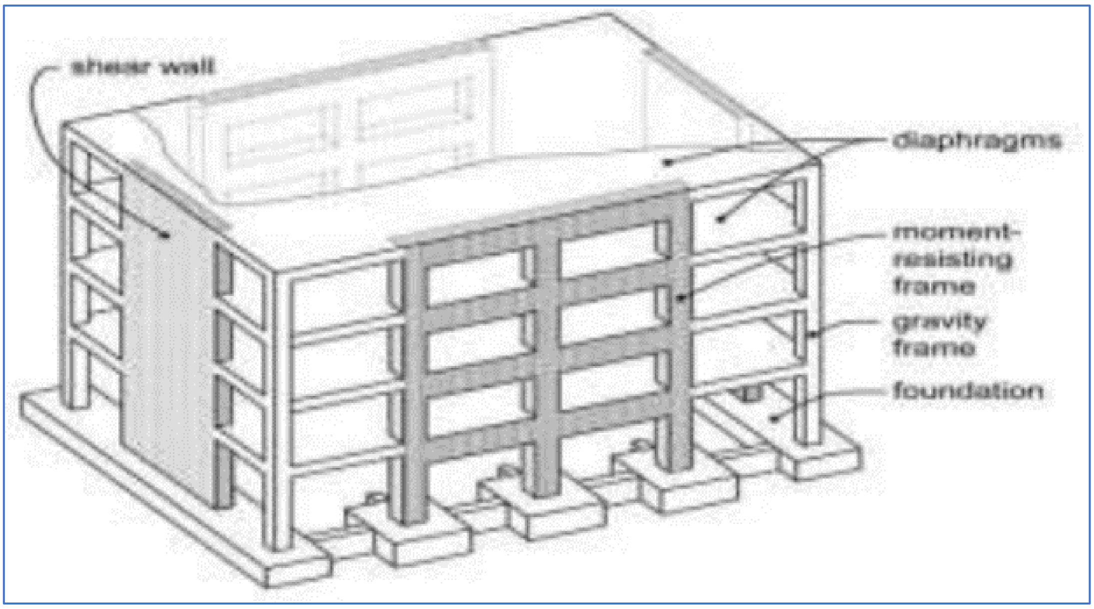


**Figure 7** Diaphragm illustration.

### 2.2.2 Flexible Diaphragms

Unlike rigid diaphragms, flexible diaphragms distribute the lateral forces to the vertical resisting system based on the in-plan tributary area of the element acting as diaphragm (e.g., roof or floor members). Diaphragms are considered flexible when its maximum lateral deformation is > 200% of the common story drift of the associated story, which can be determined by comparing the in-plan deflection of the diaphragm center under lateral load , to adjacent vertical component under tributary lateral load (Rahman, and Jamshetty, 2019).

### 2.2.3 Semi-Rigid Diaphragms

In real-life applications no diaphragm can be considered 100% rigid nor 100% versatile. However, when the diaphragm is very stiff comparing to the vertical resisting system, it is considered to be rigid diaphragm to make calculations easy, and when the diaphragm is much more flexible comparing to the vertical resisting system it is considered to be flexible diaphragm. However, when the diaphragm has similar or near rigidity to the vertical resisting system, it is not suitable to say that it is 100% rigid or 100% flexible, in such case the semi-rigid analysis takes place, and complex analysis should be done instead of the simplified procedures of the rigid and flexible diaphragms. In this case the stiffness of the diaphragm and the vertical resisting system should be taken into consideration where finite element analysis usually used.

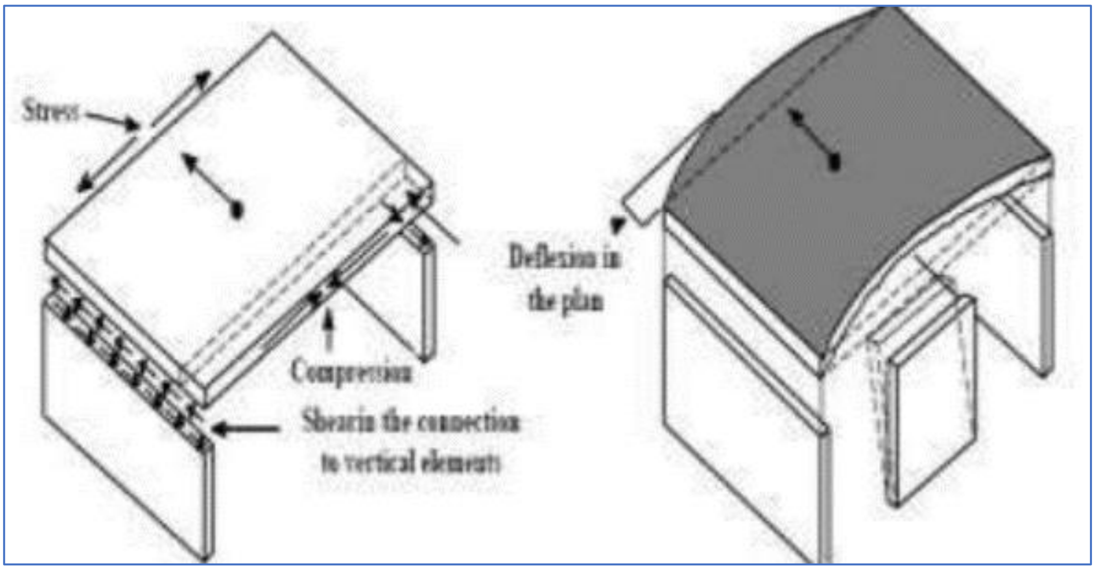


**Figure 8** Rigid diaphragm concentration of stresses (left), flexible diaphragm deflection of stresses (right).

### 2.2.4 Diaphragms Actions

Behavior of horizontal diaphragm in buildings can be similar to simply supported deep beam under uniform load, as shown in the Figure 9. Where the chords are the perimeter elements where the diaphragm resists the bending moment thorough. The cord axial forces are either tension or compression forces as shown in Figure 10 where they result from resolving the internal bending moment into coupling force with b being the moment arm. Therefore. $C = T = M/b$ (The Structural World, 2021; Guzman, 2019). Floor diaphragm rigid body movements can be classified into longitudinal translation, transverse translation, rotational about the third axis, and combination of both transverse and rotational translations. Internal shear forces carried by the diaphragm are fairly uniform across the depth of the slab, therefore, the shear v can be expressed as shear per unit depth taking $v = V/b$.

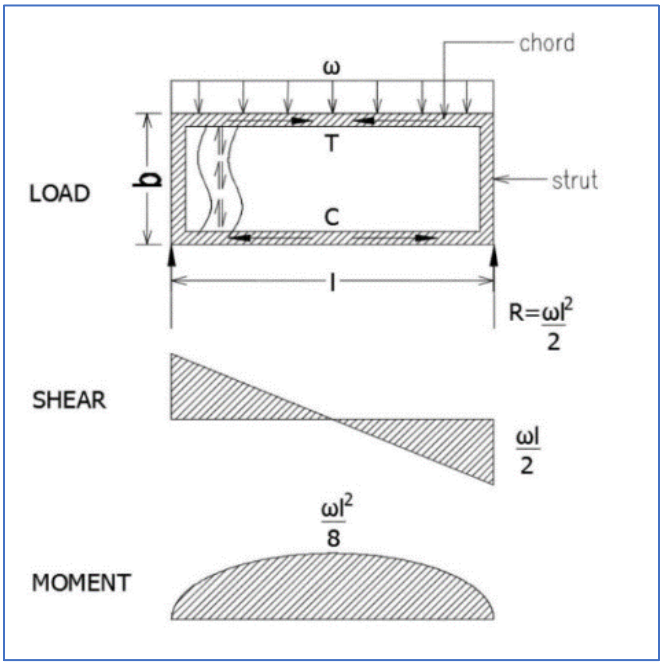


**Figure 9** stresses within the diaphragm cords (above), shear and moment as simply supported beam (below).

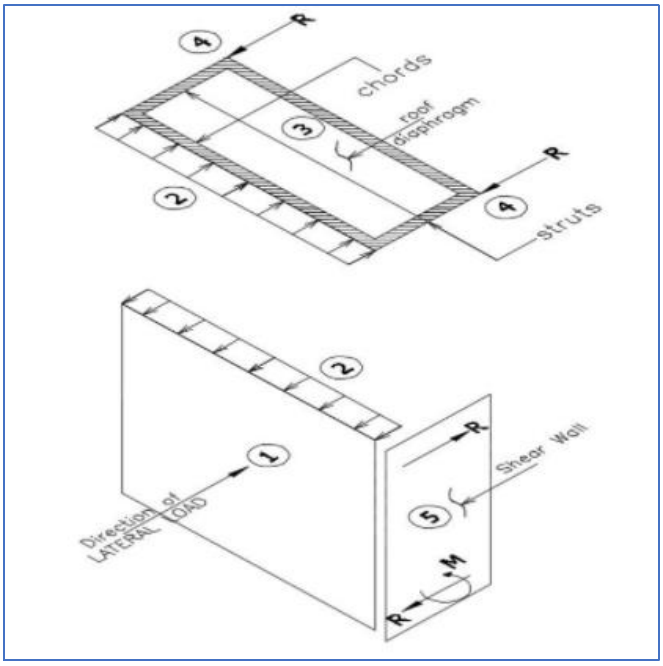


**Figure 10** Diaphragm actions under horizontal actions.

When proper connection is provided between slabs and vertical resisting system (frames or shear walls) then the support reactions can be directly transmitted by the slab to the vertical horizontal system.

The process and the role of diaphragm can be ordered within the following points:

1. The applied lateral forces are firstly carried by the walls (which are assumed to be spanning vertically) to the slabs of the structure.
2. Then the developed horizontal reactions are picked by the slabs which are attached to these vertically spanning walls.
3. At the roof plan level, the developed horizontal reactions turn the loads into the plan roof system which can be said to be a diaphragm.
4. This diaphragm act as a large horizontal beam spanning between the supporting shear walls or moment resisting frames, transferring the horizontal loads to vertical loads (diaphragm actions).
5. The diaphragm actions are resisted by these shear walls or moment resisting frames transferring the shear loads and possible overturning moment to the ground through foundations.

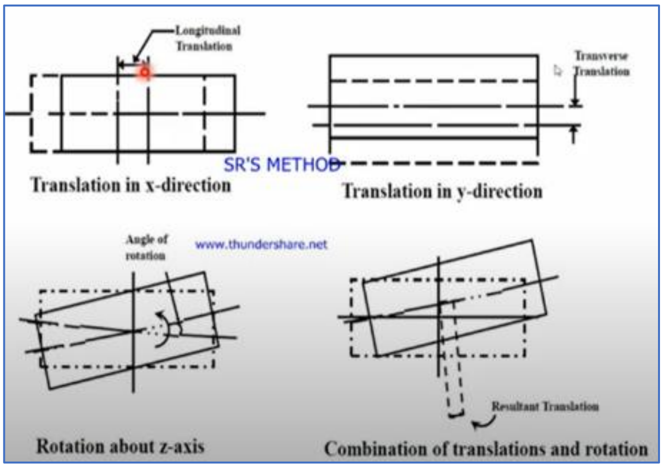


**Figure 11** Possible rigid body movements of diaphragms.

## 2.3 Time History Analysis

Time History Analysis provides a way to evaluate dynamic response of structures under loading that is varying with time with a specified time function. It can be either linear or nonlinear evaluation. Its dynamic equilibrium equation can be solved using direct integration or using modal method, with the initial conditions can be taken from the end of the previously done analysis.

Nonlinear Time history analysis is a nonlinear dynamic technique used for structural seismic analysis specially in cases that the structure could show nonlinear response to earthquake forces. To evaluate a structural behavior with this method, a representative earthquake time history is needed for that structure. It is a step-by-step analysis along with known loading function that is varying with time. (Patil & Kumbhar, 2013). Should be taken into consideration that direct integration method can be sensitive to step-size of time, where the step size should be decreased to a certain point until the results can be affected. Another thing to be taken into consideration is HHT, which is Hibler-Hughes-Tylor negative value of alpha, which can be added to the system in order to help the nonlinear solution to converge. Furthermore, both nonlinearity of material and geometry can be included during this type of nonlinear analysis.

Linear time history analysis is also a step-by-step analysis technique where both loading, and response histories are evaluated rapidly at each step. It considers the interaction of the vibrational modes along with the earthquake's typical frequencies (Di Cuia et al., 2017).

# CHAPTER 3

# 3. STRUCTURAL DESIGN

## 3.1 Description of the Building

In this study, two structures are being designed and studied, both are plan irregular two-story buildings, both have the same plan and vertical layouts, with an asymmetrical plan shape, and re-entrant corners, and one of them has a diaphragm discontinuity. They are considered to be modeled as intermediate moment resisting steel frame structures. The two structures will be referred to as Structure 1 and Structure 2, and the difference between them will be illustrated next. Figure 12 shows the plan view of the structural layout of both Structure 1 and Structure 2. It is noticed that they are asymmetric in both x and y directions consisted of three rectangular each has an envelope of 8 x 5 m floor, and the two stories have a 3 m height each. Structure 1 has a floor gap in its roof floor, having its first floor to be a rigid diaphragm, and the roof slab to be a flexible diaphragm. On the other hand, Structure 2 has its both floors to be rigid with no void in any of them. All floors are made of reinforced concrete supported by steel beams at their edges. A 3D view of Structure 1 is shown in Figure 13.

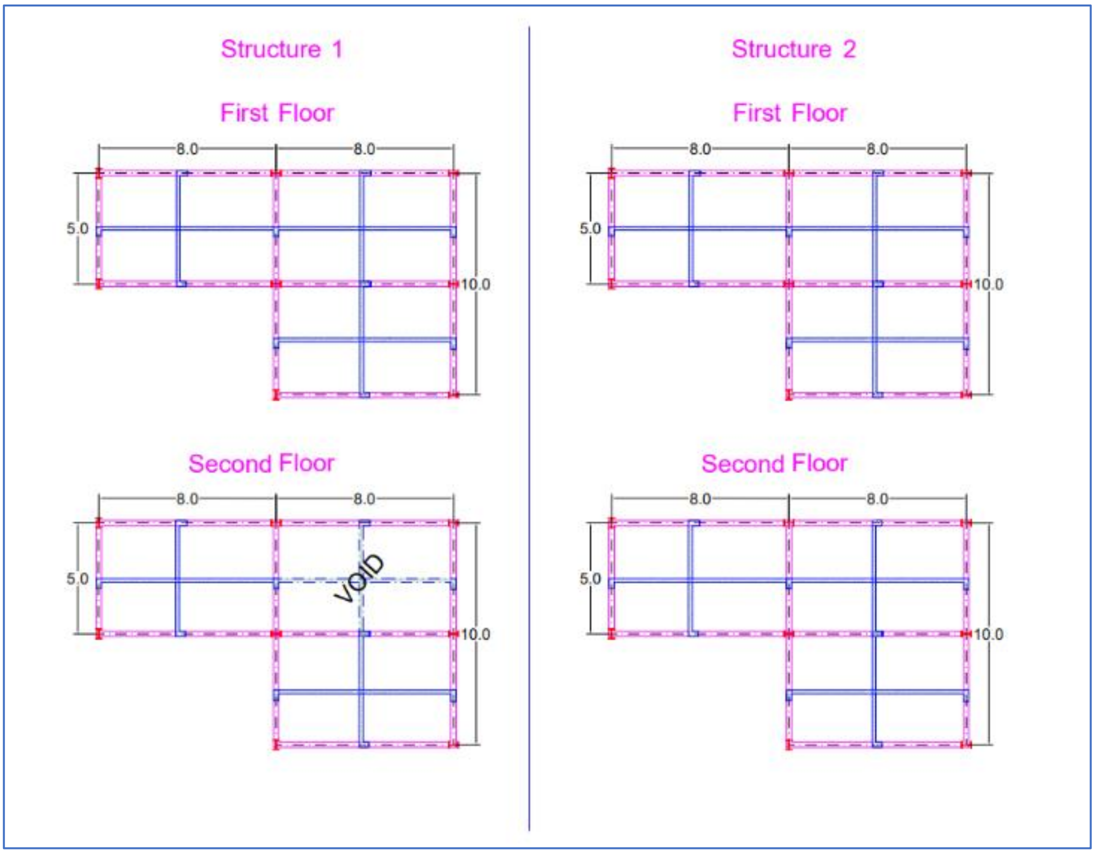


**Figure 12** Structural plan view and layout.

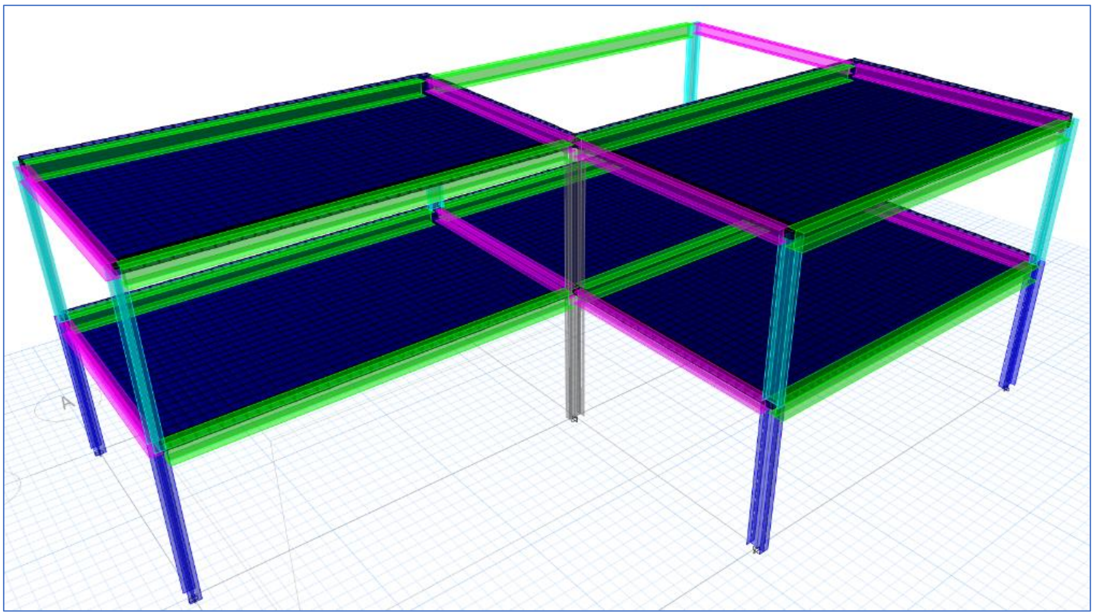

**Figure 13** 3D view of Structure 1.

### 3.2 Codes, Methods, and References Used

ASCE 7-16: Minimum Design Loads and Associated Criteria for Buildings and Other Structures. Describes the means for determining dead, live, soil, flood, tsunami, snow, rain, atmospheric ice, earthquake, and wind loads, and their combinations for general structural design.

ACI318M-19: Building Code Requirements for Structural Concrete and Commentary (SI Units). Provides minimum requirements for the materials, design, and detailing of structural concrete buildings.

AISC 360-16: Specification for Structural Steel Buildings. The specification provides the generally applicable requirements for the design and construction of structural steel buildings and other structures.

AISC Steel Construction Manual 15th Edition: Includes updated specifications, codes, and standards, tabular information as well as discussions, shape information, slenderness limits, provided by the AISC complying with the 2016 Specifications for Structural Buildings.

LRFD: Load and Resistance Factor Design Method.

AFAD: Disaster and Emergency Management Presidency in Turkey.

### 3.3 Modeling of the Structures and Load Inputs

The nonlinear static and dynamic analysis are carried out using ETABS software, where Structure 1 model is constructed with steel sections taken from the AISC steel manual with known section properties and load capacity. In addition, the slabs are meshed during the analysis process with their stiffness taken from their material and thickness. The initial designed started with manual calculations and then sections are carried out to the software where more accurate analysis has been done including the earthquake forces. Trial and error design procedure is used in the software until safe and sufficient sections are being founded. Further information are available in the design appendix. Then, Structure 2 which is as defined previously, is a similar to Structure 1 with the exact same plans, sections, and loads but with no void in the roof floor and rigid diaphragms, is also analyzed and designed in the software to check which structure controls the failure and generalize the design on both structures to avoid any unwanted variability.

### 3.3.1 Load Types on the Structures

The structures are designed as Steel Intermediate Moment Frame structure, and are taken as normal occupancy buildings (Residential buildings) located in Istanbul – Turkey and using the government official Turkey earthquake hazard map, and ASCE7-17, the following indexes are obtained:

- Superimposed Dead Load (gravitational): 0.9 KN/m$^2$.
- Superimposed Live Load (gravitational): 2.0 KN/m$^2$. ASCE7-16 Table 4.3-1

- Earthquake ground motion level: DD-2 (An earthquake with a probability of exceedance of 10% in 50 years (recurrence period of 475 years) movement level.

- Site soil class: ZC (Very tight layers of sand, gravel and hard clay or weathered, very cracked weak rocks).

**Table 3** Seismic parameters for the structure

| | | | |
|---|---|---|---|
| Short period spectral response accelerations at 0.2 | Ss (sec) | 1.159 | Turkey Hazard Map [1] |
| 1-second period spectral response accelerations | S1 **(sec)** | 0.314 | Turkey Hazard Map [1] |
| Long-period transition period | TL (sec) | 6 | H. Elastic Design Spectrum |
| Period Calculated by software | T | 0.695 | ETABS MODAL 1$^{st}$ |
| Response modification factor | R | 4.5 | ASCE7-16 Table 12.2-1 |
| Over strength factor | Ω | 3 | ASCE7-16 Table 12.2-1 |
| Deflection Amplification factor | Cd | 4 | ASCE7-16 Table 12.2-1 |
| Risk category | **-** | II | ASCE7-16 Table 1.5-1 |

| | | | |
|---|---|---|---|
| Occupancy importance factor | I | 1.0 | ASCE7-16 Table 1.5-2 |

- Wind Load (Lateral): The buildings are classified as partially enclosed buildings, assumed the wind speed to be 80 mph (129 Km/h), and terrain/exposure category C.

**Table 4** Wind parameters for the structure

| | | | |
|---|---|---|---|
| Basic Wind Speed | V (mph-Km/h) | 80 - 129 | Wind Hazard Map |
| Exposure Type | - | C | ASCE7-16 C26.7.2 Surface Roughness Category |
| Ground Elevation Factor | Ke | 1 | ASCE7-16 Table 26.9-1 |
| Topographic Factor | Kzt | 1 | ASCE7-16 Fig26.8-1 |
| Gust-Effect Factor | G | 0.85 | ASCE7-16 C26.11.1 Gust for rigid structures |
| Directionality Factor | Kd | 0.85 | ASCE7-16 Table 26.6-1 |
| E1 Ratio | e1 | 0.15 | ASCE 7-16 Fig27.3-8 |
| E2 Ratio | e2 | 0.15 | ASCE 7-16 Fig27.3-8 |

### 3.3.2 Load Combinations

According to ASCE 7-16 in section 2.3.1 the basic load combinations considering LRFD method are taken, shown in Table 6, where 36 load combinations are included. And Table 5 explains the symbols used to define loads.

**Table 5** Load Combination Symbol Explanation.

| **Symbol of the force** | **Explanation** | **Direction** |
|---|---|---|
| **Dead** | Dead load assigned including self-weight and superimposed. | Vertical |
| **Live** | Live load assigned to the structural floor. | Vertical |
| **EQx** | Earthquake force in x-direction | Lateral |
| **EQy** | Earthquake force in y-direction | Lateral |
| **EQx ecc** | Earthquake force in x-direction with 5% eccentricity | Lateral |
| **EQy ecc** | Earthquake force in y-direction with 5% eccentricity | Lateral |

| | | |
|---|---|---|
| **EQx eccM** | Earthquake force in negative x-direction with 5% eccentricity | Lateral |
| **EQy eccM** | Earthquake force in negative y-direction with 5% eccentricity | Lateral |
| **Wind X** | Wind force in x-direction | Lateral |
| **Wind Y** | Wind force in x-direction | Lateral |

**Table 6** Load Combinations Assigned to the Structure.

| Case Number | Load Name | SF | Notes |
|---|---|---|---|
| **1** | Dead | 0.8 | Dead (min) + Static Earthquake [Strength] |
| | EQx | 1 | |
| **2** | Dead | 0.8 | Dead (min) + Static Earthquake [Strength] |
| | EQx ecc | 1 | |
| **3** | Dead | 0.8 | Dead (min) - Static Earthquake [Strength] |
| | EQx ecc | -1 | |
| **4** | Dead | 0.8 | Dead (min) - Static Earthquake [Strength] |
| | EQx | -1 | |
| **5** | Dead | 0.8 | Dead (min) + Static Earthquake [Strength] |
| | EQy | 1 | |
| **6** | Dead | 0.8 | Dead (min) + Static Earthquake [Strength] |
| | EQy ecc | 1 | |
| **7** | Dead | 0.8 | Dead (min) - Static Earthquake [Strength] |
| | EQy ecc | -1 | |
| **8** | Dead | 0.8 | Dead (min) - Static Earthquake [Strength] |
| | EQy | -1 | |
| **9** | Dead | 0.9 | Dead (min) + Wind [Strength] |
| | Wind X | 1 | |
| **10** | Dead | 0.9 | Dead (min) - Wind [Strength] |
| | Wind X | -1 | |
| **11** | Dead | 0.9 | Dead (min) + Wind [Strength] |
| | Wind Y | 1 | |
| **12** | Dead | 0.9 | Dead (min) - Wind [Strength] |
| | Wind Y | -1 | |
| **13** | Dead | 1.2 | Dead + Live [Strength] |
| | Live | 1.6 | |

| | | | |
|---|---|---|---|
| **14** | Dead | 1.2 | Dead + Live + Wind + Snow  [Strength] |
| | Live | 1 | |
| | Wind X | 1 | |
| **15** | Dead | 1.2 | Dead + Live + Wind + Snow  [Strength] |
| | Live | 1 | |
| | Wind Y | 1 | |
| **16** | Dead | 1.2 | Dead + Live - Wind + Snow  [Strength] |
| | Live | 1 | |
| | Wind X | -1 | |
| **17** | Dead | 1.2 | Dead + Live - Wind + Snow  [Strength] |
| | Live | 1 | |
| | Wind Y | -1 | |
| **18** | Dead | 1.3 | Dead + Live + Static Earthquake  [Strength] |
| | Live | 1 | |
| | EQx | 1 | |
| **19** | Dead | 1.3 | Dead + Live + Static Earthquake  [Strength] |
| | Live | 1 | |
| | EQx ecc | 1 | |
| **20** | Dead | 1.3 | Dead + Live - Static Earthquake  [Strength] |
| | Live | 1 | |
| | EQx ecc | -1 | |
| **21** | Dead | 1.3 | Dead + Live - Static Earthquake  [Strength] |
| | Live | 1 | |
| | EQx | -1 | |
| **22** | Dead | 1.3 | Dead + Live + Static Earthquake  [Strength] |
| | Live | 1 | |
| | EQy | 1 | |
| **23** | Dead | 1.3 | Dead + Live + Static Earthquake  [Strength] |
| | Live | 1 | |
| | EQy ecc | 1 | |
| **24** | Dead | 1.3 | Dead + Live - Static Earthquake  [Strength] |
| | Live | 1 | |
| | EQy ecc | -1 | |
| **25** | Dead | 1.3 | Dead + Live - Static Earthquake  [Strength] |
| | Live | 1 | |
| | EQy | -1 | |
| **26** | Dead | 1.4 | Dead  [Strength] |

| | | | |
|---|---|---|---|
| **27** | Dead | 1 | |
| | EQx | 1 | |
| | EQy | 1 | |
| | Live | 0.5 | |
| **28** | Dead | 1 | |
| | Live | 0.3 | |
| **29** | Dead | 1.3 | Dead + Live + Static Earthquake [Strength] |
| | Live | 1 | |
| | EQx eccM | 1 | |
| **30** | Dead | 1.3 | Dead + Live - Static Earthquake [Strength] |
| | Live | 1 | |
| | EQx eccM | -1 | |
| **31** | Dead | 1.3 | Dead + Live + Static Earthquake [Strength] |
| | Live | 1 | |
| | EQy eccM | 1 | |
| **32** | Dead | 1.3 | Dead + Live - Static Earthquake [Strength] |
| | Live | 1 | |
| | EQy eccM | -1 | |
| **33** | Dead | 0.8 | Dead (min) + Static Earthquake [Strength] |
| | EQx eccM | 1 | |
| **34** | Dead | 0.8 | Dead (min) - Static Earthquake [Strength] |
| | EQx eccM | -1 | |
| **35** | Dead | 0.8 | Dead (min) + Static Earthquake [Strength] |
| | EQy eccM | 1 | |
| **36** | Dead | 0.8 | Dead (min) - Static Earthquake [Strength] |
| | EQy eccM | -1 | |

### 3.3.3 Materials Used for Structural Elements

**Table 7** Materials Used in the Structure.

| Member | Material | Modulus of Elasticity E | Poisson's Ratio | Shear Modulus G | Specified Weight Density |
|---|---|---|---|---|---|
| | | (MPa) | | (MPa) | (KN/m$^3$) |
| **Beams** | A992 Steel | 199947.98 | 0.3 | 76903.07 | 76.9729 |
| **Columns** | A992 Steel | 199947.98 | 0.3 | 76903.07 | 76.9729 |
| **Slabs** | 5000Psi Concrete | 27789.38 | 0.2 | 11578.91 | 23.5631 |
| **Rebars** | A615 Gr60 Steel | 199947.98 | 0.3 | 76903.07 | 76.9729 |

## 3.4 Design outcomes

Two structures have been designed and analysis to see which structure controls the section sizes. Structure 1 is the one with semi-rigid roof slab and a slab void. And Structure 2 is the one with rigid roof slab and no void. After performing the analysis, the control structure appeared to be Structure 2 where larger sections are needed in order to the design to be sufficient. After calculating the loads on the structures and designing it using hand conceptual design followed by error and trail software design using provided formulas by AISC 360-16 for LRFD method and ASCE 7-16. And taking the steel sections from AISC Steel Construction Manual 15th Edition; the sections found and are to be used in the structure are shown in Table 8.

**Table 8** Chosen Sections and Properties.

| Element | Symbol | Material | Section |
|---|---|---|---|
| Beam | B1 | A992 Steel Fy50 | W10x33 |
| Beam | B2 | A992 Steel Fy50 | W12x79 |
| Beam | B3 | A992 Steel Fy50 | W12x87 |
| Column | C1 | A992 Steel Fy50 | W12x40 |
| Column | C2 | A992 Steel Fy50 | W12x58 |
| Slabs | S1 | 5000Psi Concrete | 0.25m |

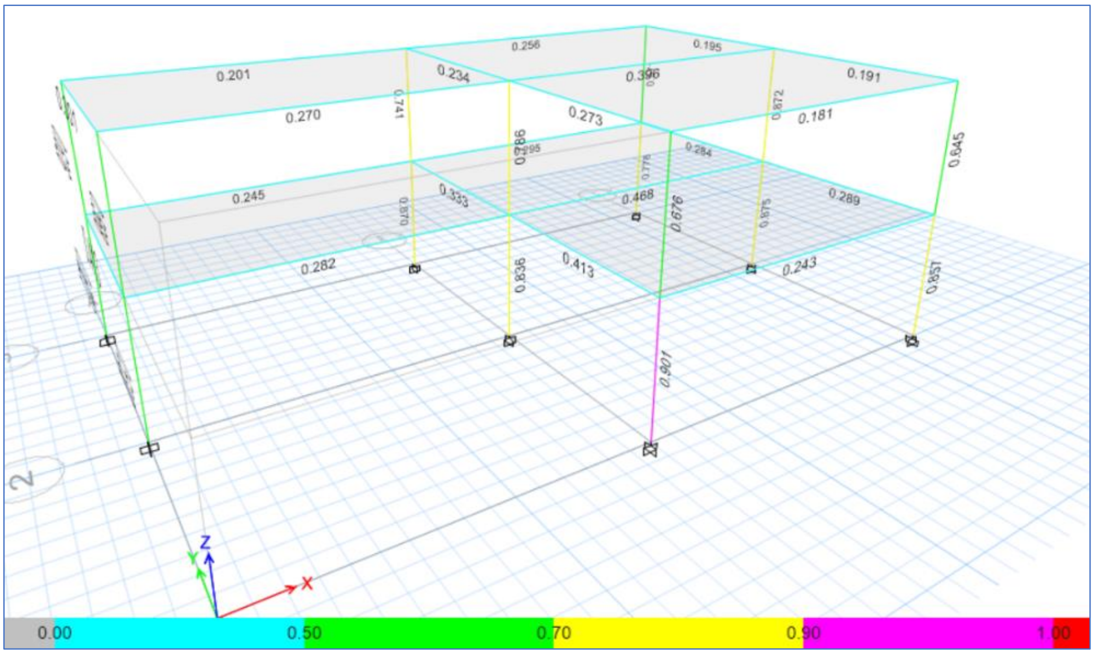


**Figure 14** Section efficiency P-M ration values for Structure 2 (control).

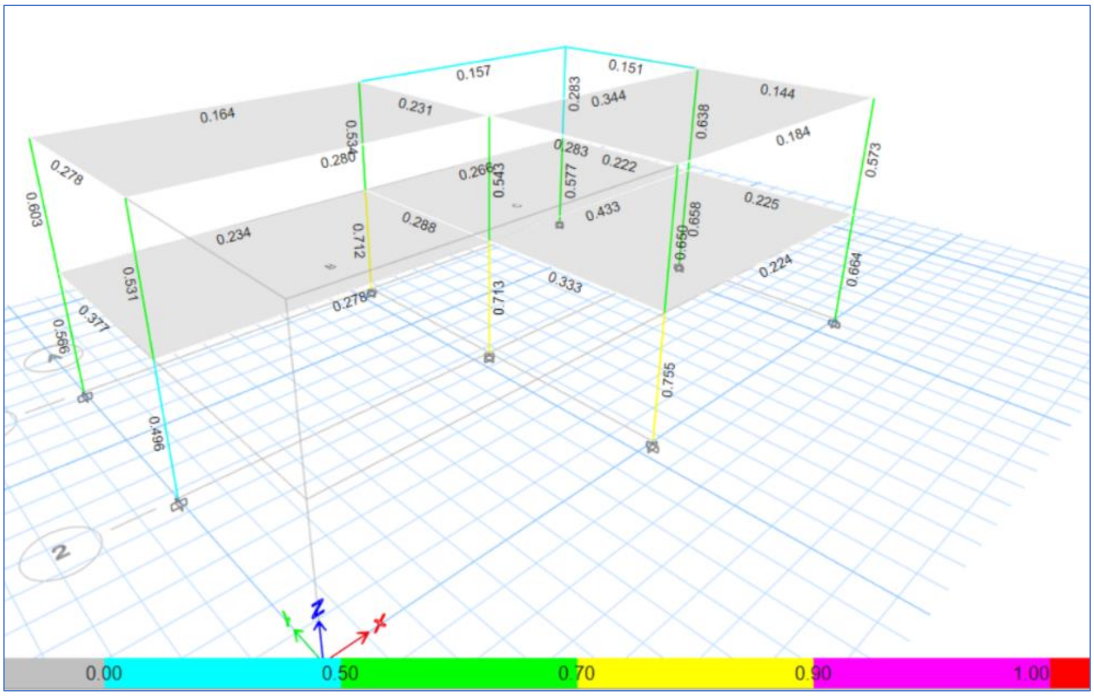


**Figure 15** Section efficiency P-M ration values for Structure 1.

# CHAPTER 4

# 4. CASE STUDY AND RESULTS

## 4.1 FREE VIBRATION ANALYSIS

If a structure is displaced by a certain amount and released suddenly, it starts vibrating under the effect of the first excitation without any additional action of external force. Free vibration analysis can be defined as the study of structural response when vibrating without external force effect. Free vibration analysis gives information about the natural periods, frequencies, and resonance of the structure for different mode shapes. Carryout Free Vibration Analysis using ETABS software for the two structures is done in this research. Since they are 3D structures, at each node there will be 3 components transactions about x, y, and rotation.

For Structure 1, with void and flexible roof slab diaphragm, the following table shows the periods, frequencies, and other values for each mode shape.

**Table 9** Modal Period and Frequencies by FVA of Structure 1.

| Case | Mode | Period | Frequency | CircFreq |
|---|---|---|---|---|
| | | sec | cyc/sec | rad/sec |
| **Modal** | 1 | 0.625 | 1.599 | 10.048 |
| **Modal** | 2 | 0.45 | 2.224 | 13.9713 |
| **Modal** | 3 | 0.389 | 2.57 | 16.146 |
| **Modal** | 4 | 0.243 | 4.124 | 25.9096 |

| | | | | |
|---|---|---|---|---|
| **Modal** | 5 | 0.169 | 5.92 | 37.1984 |
| **Modal** | 6 | 0.165 | 6.066 | 38.1116 |

For Structure 2, with no gap and rigid diaphragm, the following mode shapes are obtained:

**Table 10** Modal Period and Frequencies by FVA of Structure 2.

| **Case** | **Mode** | **Period** | **Frequency** | **CircFreq** |
|---|---|---|---|---|
| | | sec | cyc/sec | rad/sec |
| **Modal** | 1 | 0.744 | 1.345 | 8.4484 |
| **Modal** | 2 | 0.504 | 1.983 | 12.461 |
| **Modal** | 3 | 0.41 | 2.44 | 15.3329 |
| **Modal** | 4 | 0.259 | 3.856 | 24.2256 |
| **Modal** | 5 | 0.172 | 5.803 | 36.4602 |
| **Modal** | 6 | 0.132 | 7.586 | 47.6671 |

Joint displacements and drifts for the first mode shape are included in the next tables taking only the first mode shape into consideration.

**Table 11** Joint Displacements and Drifts Due to FVA for the First Mode Shape of Structure 1.

| **Story** | **Label** | **Name** | **Ux** mm | **Uy** mm | **Uz** mm | **Drift X** | **Drift Y** |
|---|---|---|---|---|---|---|---|
| **Story2** | 1 | 18 | 0.023 | -0.037 | 0.000402 | 0.000003 | 0.000006 |
| **Story2** | 2 | 20 | 0.022 | -0.09 | 0.000335 | 0.000003 | 0.000013 |
| **Story2** | 3 | 21 | 0.022 | -0.14 | 0.000162 | 0.000003 | 0.000019 |
| **Story2** | 4 | 19 | -0.01 | -0.037 | -0.00037 | 0.000002 | 0.000006 |
| **Story2** | 5 | 22 | -0.01 | -0.141 | 0.000124 | 0.000002 | 0.000019 |
| **Story2** | 6 | 23 | -0.042 | -0.141 | -0.00015 | 0.000005 | 0.000019 |
| **Story2** | 7 | 24 | -0.042 | -0.09 | -0.001 | 0.000005 | 0.000013 |
| **Story2** | 8 | 17 | -0.01 | -0.09 | 0.000131 | 0.000002 | 0.000013 |
| **Story1** | 1 | 2 | 0.014 | -0.02 | 0.000301 | 0.000005 | 0.000007 |

| | | | | | | | |
|---|---|---|---|---|---|---|---|
| **Story1** | 2 | 4 | 0.014 | -0.052 | 0.000267 | 0.000005 | 0.000017 |
| **Story1** | 3 | 6 | 0.014 | -0.084 | 0.000126 | 0.000005 | 0.000028 |
| **Story1** | 4 | 8 | -0.006 | -0.02 | -0.00028 | 0.000002 | 0.000007 |
| **Story1** | 5 | 10 | -0.006 | -0.084 | 8.88E-05 | 0.000002 | 0.000028 |
| **Story1** | 6 | 12 | -0.026 | -0.084 | -0.00012 | 0.000009 | 0.000028 |
| **Story1** | 7 | 14 | -0.026 | -0.052 | -0.001 | 0.000009 | 0.000017 |
| **Story1** | 8 | 16 | -0.006 | -0.052 | 9.39E-05 | 0.000002 | 0.000017 |

**Table 12** Joint Displacements and Drifts Due to FVA for the First Mode Shape of Structure 2.

| Story | Label | Name | **Ux** mm | **Uy** mm | **Uz** mm | Drift X | Drift Y |
|---|---|---|---|---|---|---|---|
| **Story2** | 1 | 18 | -0.024 | 0.026 | -0.0003162 | 0.000003 | 0.000004 |
| **Story2** | 2 | 20 | -0.024 | 0.075 | -0.0003319 | 0.000003 | 0.000011 |
| **Story2** | 3 | 21 | -0.024 | 0.123 | -0.0001348 | 0.000003 | 0.000018 |
| **Story2** | 4 | 19 | 0.006 | 0.026 | 0.0002659 | 0.000001 | 0.000004 |
| **Story2** | 5 | 22 | 0.006 | 0.123 | -6.176E-05 | 0.000001 | 0.000018 |
| **Story2** | 6 | 23 | 0.037 | 0.123 | 0.0001331 | 0.000005 | 0.000018 |
| **Story2** | 7 | 24 | 0.037 | 0.075 | 0.001 | 0.000005 | 0.000011 |
| **Story2** | 8 | 17 | 0.006 | 0.075 | -0.000107 | 0.000001 | 0.000011 |
| **Story1** | 1 | 2 | -0.014 | 0.013 | -0.0002339 | 0.000005 | 0.000004 |
| **Story1** | 2 | 4 | -0.014 | 0.041 | -0.0002528 | 0.000005 | 0.000014 |
| **Story1** | 3 | 6 | -0.014 | 0.068 | -0.000102 | 0.000005 | 0.000023 |
| **Story1** | 4 | 8 | 0.003 | 0.013 | 0.0001954 | 0.000001 | 0.000004 |
| **Story1** | 5 | 10 | 0.003 | 0.068 | -4.637E-05 | 0.000001 | 0.000023 |
| **Story1** | 6 | 12 | 0.021 | 0.068 | 0.0001014 | 0.000007 | 0.000023 |
| **Story1** | 7 | 14 | 0.021 | 0.041 | 0.0004533 | 0.000007 | 0.000014 |
| **Story1** | 8 | 16 | 0.003 | 0.041 | -7.917E-05 | 0.000001 | 0.000014 |

Comparing the increase or decrease in joint drift in structure 1 comparing to structure 2, the following table 13 shows that larger drift values are happening in structure 1 in both x and y directions, however, some of the joints showed no difference in drift in x direction between the two structures.

**Table 13** Drift Values Comparison Between Both Structures for x and y Directions

| Story | Label | Name | X-D | Y-D |
|---|---|---|---|---|
| Story2 | 1 | 18 | 0% | 50% |
| Story2 | 2 | 20 | 0% | 18% |
| Story2 | 3 | 21 | 0% | 6% |
| Story2 | 4 | 19 | 100% | 50% |
| Story2 | 5 | 22 | 100% | 6% |
| Story2 | 6 | 23 | 0% | 6% |
| Story2 | 7 | 24 | 0% | 18% |
| Story2 | 8 | 17 | 100% | 18% |
| Story1 | 1 | 2 | 0% | 75% |
| Story1 | 2 | 4 | 0% | 21% |
| Story1 | 3 | 6 | 0% | 22% |
| Story1 | 4 | 8 | 100% | 75% |
| Story1 | 5 | 10 | 100% | 22% |
| Story1 | 6 | 12 | 29% | 22% |
| Story1 | 7 | 14 | 29% | 21% |
| Story1 | **8** | **16** | 100% | 21% |

And the story drifts for the first six mode shapes are included in the next tables

**Table 14** Story Drift due to FVA for Structure 1.

| Story | Mode | Drift x | Drift y |
|---|---|---|---|
| Story2 | 1 | 0.000005 | 0.000019 |
| Story2 | 2 | 0.000019 | 0.000009 |
| Story2 | 3 | 0.000014 | 0.000027 |
| Story2 | 4 | 0.000027 | 0.00008 |
| Story2 | 5 | 0.000056 | 0.00000 |
| Story2 | 6 | 0.000068 | 0.00000 |
| Story1 | 1 | 0.000009 | 0.000028 |
| Story1 | 2 | 0.000022 | 0.00001 |

| | | | |
|---|---|---|---|
| **Story1** | 3 | 0.000019 | 0.000028 |
| **Story1** | 4 | 0.000012 | 0.000037 |
| **Story1** | 5 | 0.000024 | 0.000017 |
| **Story1** | 6 | 0.000031 | 0.000022 |

**Table 15** Story Drift due to FVA for Structure 2.

| Story | Mode | Drift x | Drift y |
|---|---|---|---|
| **Story2** | 1 | 0.000000 | 0.000018 |
| **Story2** | 2 | 0.000014 | 0.000000 |
| **Story2** | 3 | 0.000014 | 0.00003 |
| **Story2** | 4 | 0.000000 | 0.000065 |
| **Story2** | 5 | 0.000046 | 0.00000 |
| **Story2** | 6 | 0.000045 | 0.00009 |
| **Story1** | 1 | 0.000000 | 0.000023 |
| **Story1** | 2 | 0.000016 | 0.00000 |
| **Story1** | 3 | 0.000019 | 0.00003 |
| **Story1** | 4 | 0.000000 | 0.000041 |
| **Story1** | 5 | 0.00003 | 0.00000 |
| **Story1** | 6 | 0.000029 | 0.00006 |

## 4.2 EQUIVALENT LATERAL FORCES

Finding equivalent lateral force for Structure 1, the one with the void and flexible diaphragm, and locating the building in Istanbul – Turkey where the site soil class: ZC (Very tight layers of sand, gravel and hard clay or weathered, very cracked weak rocks). Using Turkish Hazard Map, The building's short periodic spectral response acceleration at 0.2 is Ss = 1.159, and its one-second periodic spectral response acceleration is S1 = 0.314. With response modification factor R = 4.5, and Importance factor I = 1. The calculated period of the first structure for the first mode shape T =

0.625 and the calculated period of the second structure of the first mode shape T = 0.744.

- Fa = 1.2 for soil classification of ZC and Ss > 0.75.
- Fv = 1.5 for soil classification of ZC and S1 < 0.6.

$$S_{DS} = 0.9272$$

$$S_{D1} = 0.314$$

Since $S_{DS} = 0.9272 \geq 0.5$ The seismic design category is: D ASCE7-16 Table 11.6-1

Since $S_{D1} = 0.314 \geq 0.2$ The seismic design category is: D ASCE7-16 Table 11.6-2

Where $S_{DS}$ and $S_{D1}$ are calculated according to equations 11.4-1, 11.4-2, 11.4-3, and 11.4-4 ASCE 7-16, and the same is applied to Fa and Fv values which are also taken according to ASCE 7-16.

Therefore, the structure needs to be analyzed according to seismic design category D, which is corresponding to buildings and structures in areas expected to experience severe and destructive ground shaking But NOT located close to a major fault.

Calculating Seismic Response Coefficient Cs for structure 1:

$$Cs = \frac{S_{DS}}{\frac{R}{I}} = 0.2060$$

$$Csmin = 0.044 S_{DS} * I = 0.0408$$

$$Csmax = \frac{S_{D1}}{T * \frac{R}{I}} = 0.1116$$

Therefore $Cs = 0.1116$

**Table 16** Effective Weight for Structure 1.

| Story Number | Effective mass Kg | Effective weight KN | Height m |
|---|---|---|---|
| **Story2** | 66845.09 | 655.53 | 6 |
| **Story1** | 97648.16 | 957.60 | 3 |
| **Total** | 164493.25 | 1613.13 | - |

Calculating Structure 1 Base Shear V

$$V = Cs * W = 0.1116 * 1613.13 = 180.025\ KN$$

Calculating vertical distribution of seismic forces:

$$Fx = Cvx * V \qquad \text{Where } Cvx = \frac{wx * Hx^k}{\sum wi * Hi^k}$$

And k is exponent related to structure period.

k = 1 for T < 0.5 k = 2 for T > 2.5

Interpolating for T = 0.625; K = 1.0625

**Table 17** Equivalent Lateral Force for Structure 1.

| Story | Height | Weight KN | Weight*Height | Cvx | Lateral force KN |
|---|---|---|---|---|---|
| **2** | 6 | 655.53 | 4399.246 | 0.58843 | 105.93 |
| **1** | 3 | 957.60 | 3076.986 | 0.41157 | 74.093 |
| **Base** | 0 | | | | 180.025 |

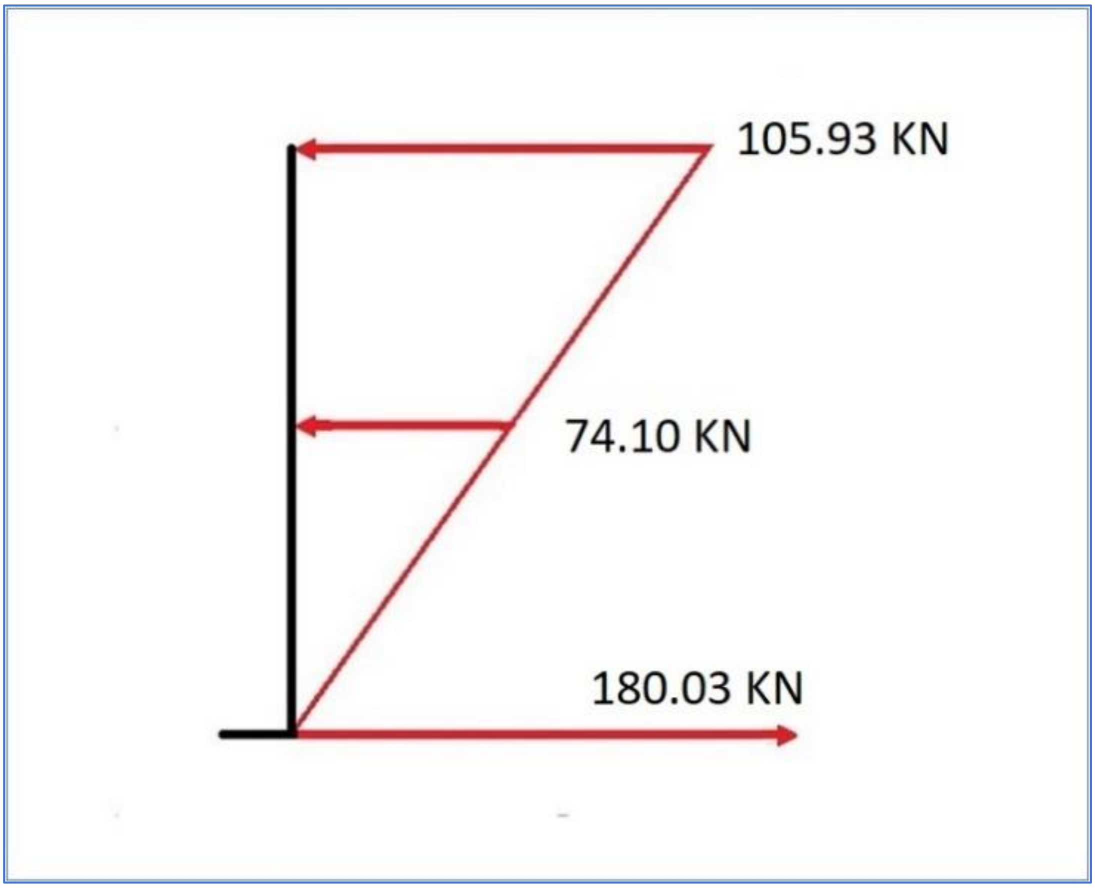


**Figure 16** Equivalent lateral forces for Structure 1

Calculating Seismic Response Coefficient Cs for Structure 2:

$$Cs = \frac{S_{DS}}{\frac{R}{I}} = 0.2060$$

$$Csmin = 0.044S_{DS} * I = 0.0408$$

$$Csmax = \frac{S_{D1}}{T * \frac{R}{I}} = 0.0938$$

Therefore $Cs = 0.0938$

**Table 18** Effective Weight for Structure 2.

| Story Number | Effective mass Kg | Effective weight KN | Height m |
|---|---|---|---|
| **Story2** | 96991.09 | 951.16 | 6 |
| **Story1** | 97648.16 | 957.60 | 3 |
| **Total** | 164493.25 | 1908.76 | - |

Calculating Structure 2 Base Shear V

$$V = Cs * W = 0.0938 * 1908.76 = 179.04\ KN$$

Calculating vertical distribution of seismic forces:

$Fx = Cvx * V$ Where $Cvx = \frac{wx * Hx^k}{\sum wi * Hi^k}$

And k is exponent related to structure period.

k=1 for T < 0.5 k=2 for T > 2.5

Interpolating for T = 0.744; K = 1.122

**Table 19** Equivalent Lateral Force for Structure 2.

| Story | Height | Weight KN | Weight*Height | Cvx | Lateral force KN |
|---|---|---|---|---|---|
| **2** | 6 | 951.16 | 7101.323 | 0.683729 | 122.4149 |
| **1** | 3 | 957.60 | 3284.84 | 0.316271 | 56.62512 |
| **Base** | 0 | | | | 179.040 |

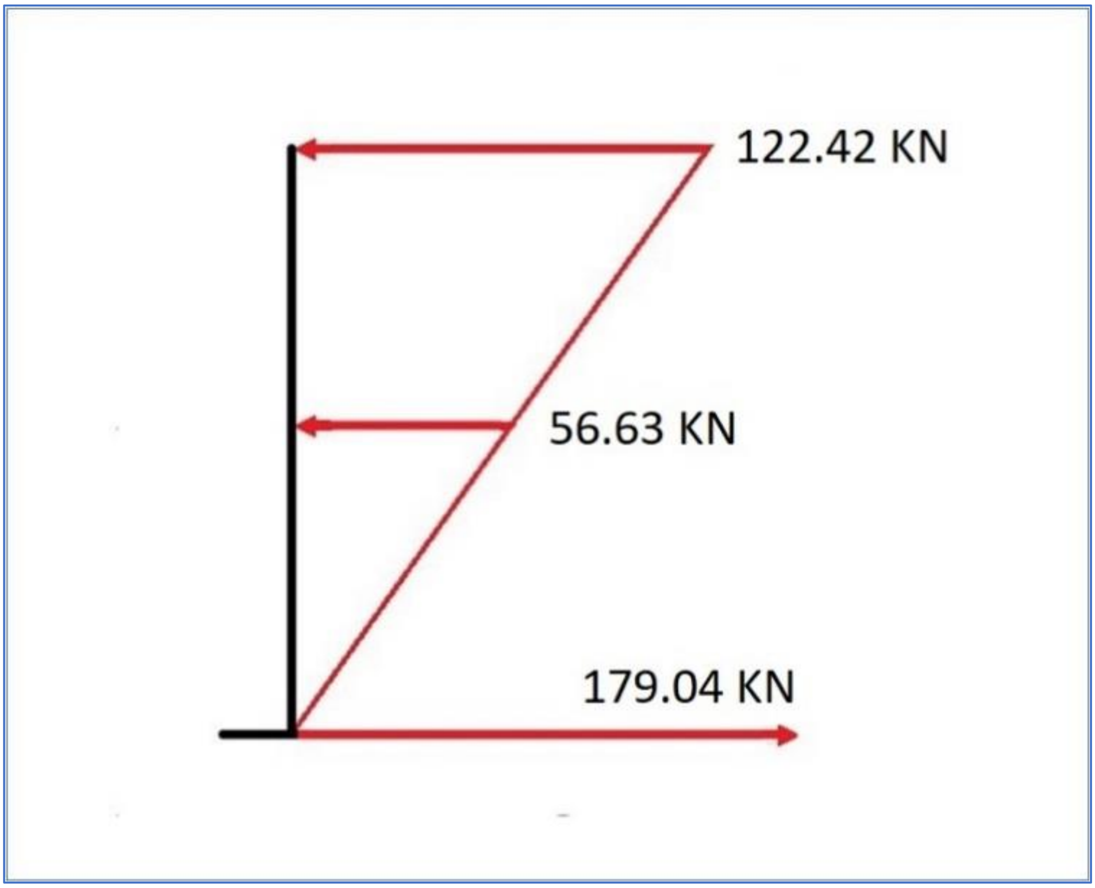


**Figure 17** Equivalent lateral forces for Structure 2.

### 4.3 TIME HISTORY ANALYSIS

Before applying time history analysis, different earthquakes shall be chosen, and in this study, 11 different records for 6 different earthquakes will be taken using PEER Ground Motion Database using NGA-West2 horizontal ground motion prediction equations (GMPEs) with 5% damped spectra of vertical ground motion where their velocity (Vs30) is between 300 and 700 m/s, their rupture distance (Rrup) is between 20 to 100 and their scale factor with the response spectrum is between 0.2 and 4.0 km, as following:

**Table 20** Chosen Earthquakes to be Used in THA.

| RSN | Earthquake Name | Scale Factor | Station Name | Year | Rrup (KM) | Vs30 (m/sec) | Earthquake Magnitude |
|---|---|---|---|---|---|---|---|
| **288** | Irpinia | 1.57 | Brienza | 1980 | 22.6 | 561.0 | 6.9 |
| **534** | N. Palm Springs | 2.16 | San Jacinto - Soboba | 1986 | 23.3 | 447.2 | 6.06 |
| **963** | Northridge-01 | 0.46 | Castaic | 1994 | 20.7 | 450.3 | 6.69 |
| **1006** | Northridge-01 | 0.91 | LA - UCLAG | 1994 | 22.5 | 398.4 | 6.69 |
| **1144** | Gulf of Aqaba | 2.09 | Eilat | 1995 | 44.1 | 354.9 | 7.2 |
| **1487** | Chi-Chi | 0.66 | TCU047 | 1999 | 35.0 | 520.4 | 7.62 |
| **1524** | Chi-Chi | 0.55 | TCU095 | 1999 | 45.2 | 446.6 | 7.62 |
| **4226** | Niigata | 1.24 | NIGH09 | 2004 | 22.7 | 462.9 | 6.63 |
| **4455** | Montenegro | 1.62 | Herceg Novi - O.S.D. | 1979 | 25.6 | 585.0 | 7.1 |
| **4889** | Chuetsu-oki | 1.25 | Joetsu Otemachi | 2007 | 32.9 | 314.6 | 6.8 |
| **6915** | Darfield | 0.71 | Heathcote Valley | 2010 | 24.5 | 422.0 | 7 |

Using $Sd_1$ and $Sd_s$ obtained in the equivalent lateral force section, the response spectrum is calculated and plotted where $Ta = 0.2\ Sd_1 / Sd_s = 0.067731$, and $Tb = Sd_1 / Sd_s = 0.338654$. The plot is shown in Figure 18. Then it is inserted in the ETABS model.

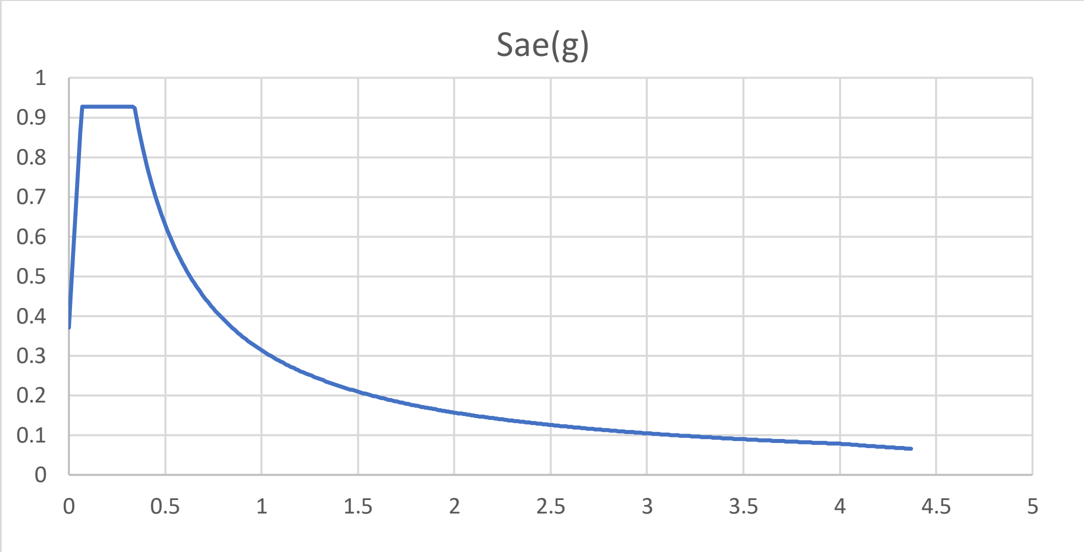


**Figure 18** Defined response spectrum used.

Using the Defined Response Spectrum, each earthquake record has been matched in its both direction using response spectrum matching with either time domain or frequency domain depending on the better matching of both cases. Where all the matched earthquakes had a scale factor between 0.2 and 4.0, and the average matched earthquake spectrum is higher than the design earthquake spectrum.

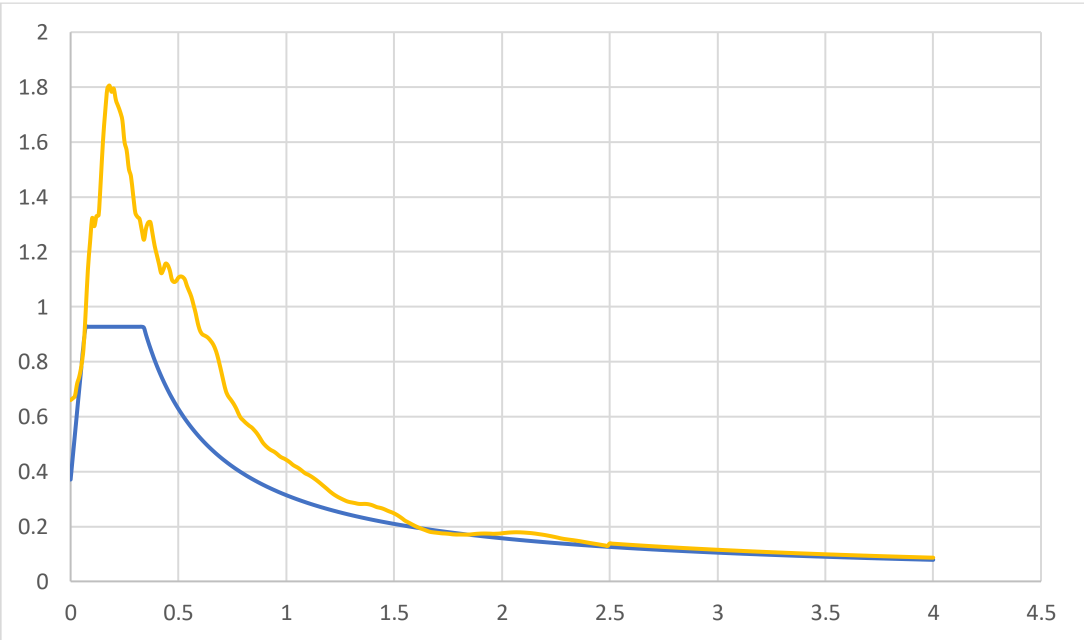


**Figure 19** Average and Design Response Spectrums.

After matching, Load cases have been created where two components of earthquake are inserted at each case acting at the same time to take into account the irregularity of the structure in its plane view, since only one component a time could not give accurate results for such structure. The analysis used in nonlinear direct integration with a scale factor of $9.81/R$, so $9.81/4.5 = 2.18$ The geometrical nonlinearity chosen is P-delta, with each of the time step is taken into consideration, and time integration parameters are from Hibler-Hughes-Tylor.

### 4.3.1 Results Obtained of Both Structures

The results obtained from structure 1 which is the structure with the void in the second-floor slab and flexible diaphragm, and the results obtained from structure 2 which is the one with no voids and with rigid diaphragms are written next starting form base shear, story displacements, story drifts, maximum actions in beams, maximum actions in columns, and finally torsion coefficient of the structures.

### 4.3.2 Base Shear Results

Maximum base shear in the x-direction happens with Gulf of Aqaba Earthquake record 1144 at an amount of 450.0 KN and the Maximum base shear of in y-direction happens also with Gulf of Aqaba Earthquake record 1144 at an amount of 260.7 KN. Table 21 shows the 6 most significant earthquake records regarding base reactions.

**Table 21** Base Reactions for Structure 1.

| Output Case | Step Type | FX | FY | MX | MY | MZ |
|---|---|---|---|---|---|---|
| | | kN | kN | kN-m | kN-m | kN-m |
| **Gulf 1144** | Max | 450.0 | 250.1 | 10225.0 | 12048.7 | 4372.7 |
| **Gulf 1144** | Min | 444.2 | 260.7 | 7732.7 | 16322.9 | 3894.5 |
| **Palm 534** | Max | 272.7 | 234.7 | 9972.1 | 13006.6 | 2391.6 |
| **Palm 534** | Min | 269.5 | 207.7 | 7865.9 | 15518.4 | 2940.7 |

| | | | | | | |
|---|---|---|---|---|---|---|
| **Montenegro 4455** | Max | 269.8 | 242.6 | 9973.1 | 12941.8 | 2631.5 |
| **Montenegro 4455** | Min | 227.2 | 200.9 | 7931.1 | 15321.0 | 2578.3 |
| **Chi-Chi 1524** | Max | 266.0 | 139.8 | 9631.8 | 13045.7 | 2237.9 |
| **Chi-Chi 1524** | Min | 272.5 | 138.3 | 8292.2 | 15491.2 | 2088.7 |
| **Oki 4889** | Max | 196.2 | 190.6 | 9737.1 | 13391.8 | 2488.0 |
| **Oki 4889** | Min | 206.8 | 170.4 | 8000.1 | 15159.3 | 2991.7 |
| **Northridge 964** | Max | 191.6 | 166.5 | 9520.8 | 13356.6 | 2095.2 |
| **Northridge 964** | Min | 238.5 | 119.3 | 8190.0 | 15297.9 | 2076.7 |

However, maximum base shear in the x-direction for Structure 2 happens with Montenegro Earthquake record 4455 at an amount of 353.9 KN and the Maximum base shear of in y-direction happens with Northridge Earthquake record 963 at an amount of 236.8 KN. Base actions obtained from structure 2 for the same 6 earthquakes are shown in Table 22.

**Table 22** Base Reactions for Structure 2.

| **Output Case** | **Step Type** | **FX** | **FY** | **MX** | **MY** | **MZ** |
|---|---|---|---|---|---|---|
| | | kN | kN | kN-m | kN-m | kN-m |
| **Gulf 1144** | Max | 298.1 | 97.1 | 11873.6 | 16365.9 | 2243.6 |
| **Gulf 1144** | Min | 249.9 | 138.6 | 10705.3 | 19097.9 | 2290.3 |
| **Palm 534** | Max | 289.4 | 154.4 | 11707.0 | 16380.7 | 2460.0 |
| **Palm 534** | Min | 265.5 | 99.0 | 10371.3 | 19150.6 | 2561.3 |
| **Montenegro 4455** | Max | 335.0 | 178.6 | 12281.5 | 16179.8 | 3570.2 |
| **Montenegro 4455** | Min | 353.9 | 210.9 | 10222.2 | 19584.4 | 3824.5 |
| **Chi-Chi 1524** | Max | 274.1 | 124.1 | 11811.1 | 16460.6 | 2353.7 |
| **Chi-Chi 1524** | Min | 302.5 | 114.4 | 10602.0 | 19277.6 | 1987.7 |
| **Oki 4889** | Max | 290.9 | 137.0 | 11779.7 | 16377.8 | 2536.7 |
| **Oki 4889** | Min | 285.0 | 112.5 | 10435.7 | 19304.3 | 2941.4 |
| **Northridge 964** | Max | 315.5 | 224.1 | 12317.7 | 16244.2 | 3518.0 |
| **Northridge 964** | Min | 306.8 | 236.8 | 10055.3 | 19380.9 | 3265.7 |

Comparing results from both structures, the increase and decrease in the base actions in structure 1 comparing to structure 2 is shown in Table 23, noting that minus sign indicates decrease and positive sign indicates increase. Comparing maximum cases in both directions for the two structures, shows that there is an increase in both direction in structure 1 comparing to structure 2 by 27% and 10% for x and y directions respectively. And from Table 23, it can be noticed that in most cases significant increase in base shear in y-direction is happening in structure 1 compared to structure 2, and that is not the case for x-direction, knowing that y-direction is along the longer side of the gap so the ratio of the gap could hurt the structural behavior overall.

**Table 23** Difference Increase and Decrease of Base Reaction in Structure 1 Compared to Structure 2.

| Output Case | Step Type | FX | FY | MX | MY |
|---|---|---|---|---|---|
| **Gulf 1144** | Max | 51% | 158% | -14% | -26% |
| **Gulf 1144** | Min | 78% | 88% | -28% | -15% |
| **Palm 534** | Max | -6% | 52% | -15% | -21% |
| **Palm 534** | Min | 2% | 110% | -24% | -19% |
| **Montenegro 4455** | Max | -19% | 36% | -19% | -20% |
| **Montenegro 4455** | Min | -36% | -5% | -22% | -22% |
| **Chi-Chi 1524** | Max | -3% | 13% | -18% | -21% |
| **Chi-Chi 1524** | Min | -10% | 21% | -22% | -20% |
| **Oki 4889** | Max | -33% | 39% | -17% | -18% |
| **Oki 4889** | Min | -27% | 51% | -23% | -21% |
| **Northridge 964** | Max | -39% | -26% | -23% | -18% |
| **Northridge 964** | Min | -22% | -50% | -19% | -21% |

Figures 20 and 21 show the base shear for Gulf of Aqaba earthquake record 1144 in both directions for structure 1, while Figures 22 and 23 show the base shear for Montenegro Earthquake record 4455 in x-direction and Northridge Earthquake record 963 in y-direction for structure 2.

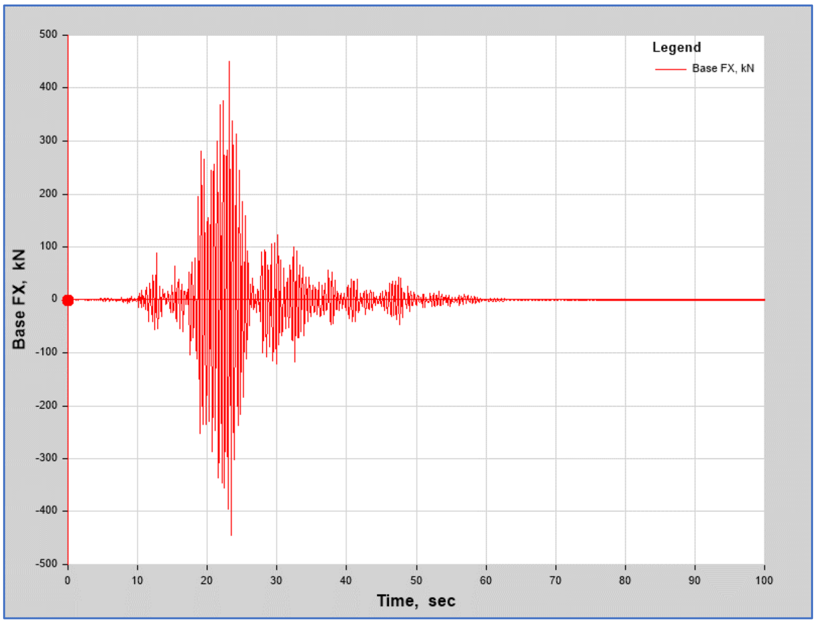


**Figure 20** Gulf of Aqaba Record 1144 Base Shear for Structure 1 in X-Direction.

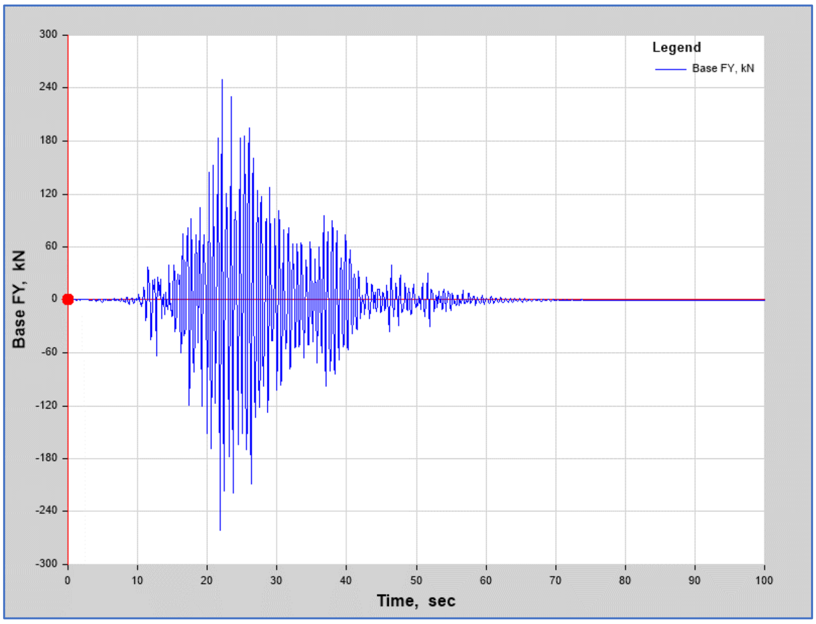


**Figure 21** Gulf of Aqaba Record 1144 Base Shear for Structure 1 in Y-Direction.

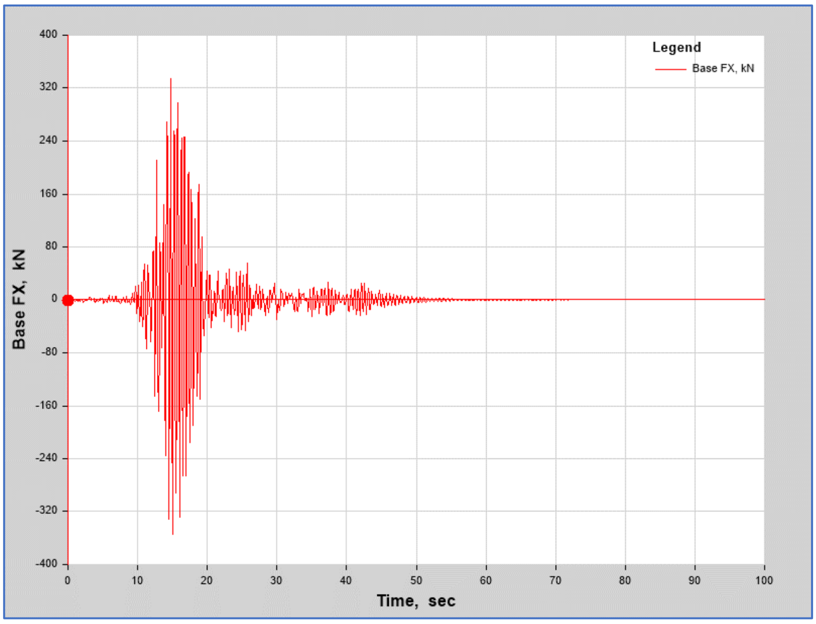


**Figure 22** Montenegro Earthquake record 4455 X-Direction Structure 2 Base shear.

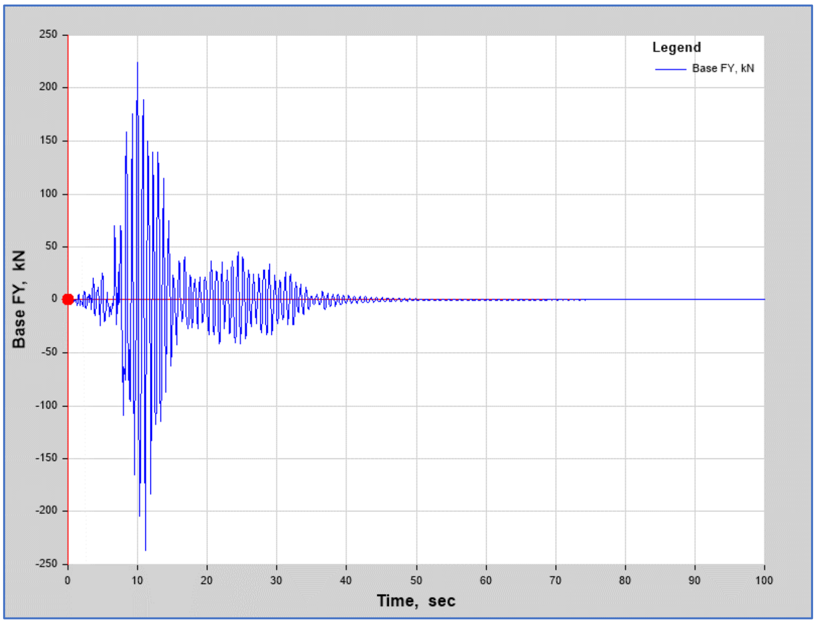


**Figure 23** Northridge Earthquake record 963 Y-Direction Structure 2 Base shear.

Therefore, the six major earthquakes are shown in Table 24. And the 2 structures will be compared according to the 11 earthquakes records mentioned earlier in Table 20.

**Table 24** Chosen six Earthquake for both directions x and y.

| RSN | Earthquake Name | Year | Station Name | Earthquake Magnitude |
|---|---|---|---|---|
| **1144** | Gulf of Aqaba | 1995 | Eilat | 7.2 |
| **534** | N. Palm Springs | 1986 | San Jacinto - Soboba | 6.06 |
| **4455** | Montenegro | 1979 | Herceg Novi - O.S.D. | 7.1 |
| **1524** | Chi-Chi | 1999 | TCU095 | 7.62 |
| **4889** | Chuetsu-oki | 2007 | Joetsu Otemachi | 6.8 |
| **963** | Northridge-01 | 1994 | Castaic | 6.69 |

### 4.3.3 Story Displacements

For structure 1, maximum story displacement in x-direction happens in Gulf of Aqaba earthquake record 1144 at an amount of 0.0209m. Figure 24 shows the maximum story displacement in this record for x direction.

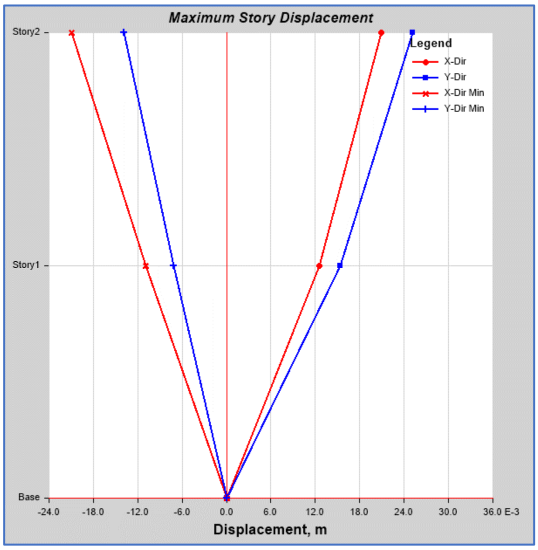


**Figure 24** Maximum Story Displacement of Structure 1 in X-Direction.

And for the same structure, maximum story displacement in y-direction happens in Darfield Earthquake record 6915 at an amount of 0.029m. Figure 25 shows the maximum story displacement in this record.


**Figure 25** Maximum Story Displacement of Structure 1 in Y-Direction.

For structure 2, maximum story displacement in x-direction happens in Montenegro Earthquake record 4455 at an amount of 0.0178. Figure 26 shows the maximum story displacement in this record.

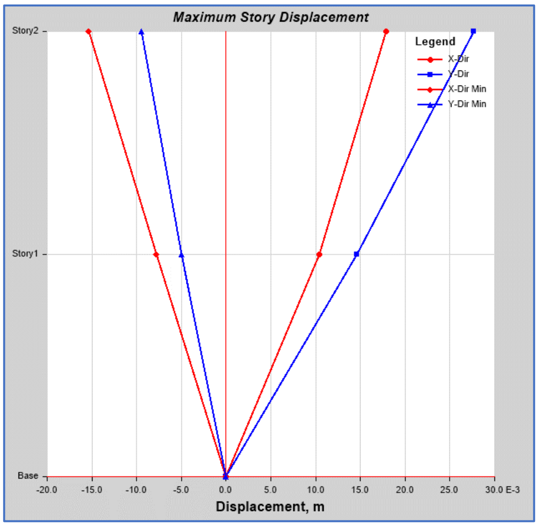


**Figure 26** Maximum Story Displacement of Structure 2 in X-Direction.

And for the same structure, maximum story displacement in y-direction happens in Northridge-01 Earthquake record 963 at an amount of 0.0276. Figure 27 shows the maximum story displacement in this record.

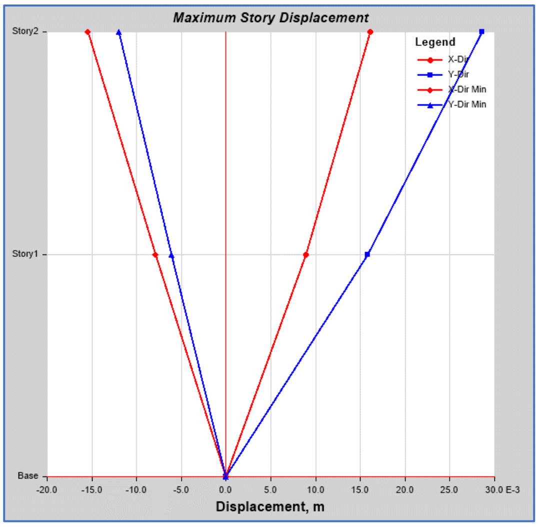


**Figure 27** Maximum Story Displacement of Structure 2 in Y-Direction

Comparing maximum cases for both structures show that there is 17% increase of story displacement in Structure 1 along x-direction, and 5% increase of story displacement in Structure 1 along y-direction. This increase could be due to the existence of gap in the second story slab and its diaphragm flexibility.

### 4.3.4 Story Drift

For structure 1, x-direction maximum story drift happens in first story at Gulf of Aqaba earthquake record 1144 at an amount of 0.00464, and y-direction maximum story drift happens in Darfield Earthquake record 6915 at an amount of 0.00574. Figures 28 and 29 show the maximum drift in structure 1 for both directions.

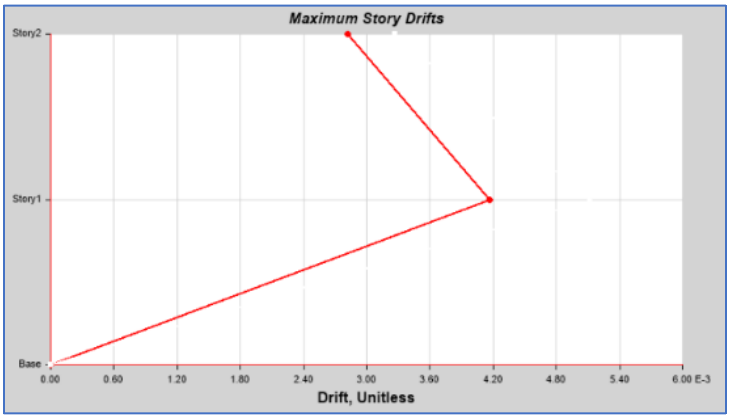


**Figure 28** Structure 1 Maximum Drift in x-direction.

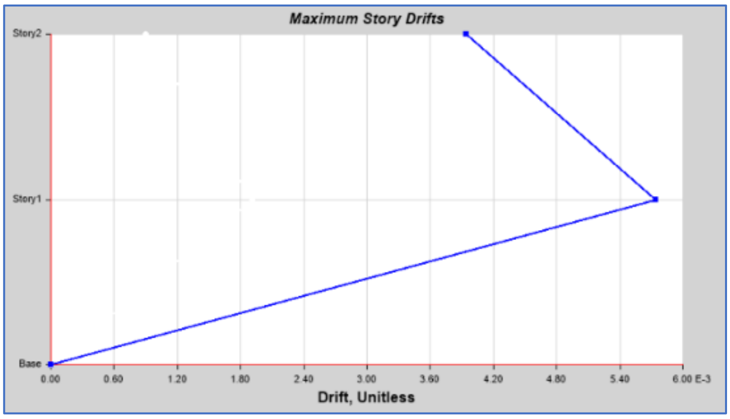


**Figure 29** Structure 1 Maximum Drift in x-direction.

In structure 2, for x direction, maximum story drift happens in the first story in Northridge-01 Earthquake record 963 at an amount of 0.0043. Also, for y direction, maximum story drift happens in the same earthquake at an amount of 0.0054. Figure 30 shows the maximum drift in structure 2 for both x and y directions.

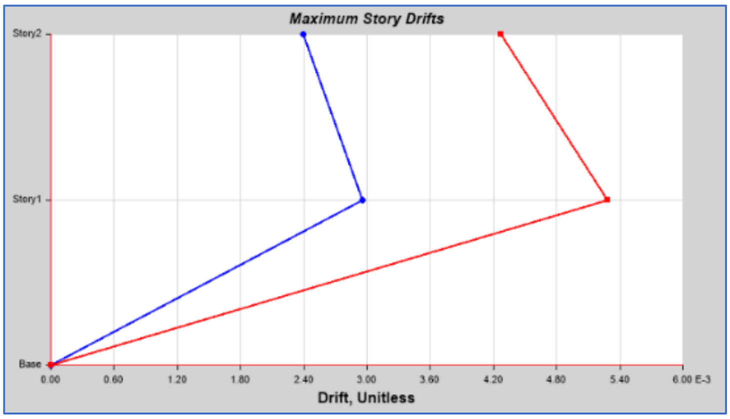


**Figure 30** Structure 2 Maximum Drift in x and y directions.

Comparing maximum cases for both structures show that there is 8% increase of story drift in Structure 1 along x-direction, and 6% increase of story drift in Structure 1 along y-direction. Which is a slight and not significant increase.

Comparing story drift for the second story for both structures for the rest earthquakes for x and y directions are shown in Tables 25 and 26.

**Table 25** Story Drift of Both Cases. Increase or Decrease Percentage in Structure 1 Compared to Structure 2 in x-direction.

| Output Case | Direction | Structure 1 Drift | Structure 2 Drift | Increase or decrease |
|---|---|---|---|---|
| **Gulf 1144** | Max | 0.002817 | 0.001801 | 56% |
| **Gulf 1144** | Min | 0.004146 | 0.002542 | 63% |
| **Palm 534** | Max | 0.002192 | 0.001513 | 45% |
| **Palm 534** | Min | 0.003392 | 0.002467 | 37% |
| **Montenegro 4455** | Max | 0.001589 | 0.002566 | -38% |
| **Montenegro 4455** | Min | 0.003491 | 0.003591 | -3% |
| **Chi-Chi 1524** | Max | 0.001557 | 0.001517 | 3% |
| **Chi-Chi 1524** | Min | 0.002956 | 0.002687 | 10% |
| **Oki 4889** | Max | 0.001616 | 0.002453 | -34% |
| **Oki 4889** | Min | 0.002761 | 0.003362 | -18% |
| **Northridge 963** | Max | 0.000934 | 0.002398 | -61% |
| **Northridge 963** | Min | 0.002489 | 0.003706 | -33% |

**Table 26** Story Drift of Both Cases. Increase or Decrease Percentage in Structure 1 Compared to Structure 2 in y-direction.

| Output Case | Direction | Structure 1 Drift | Structure 2 Drift | Increase or decrease |
|---|---|---|---|---|
| **Gulf 1144** | Max | 0.003264 | 0.003396 | -4% |
| **Gulf 1144** | Min | 0.004019 | 0.00281 | 43% |
| **Palm 534** | Max | 0.00369 | 0.002509 | 47% |
| **Palm 534** | Min | 0.004391 | 0.00304 | 44% |
| **Montenegro 4455** | Max | 0.003236 | 0.004505 | -28% |
| **Montenegro 4455** | Min | 0.003413 | 0.004575 | -25% |
| **Chi-Chi 1524** | Max | 0.002066 | 0.002415 | -14% |
| **Chi-Chi 1524** | Min | 0.002317 | 0.003365 | -31% |
| **Oki 4889** | Max | 0.002992 | 0.002772 | 8% |
| **Oki 4889** | Min | 0.003262 | 0.003629 | -10% |

| | | | | |
|---|---|---|---|---|
| **Northridge 963** | Max | 0.002145 | 0.004269 | -50% |
| **Northridge 963** | Min | 0.002816 | 0.003839 | -27% |

The previous table shows that although the maximum cases of both structures tend to be more in Structure 1 with slight differences, however, the overall performance is diverse in the other earthquakes varying from earthquake to earthquake along both x and y directions.

### 4.3.5 Actions in Beams

Regarding beams, the actions in focus will be V2 and M3 which are the primary actions.

**Table 27** Maximum Beam Actions in Structure 1

| Action | Case | Earthquake | Beam | Amount | Unit |
|---|---|---|---|---|---|
| **V2** | Maximum | 1144 | B7 -33 | 74.41 | KN |
| **V2** | Minimum | 1144 | B4 -32 | 99.92 | KN |
| **M3** | Maximum | 1144 | B7 -33 | 75.42 | KN-m |
| **M3** | Minimum | 1144 | B4 -32 | 162.38 | KN-m |

For structure 1, the most critical beam regarding moment is beam B4-32 followed by beam B7 – 33. The former, is located at the middle of the structure where one of its ends is located at the center of the structure at the re-entrant corner, and the latter is located at the far edge of the structure in the longitudinal direction with 8m spans for both. Both are shown in figure 31. The same is applied for shear where the maximum shear happens in beam B4-32 for both cases. And Figure 32 shows the shear and moment diagrams of the maximum case of beam B4-32 in structure 1 since it is the most critical beam for both moment and shear forces. Where it can be noticed that the end with higher shear and moment forces is the re-entrant corner joint which is the logical thing to happen since it is located at a critical point.

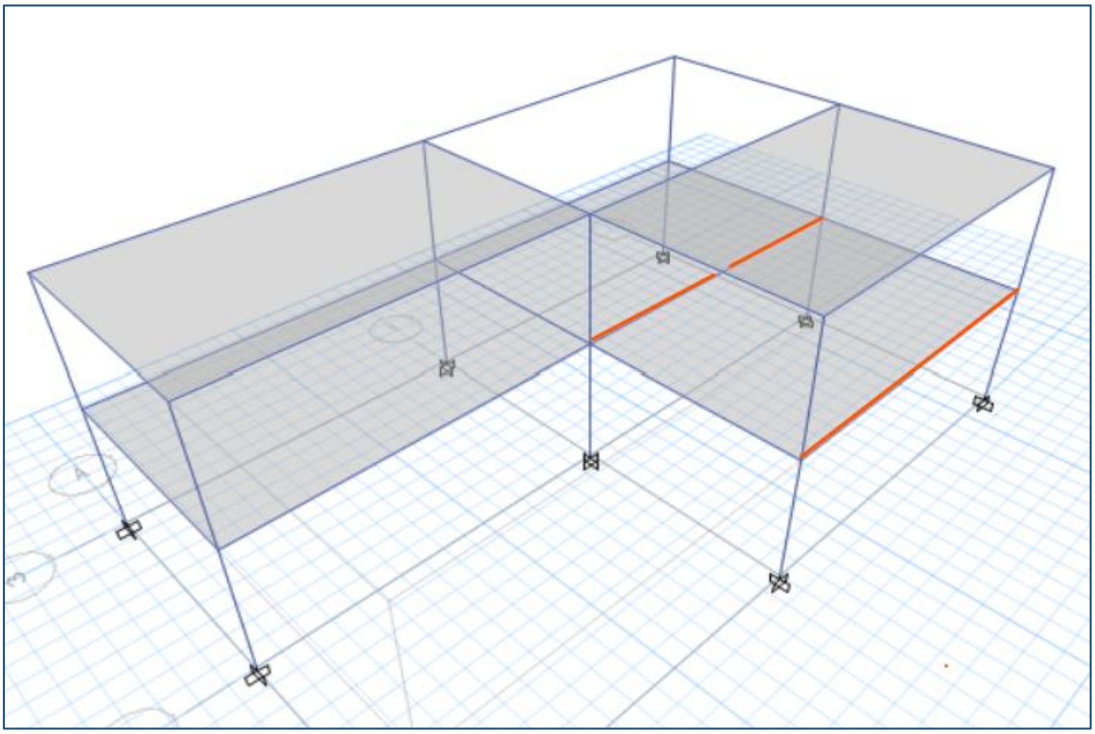

**Figure 31** Beams B4-32 and B7-33 in Structure 1 marked with orange color.

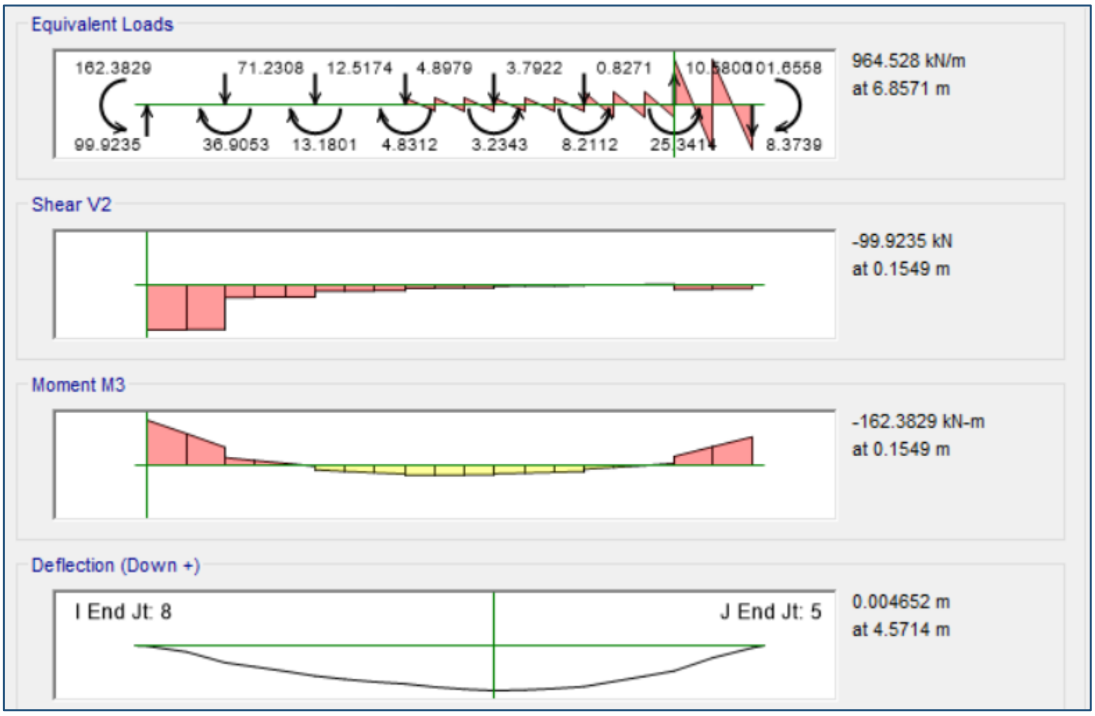


**Figure 32** Equivalent loads, shear V2, moment M3, and deflection of beam B4-32 in Structure 1.

In structure 2, Maximum shear and moment actions happen also in beam B4-32, followed by beams B5-31 B7-33 which are parallel to each other's.

**Table 28** Maximum Beam Actions in Structure 2

| Action | Case | Earthquake | Beam | Amount | Unit |
|---|---|---|---|---|---|
| **V2** | Maximum | 4455 | B7 - 33 | 66.89 | KN |
| **V2** | Minimum | 4226 | B4 - 32 | 87.05 | KN |
| **M3** | Maximum | 4455 | B5 - 31 | 71.75 | KN-m |
| **M3** | Minimum | 4226 | B4 - 32 | 138.87 | KN-m |

Figure 33 shows the location of both beams. And Figure 33 shows the shear and moment diagrams of the maximum case of beam B4-32 in structure 2 since it is the most critical beam for both moment and shear forces.

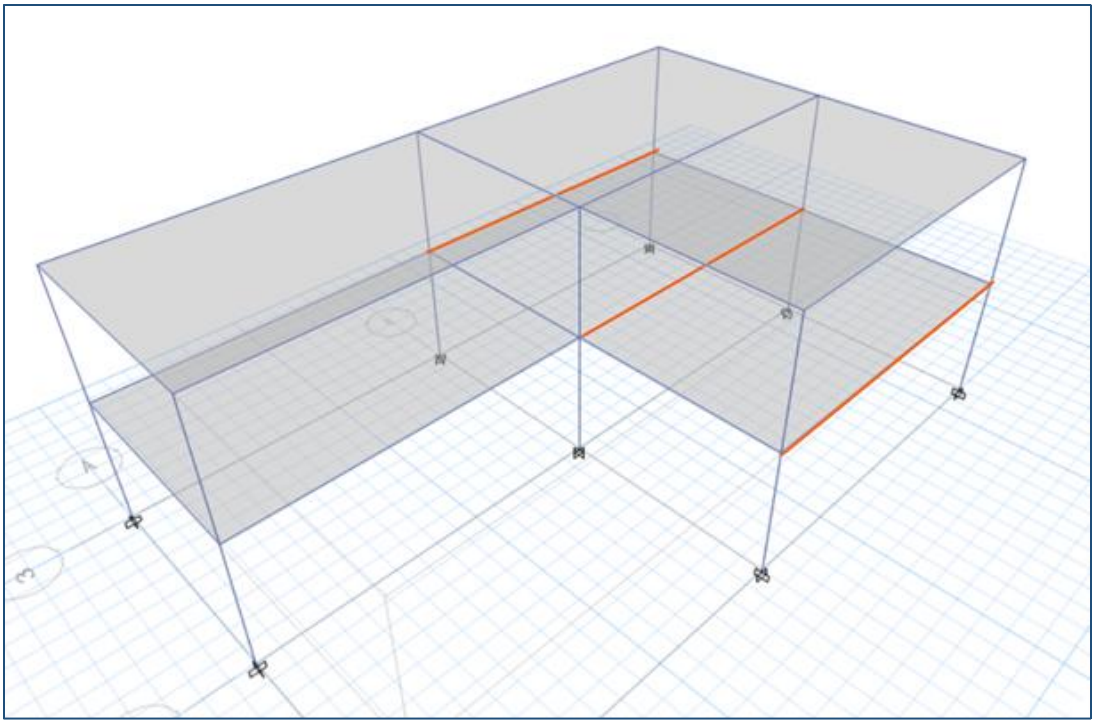

**Figure 33** Beams B4-32 and B5-31 in Structure 2 marked with orange color.

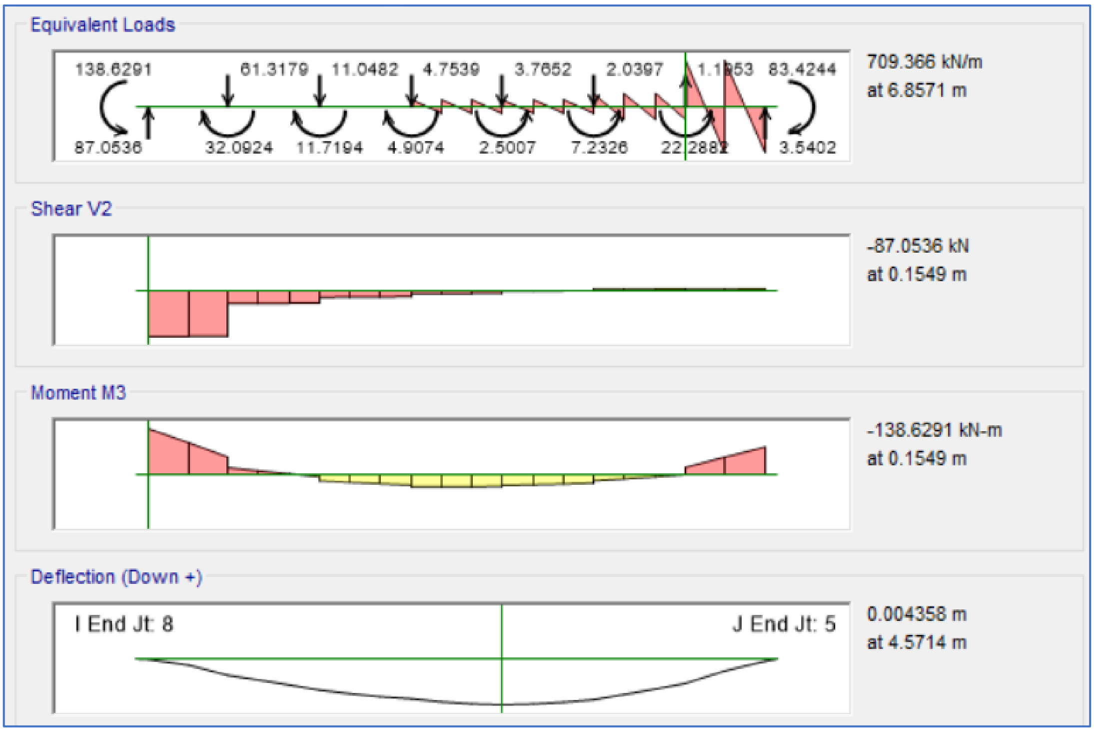


**Figure 34** Equivalent loads, shear V2, moment M3, and deflection of beam B4-32 in Structure 2.

Comparing the two cases together, beam B4-32 is compared regarding shear and moment by the maximum case of both structures as shown in Table 29.

**Table 29** Comparison of Beam B4-32 Actions for Both Cases.

| Action | Structure 1 | Structure 2 | Unit | Dif. Percentage |
|---|---|---|---|---|
| **M3** | 162.38 | 138.87 | KN-m | 17% |
| **V2** | 99.92 | 87.05 | KN | 15% |
| **Deflection** | 0.004652 | 0.004358 | m | 07% |

Comparing two cases together, increasing in both M3 and V2 is noticed in Structure 1. However, the increasing is not significant and that is because the lateral loads usually effect vertical elements like columns more than horizontal elements like diaphragms and beams.

### 4.3.6 Actions in Columns

Regarding Columns, the actions in focus will be V2 and M3, which are the primary actions, in addition, V3, and M2 will be taken into consideration.

**Table 30** Void Structure 1 Maximum V2, M3, V3, M2 Actions.

| Action | Case | Earthquake | Column | Amount | Unit |
|---|---|---|---|---|---|
| **V2** | Maximum | Gulf 1144 | C8 – 8 | 94.37 | KN |
| **V2** | Minimum | Gulf 1144 | C8 – 8 | 130.76 | KN |
| **V3** | Maximum | Gulf 1144 | C8 – 8 | 33.25 | KN |
| **V3** | Minimum | Gulf 1144 | C8 – 8 | 37.07 | KN |
| **M3** | Maximum | Gulf 1144 | C8 – 8 | 165.68 | KN-m |
| **M3** | Minimum | Gulf 1144 | C8 – 8 | 215.58 | KN-m |
| **M2** | Maximum | Gulf 1144 | C8 – 8 | 56.53 | KN-m |
| **M2** | Minimum | Gulf 1144 | C8 – 8 | 58.15 | KN-m |

It can be noticed from Table 30, that for structure 1, most critical column regarding V2, M3, V3, and M2 is column C8–8, which is located at the first floor at the re-entrant corner of the structure. Figure 35 shows the location of column C8–8, where it is marked with orange color.

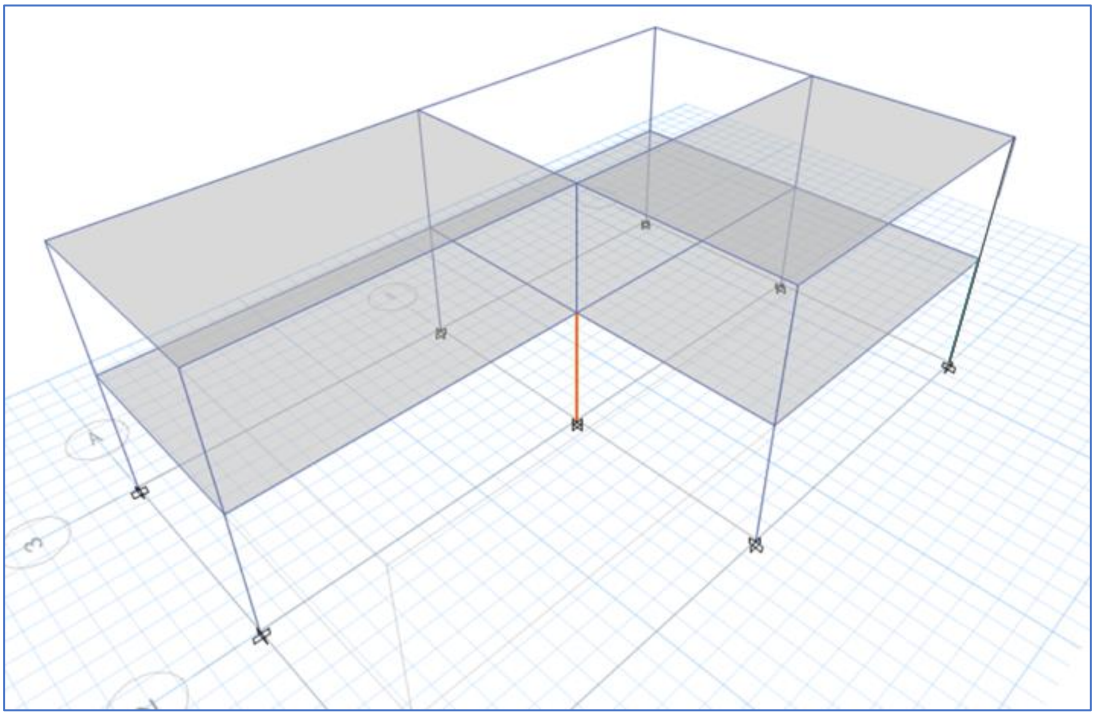

**Figure 35** Columns C8-8 shown with orange color in Structure 1.

Figure 36 shows the shear and moment diagrams of the maximum case of column C8–8 in structure 1 since it is the most critical column for both moment and shear forces.

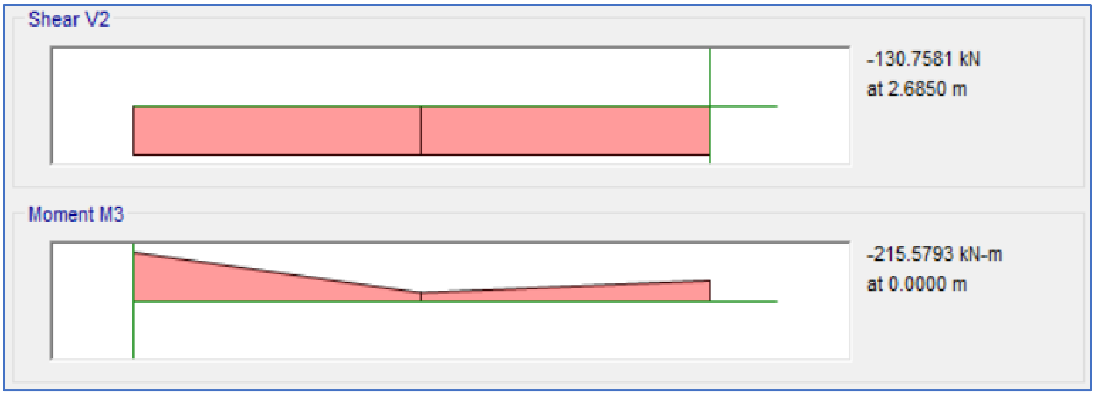


**Figure 36** Shear V2, and moment M3 at column C8 – 8 in Structure 1.

Regarding Structure 2, Table 31shows that most critical actions V3, M3, V2, and M2 happen in column C8–8 which is located at the first floor at the re-entrant corner of the structure, followed by column C6–6. Where the location of both columns is shown in figure 37.

**Table 31** No Void Structure 2 Maximum V2, M3, V3, M2 Actions.

| Action | Case | Earthquake | Column | Amount | Unit |
|---|---|---|---|---|---|
| **V2** | Maximum | 4455 | C6 – 6 | 79.72 | KN |
| **V2** | Minimum | 6915 | C8 – 8 | 95.44 | KN |
| **V3** | Maximum | 1487 | C8 – 8 | 30.41 | KN |
| **V3** | Minimum | 963 | C8 – 8 | 34.76 | KN |
| **M3** | Maximum | 4455 | C8 – 8 | 139.43 | KN-m |
| **M3** | Minimum | 6915 | C8 – 8 | 157.61 | KN-m |
| **M2** | Maximum | 1487 | C8 – 8 | 51.95 | KN-m |
| **M2** | Minimum | 963 | C8 – 8 | 55.19 | KN-m |

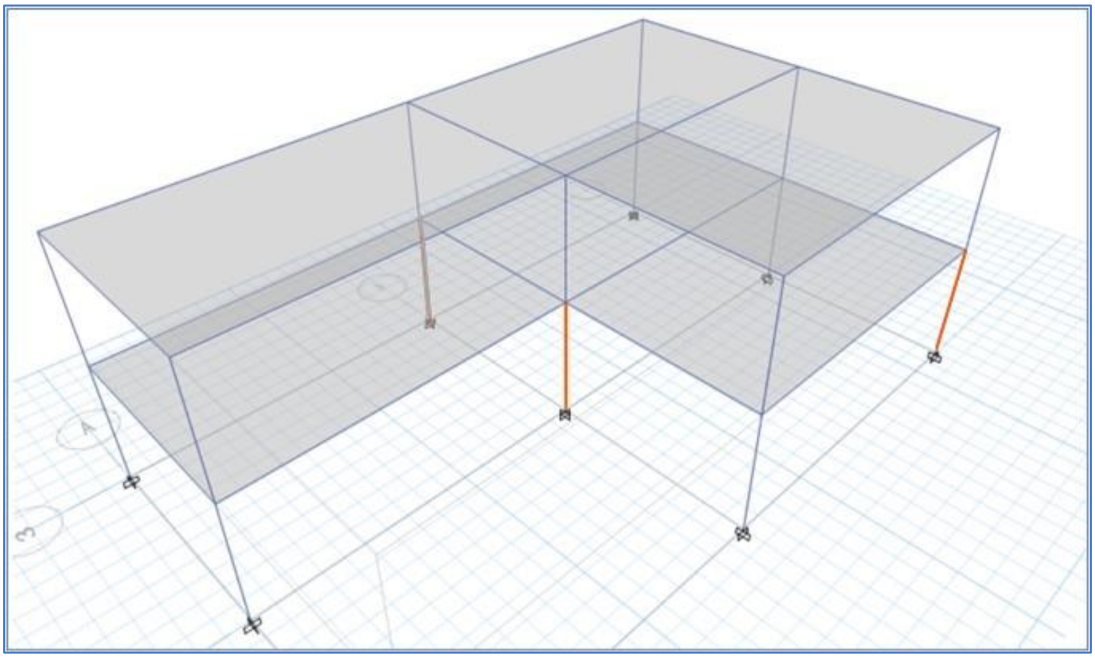

**Figure 37** Columns C8-8 and C6-6 are shown with orange color in Structure 2.

Figure 38 shows the shear and moment diagrams of the maximum case of column C8–8 in structure 2 since it is the most critical column for both moment and shear forces.

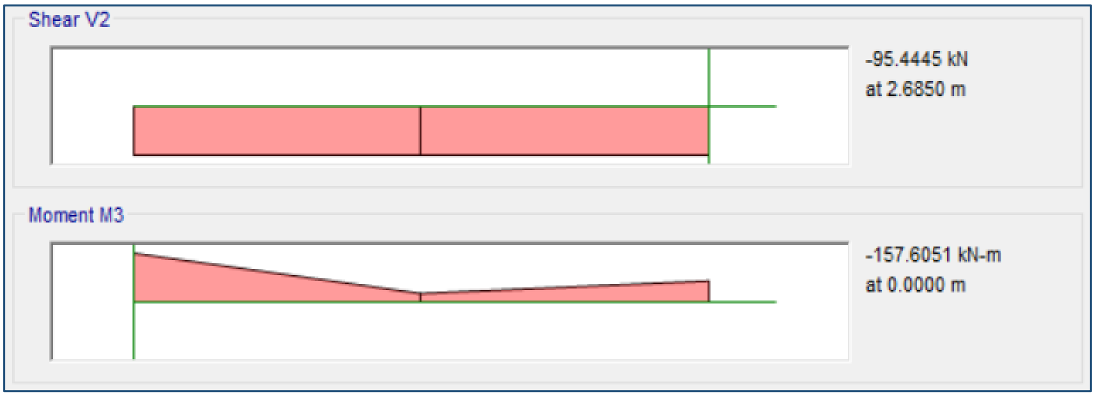


**Figure 38** Shear V2, and moment M3 at column C8 – 8 in Structure 2.

Comparison between both structures for column C8–8 is shown in Table 39 regarding actions on the column.

**Table 32** Comparison of Beam B4-32 Actions for Both Cases.

| Action | Structure 1 | Structure 2 | Unit | Dif. Percentage |
|---|---|---|---|---|
| **M3** | 215.00 | 157.61 | KN-m | 36% |
| **V2** | 130.76 | 95.44 | KN | 37% |
| **M2** | 58.15 | 55.19 | KN-m | 05% |
| **V3** | 37.07 | 34.76 | KN | 07% |

It can be noticed that both primary actions M3 and V2 are significantly increased in structure 1. However, secondary actions are similar in both structure with no significant differences.

# CHAPTER 5

# 5. DISCUSSION

After performing the analysis and obtaining the results, it is found that regarding free vibration analysis, Structure 1 showed smaller periods and higher natural frequencies for the first mode shape and other mode shapes when compared to Structure 2, and that is normal and logical thing to happen since structure 1 has less mass in the second story. For the first mode shape, joint displacements are much higher in both x and y directions in structure 1, even though the mass is larger in structure 2, this could be due to the void existence is structure 1 in its second floor, that encouraged the drift to be higher up to 100% at some points in x-direction, and an average of 28% increase in joint drift in y-direction, knowing that x-direction is the long direction of the structure, where its length in that direction is 16m divided in two spans, and y-direction is the short direction where the structure length is 10m divided also in two spans. Also, taking the drift for the structure as a whole, drift for the first mode shape is higher in both directions in structure 1, but for higher mode shapes drift starts to be different case because both structures undergo different mode shapes due to the irregularity in mass distribution is structure 1.

Calculating the Equivalent lateral forces for both structures, both showed almost identical base shear force, however, the distribution of the forces along the stories is different. For the second floor, in structure 1 second floor took less amount of shear force than in structure 2, and that due to 2 reasons, one of which is that structure 2 has stiffer second floor allowing it to take larger portion of the lateral force unlike structure 1, the other reason is that second floor in structure 2 has more mass to it causing larger forces acting on it. For first floor, first floor in structure 1 has larger portion of the force even larger than that on structure 2, and that is as stated above that the second floor is structure 1 has less stiffness forcing the first floor to take larger bite of the lateral forces.

Finally, regarding time history analysis, which is the main analysis in this study; Although Structure 2 has more weight to it, maximum base shear forces are higher in Structure 1 27% and 10% for x and y direction respectively, and that is a direct result to the existence of the void and the flexibility of the diaphragm in structure 1. However, when comparing other earthquakes, other than the maximum cases of each structure, it shows divergence in the results and variation between the two structures from earthquake to another in both directions, and that could be due to the earthquake frequencies which can be more similar to the natural frequency of the certain structure when compared to the natural frequency of the other structure, this is also noticed in some of the weaker earthquakes from the 11 records studied, the weaker the earthquake, the larger base shear forces become in structure 2 when compared to structure 1. On the other hand, moments on base reactions are more in structure 2 in all of the cases and this is logical thing to happen since structure 2 has more mass in its second story acting as a mass source for the moment $M = F.d$ where $F$ is the earthquake lateral force, and the structure elevation acting as the force arm $d$.

Results obtained for story displacements showed that structure 1 undergoes larger story displacements in both x and y directions, with the difference being more observable in x-direction (17%) compared to 5% in y-direction, and these results are with taking into consideration all the 11 earthquake records, which means that the existence of the flexible diaphragms and voids increase the story displacements specially in the stronger axis of the building has direct relationship with the increasing in story displacements in irregular structures. Same goes for story drift, where when comparing story drifts of both structures, story drifts in structure 1 are higher in most cases in x-axis with very large difference in some cases. So when comparing maximum cases of both structures, it shows 8% and 6% increase in story drift in Structure 1 for x and y respectively.

Regarding the internal forces in the beams, the study showed that maximum actions happen in both structures in the exact same beam, which is beam B4-32, and that due to the combination of its location and its long span, where one of its ends is located at the re-entrant corner. Study showed that the beam of interest showed larger internal shear and internal moment in structure 1, showing that the void existence and the flexibility of the diaphragm in structure 1 affect the behavior of the irregular structure under the effect of seismic loads showing noticeable increase in both main internal actions in addition to the deflection in the critical beam sections. Comparing the results obtained from both structures for the most critical beam B4-32; results showed that structure 1 had an increase of in primary actions as much as 17% and 15% for M3 and V2 respectively, and deflection is also increased by 7%.

Studying the internal forces in columns, results showed that maximum actions happen in both structures in the exact same column, which is column C8-8, and that due to the combination of its location which is at the re-entrant corner and due to the gravitational load on it since it has the largest portion of the gravitational loads in the structure. Comparing the results obtained from both structures for the most critical column C8-8; results showed that structure 1 had an increase of around 37% in primary actions which is much more significant difference than those found in beams, this shows columns are more affected than beams by the void existence and type of diaphragm in irregular structures regarding the seismic performance. Also, it shows that this void existence and diaphragm flexibility are highly affect the seismic performance of the irregular structures specially in columns.

# CHAPTER 6

# 6. CONCLUSION

Two irregular steel structures one with a void and flexibility in its diaphragm in the second story, and the other structure with rigid diaphragms, and no existence of voids in its diaphragms, both have been analyzed using nonlinear time history analysis, free vibration analysis, and equivalent lateral force to study their performance under seismic loads when a void is introduced making the diaphragm a flexible diaphragm. And it is found that the existence of void and flexibility of the diaphragm affect the structural behavior of irregular structures, and these affects are stated as follows:

1- The period and natural frequency of the structures can be affected by the existence of voids in the diaphragms since it changes the variation and the amount of mass along the structure.
2- Irregular structures with voids could suffer larger joint displacements and drifts specially in the strong axis of the irregular building.
3- Base shear showed to be higher in the irregular structures with voids despite the reduction of structural mass. On the other hand, base moments are higher with the structure with no voids since it has a direct relation with the mass of the structure, especially in higher altitudes.
4- Internal forces in the beams are higher in the structure with the void, increasing the primary action in the critical beams at the re-entrant corner the increase in internal actions is 17%, 15%, & 7%, for moment, shear, and deflection, respectively.

5- Internal actions in columns are significantly increased in the structure with the void are primary moment and shear increased up to 37% in most critical column at the re-entrant corners.

So overall, as the study showed, that irregular structures can be highly influenced and dramatically change its behavior when the existence of voids in the diaphragms, and when the diaphragms act as flexible diaphragm rather than rigid diaphragms.

Therefore, when designing and constructing of such irregular structures, it is highly recommended not to include large voids in the slabs of the structures, or to take large concern and attention to the design in case of void existence specially in earthquake areas. Furthermore, re-entrant corners should be the place of interest when the structure is designed. Further studies can be done in this subject, taking the void/slab ratio and its effect of irregular structures, also other irregular structural plans could be studied to see wither this effect only L shaped irregular structures or structures in general.

# REFERENCES


Varadharajan, S., Sehgal, V. K., & Saini, B. (2012). Seismic response of multistory reinforced concrete frame with vertical mass and stiffness irregularities. *The Structural Design of Tall and Special Buildings*, *23*(5), 362–389.

Giordano, A., Guadagnuolo, M. & Faella, G. (2008). Pushover analysis of plan irregular masonry buildings. *14th World conference on earthquake engineering, Beijing, China.*

Darshan, D. & Shruthi, H.K. (2016). Study on mass irregularity of high-rise buildings. *International Research Journal of Engineering and Technology*, 3(8), pp.1123-1130.

Hasnat, A. & Rahim, M.R.I. (2013). Response of building frames with vertical and stiffness irregularity due to lateral loads. *International Journal of Engineering Research & Technology*, 2(12).

Tremblay, R. (2005). Structural irregularities: proposed changes and Additions to National Building Code of Canada. *Ecole Polytechnique* personal materials.

Sachin Maske, G., & Pajgade, P. S. (2013). Torsional behaviour of asymmetrical buildings. *Int J Modern Eng Res*, 3(2), 1146-9.

Khan, M. A. (2013). Seismic design for buildings. *Earthquake-Resistant Structures*, 283-315.

Whitman, R. V. (2003). Earthquake Engineering. *Encyclopedia of Physical Science and Technology*, 717–729.

Reyes, J. C., & Chopra, A. K. (2010). Three-dimensional modal pushover analysis of buildings subjected to two components of ground motion, including its evaluation for tall buildings. *Earthquake Engineering & Structural Dynamics*, 40(7), 789–806.

*Basics of diaphragm action.* (2018, August 11) The Structural World. https://www.thestructuralworld.com/2018/08/11/basics-of-diaphragm-action.

Guzman, T. (2019). *Rigid vs. Semi-rigid diaphragm*. Retreived from https://wiki.csiamerica.com/display/etabs/Rigid+vs.+Semi-rigid+diaphragm

Rahman, A. U., Prof, A., & Jamshetty, N. (2019). Seismic effect of rigid floor diaphragm. *International Research Journal of Engineering and Technology*, 6, 433-441.

Tso, W. K., & Bozorgnia, Y. (1986). Effective eccentricity for inelastic seismic response of buildings. *Earthquake engineering & structural dynamics*, 14(3), 413-427.

Dutta, S. C., & Das, P. K. (2002). Validity and applicability of two simple hysteresis models to assess progressive seismic damage in R/C asymmetric buildings. *Journal of Sound and vibration*, 257(4), 753-777.

Poursha, M., Khoshnoudian, F., & Moghadam, A. S. (2009). A consecutive modal pushover procedure for estimating the seismic demands of tall buildings. *Engineering structures*, 31(2), 591-599.

Kunnath, S. K. (2004). Identification of modal combinations for nonlinear static analysis of building structures. *Computer‐Aided Civil and Infrastructure Engineering*, *19*(4), 246-259.

Chopra, A. K., & Goel, R. K. (2002). A modal pushover analysis procedure for estimating seismic demands for buildings. *Earthquake engineering & structural dynamics*, *31*(3), 561-582.

Goel, R. K., & Chopra, A. K. (2004). Evaluation of modal and FEMA pushover analyses: SAC buildings. *Earthquake spectra*, *20*(1), 225-254.

Bobadilla, H., & Chopra, A. K. (2008). Evaluation of the MPA procedure for estimating seismic demands: RC-SMRF buildings. *Earthquake Spectra*, *24*(4), 827-845.

Srikanta Prasad, S., Ahmed, S. K., & Prasad, S. K. (2011). PUSHOVER ANALYSIS FOR INFLUENCE OF GROUND FLEXIBILITY ON SEISMIC PERFORMANCE OF 3-D FRAMES. In *Proceedings of Indian Geo-Technical Conference, Paper* (No. 360).

Patil, A. S., & Kumbhar, P. D. (2013). Time history analysis of multistoried RCC buildings for different seismic intensities. *International Journal of Structural and Civil Engineering Research*, *2*(3), 194-201

Di Cuia, A., Lombardi, L., De Luca, F., De Risi, R., Caprili, S., & Salvatore, W. (2017). Linear Time-History Analysis for EC8 design of CBF structures. *Procedia engineering*, *199*, 3522-3527

Turkish earthquake hazard map. *Ministry of Interior Disaster and Emergency Management Presidency AFAD*. https://tdth.afad.gov.tr/TDTH

Darshan, D., & Shruthi, H. K. (2016). Study on mass irregularity of high-rise buildings. *International Research Journal of Engineering and Technology*, *3*(8), 1123-1130.

Di Cuia, A., Lombardi, L., De Luca, F., De Risi, R., Caprili, S., & Salvatore, W.

(2017). Linear time-history analysis for EC8 design of CBF structures. *Procedia Engineering*, *199*, 3522–3527. https://doi.org/10.1016/j.proeng.2017.09.502

Dutta, S. C., & Das, P. K. (2002). Validity and applicability of two simple hysteresis models to assess progressive seismic damage in r/c asymmetric buildings. *Journal of Sound and Vibration*, *257*(4), 753–777. https://doi.org/10.1006/JSVI.2002.5093

Giordano, A., Guadagnuolo, M., & Faella, G. (2008). Pushover analysis of plan irregular masonry buildings.

Hasnat, A., & Rahim, M. R. I. (2013). Response of building frames with vertical and stiffness irregularity due to lateral loads. *International Journal of Engineering Research & Technology (IJERT) ISSN: 2278-0181*, *2*(12), 795–799.

Maske, S. G., & Pajgade, D. P. S. (2013). Torsional behaviour of asymmetrical buildings. *International Journal of Modern Engineering Research*, *3*(2), 1146–1149.

Patil, A. S., & Kumbhar, P. D. (2013). Time history analysis of multistoried rcc buildings for different seismic intensities. *International Journal of Structural and Civil Engineering Research*, *2*(3), 195–201.

Rahman, A. U., Prof, A., & Jamshetty, N. (2019). *" Seismic Effect of Rigid Floor Diaphragm ."* 433–441.

Tso, W. K., & Bozorgnia, Y. (1986). Effective eccentricity for inelastic seismic response of buildings. *Earthquake Engineering & Structural Dynamics*, *14*(3), 413–427. https://doi.org/10.1002/eqe.4290140308

Varadharajan, S., Sehgal, V. K., & Saini, B. (2016). *Review of different Structural irregularities in buildings*. *December*.

# APPENDICES

## Appendix A Earthquake Matched Response Spectrums

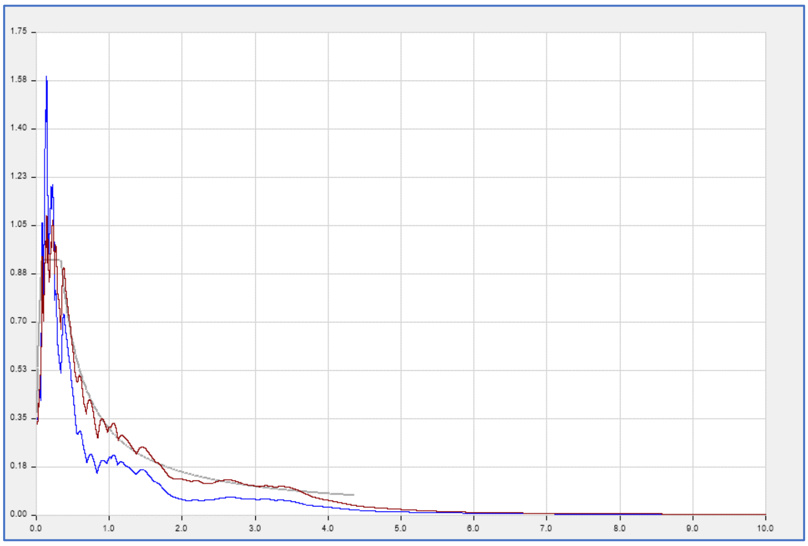


**Figure 38** 288-00 Earthquake Matched Response Spectrum.

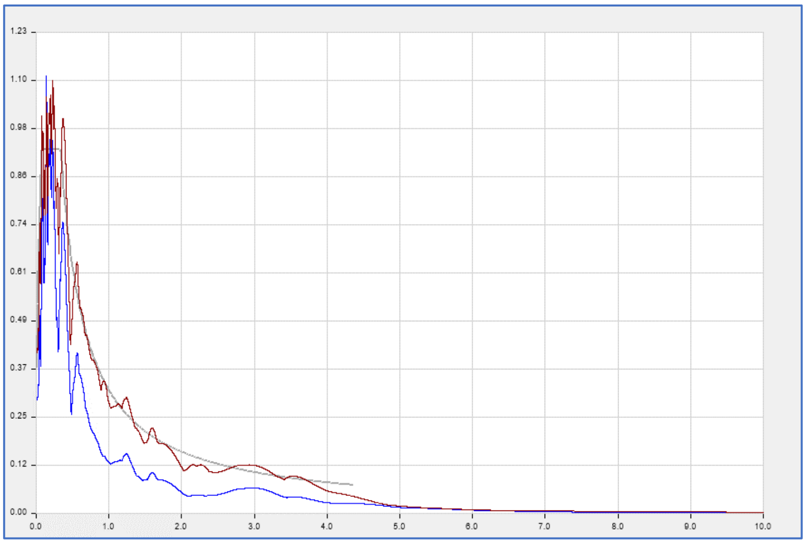


**Figure 39** 288-90 Earthquake Matched Response Spectrum.

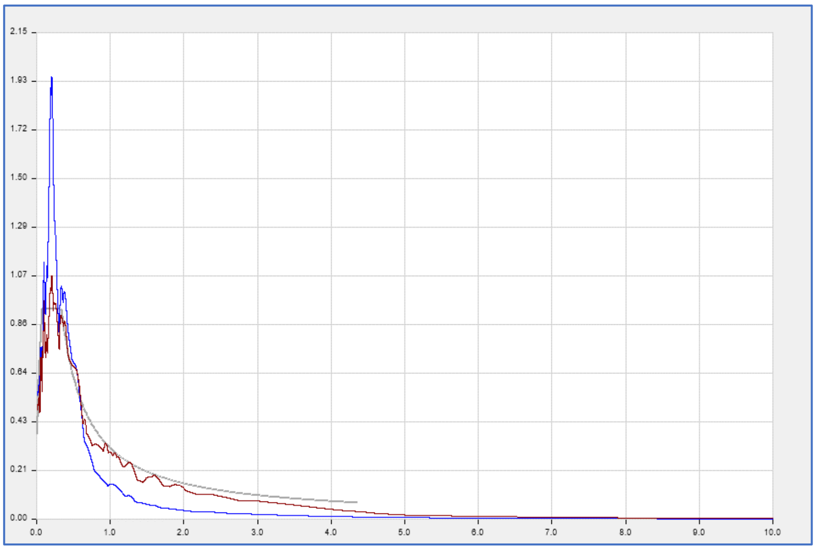


**Figure 40** 534-00 Earthquake Matched Response Spectrum.

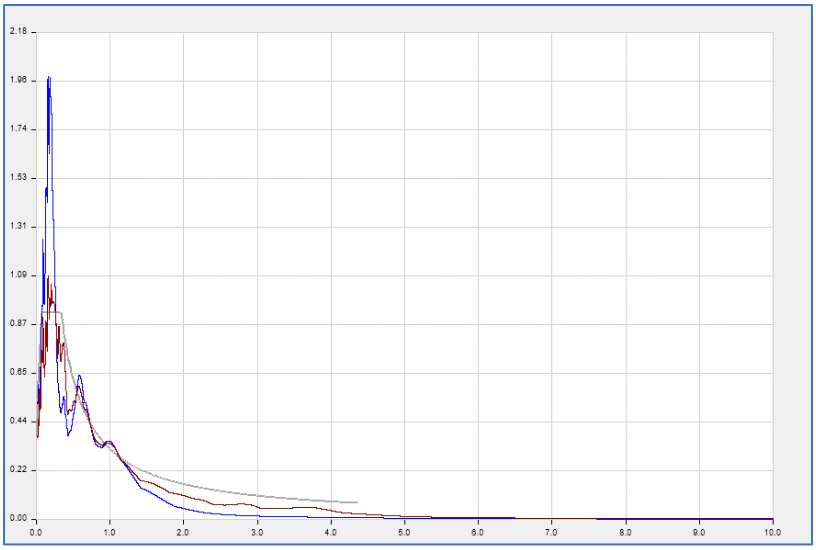


**Figure 41** 534-90 Earthquake Matched Response Spectrum.

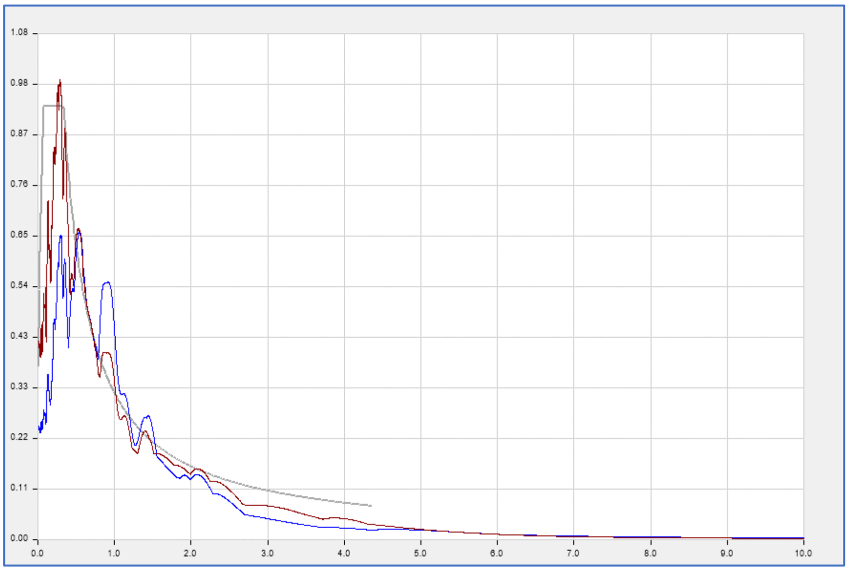


**Figure 42** 963-00 Earthquake Matched Response Spectrum.

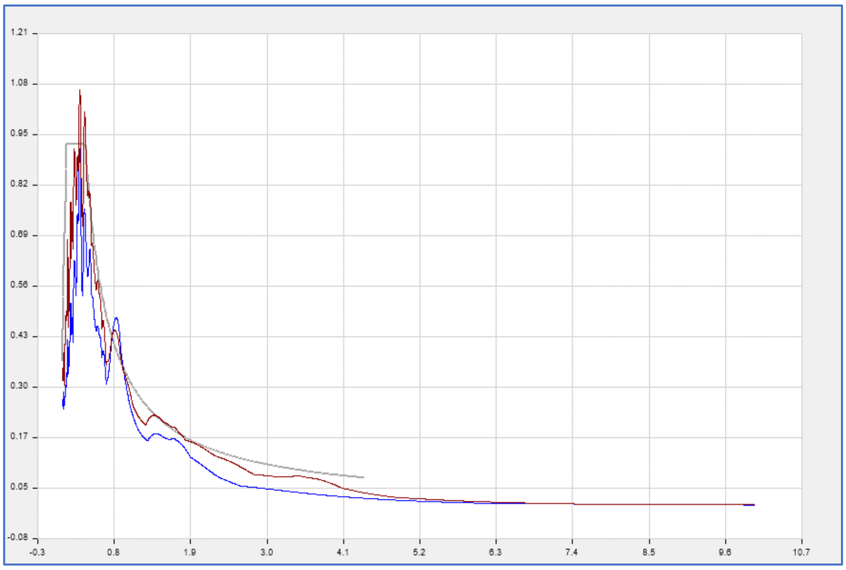


**Figure 43** 963-90 Earthquake Matched Response Spectrum.

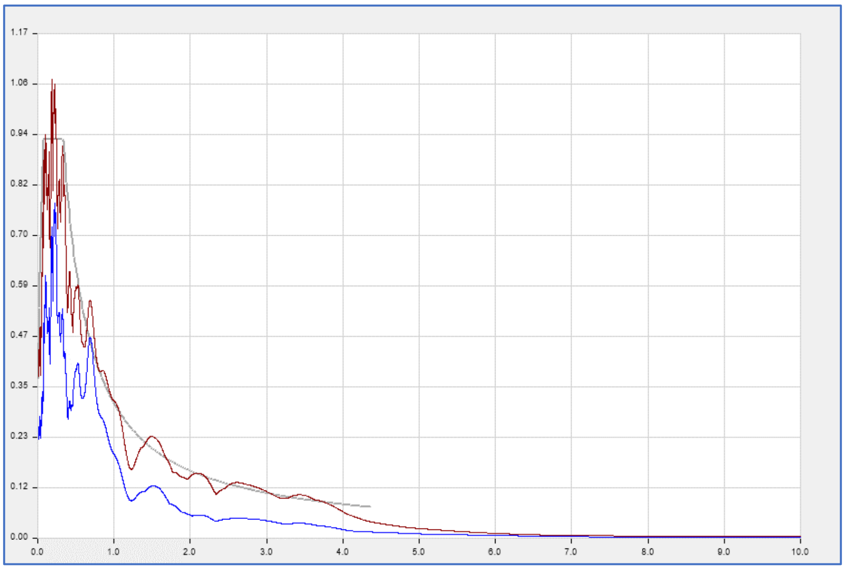


**Figure 44** 1006-00 Earthquake Matched Response Spectrum.

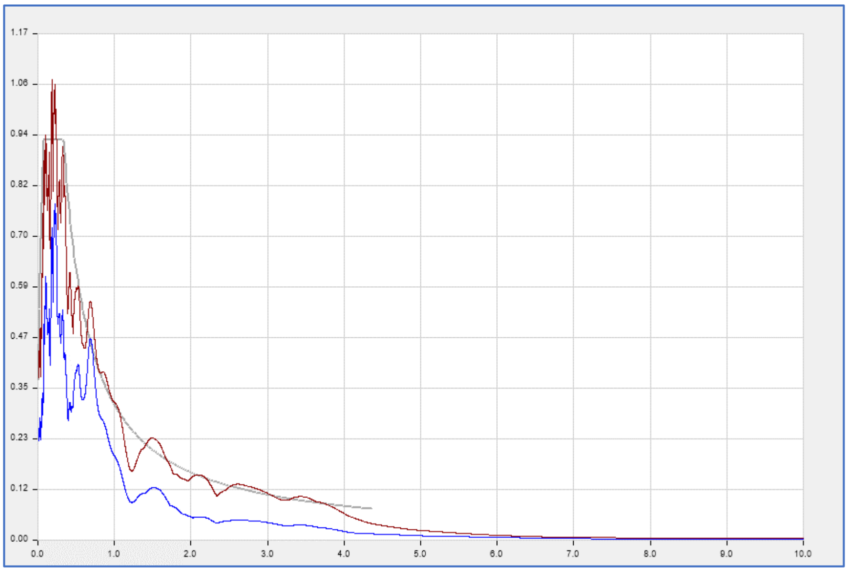


**Figure 45** 1006-90 Earthquake Matched Response Spectrum.

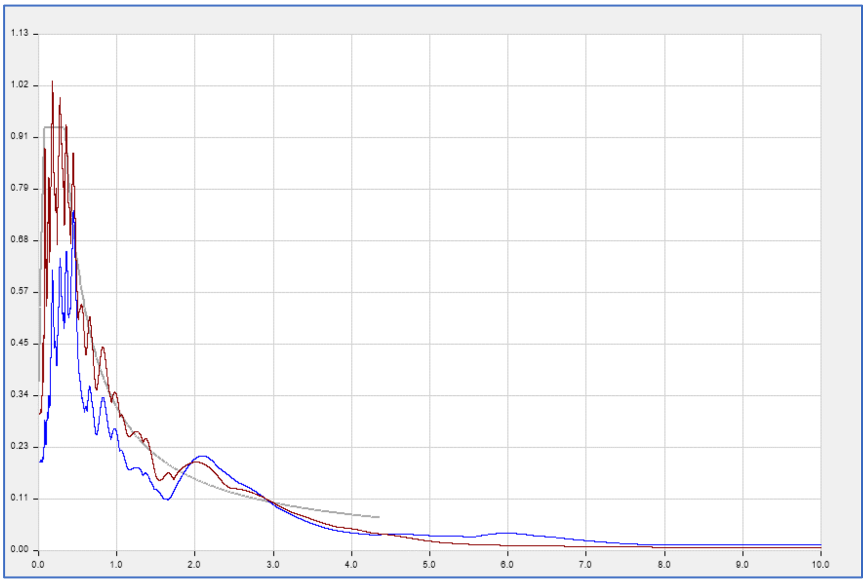


**Figure 46** 1144-00 Earthquake Matched Response Spectrum.

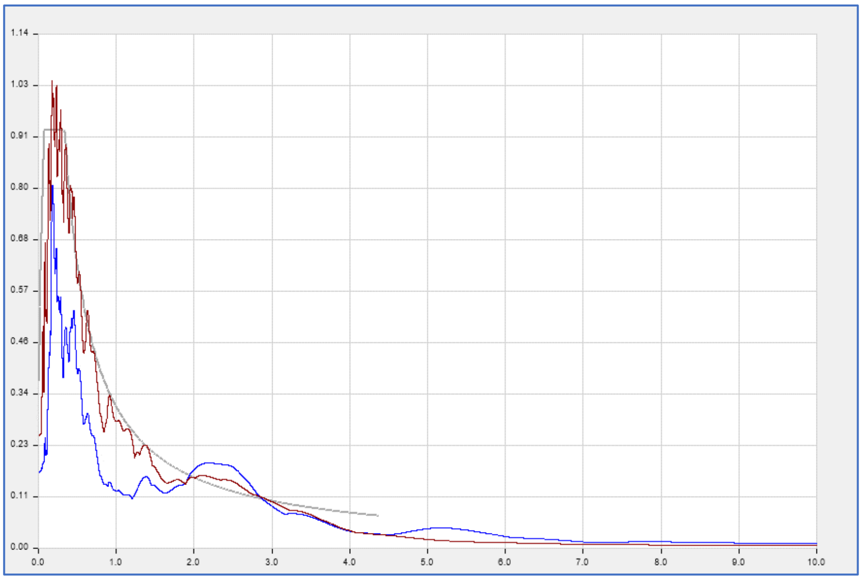


**Figure 47** 1144-90 Earthquake Matched Response Spectrum.

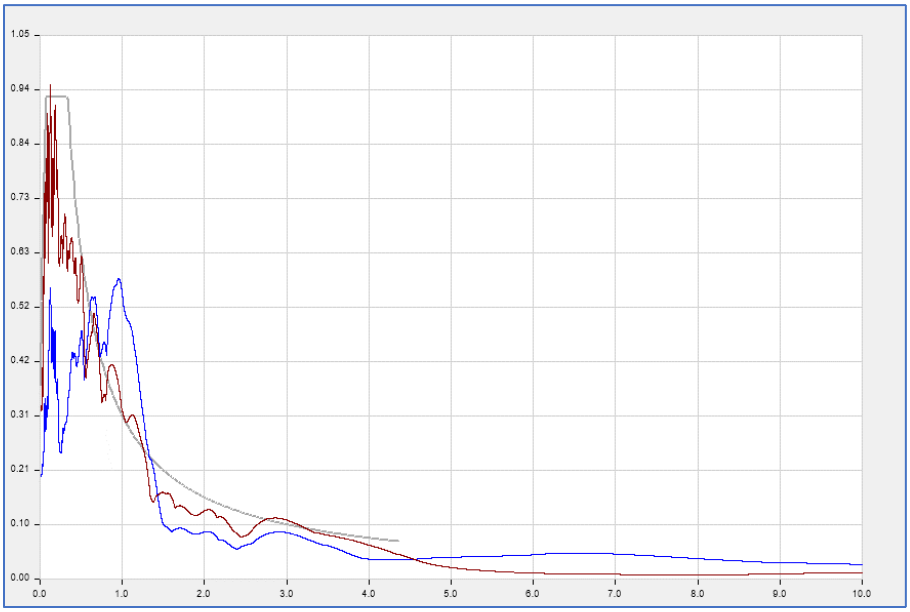


**Figure 48** 1487-00 Earthquake Matched Response Spectrum.

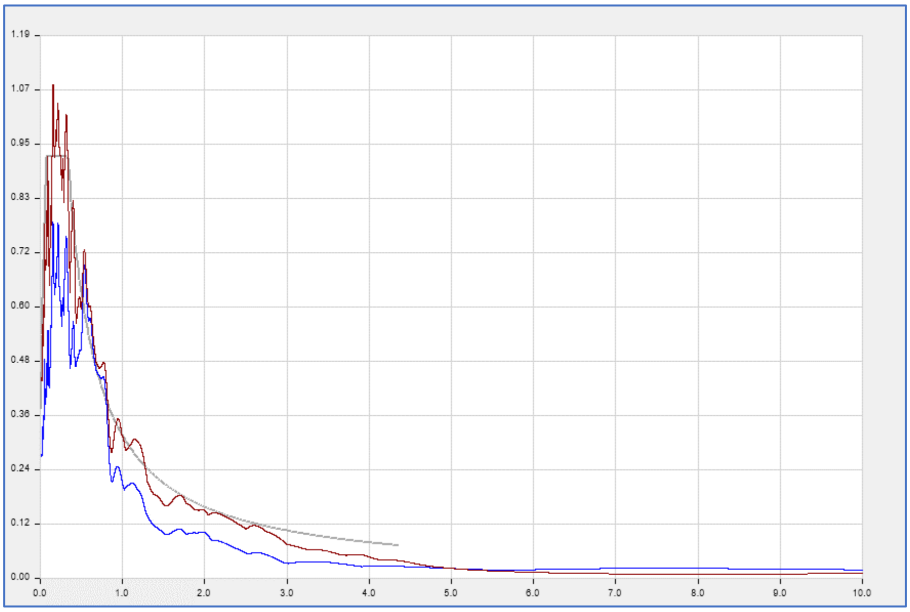


**Figure 49** 1487-90 Earthquake Matched Response Spectrum.

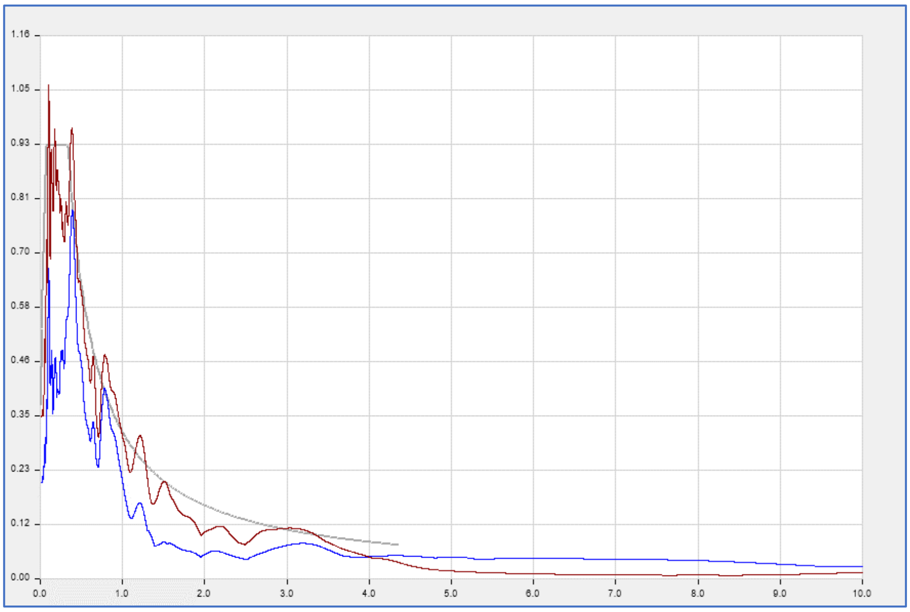


**Figure 50** 1524-00 Earthquake Matched Response Spectrum.

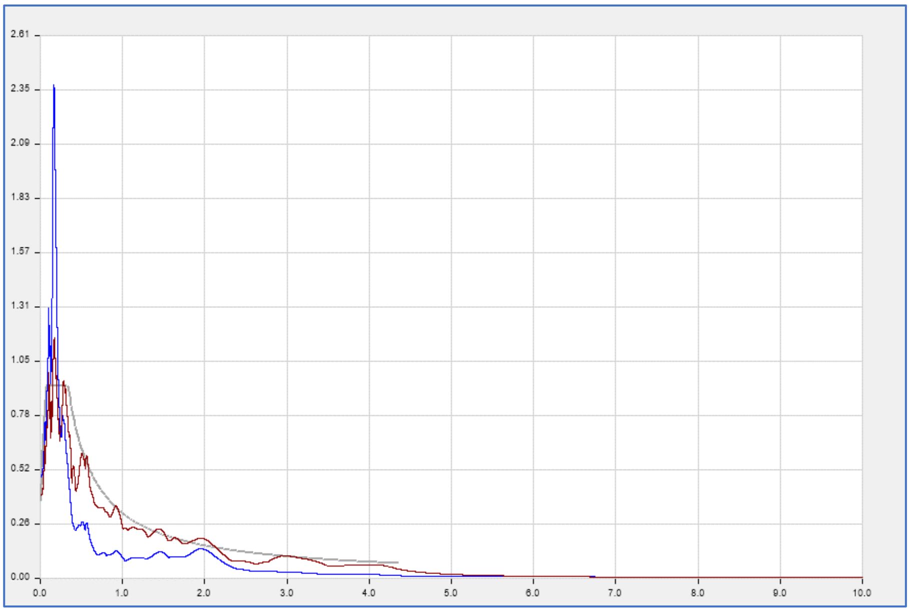


**Figure 51** 4226-00 Earthquake Matched Response Spectrum.

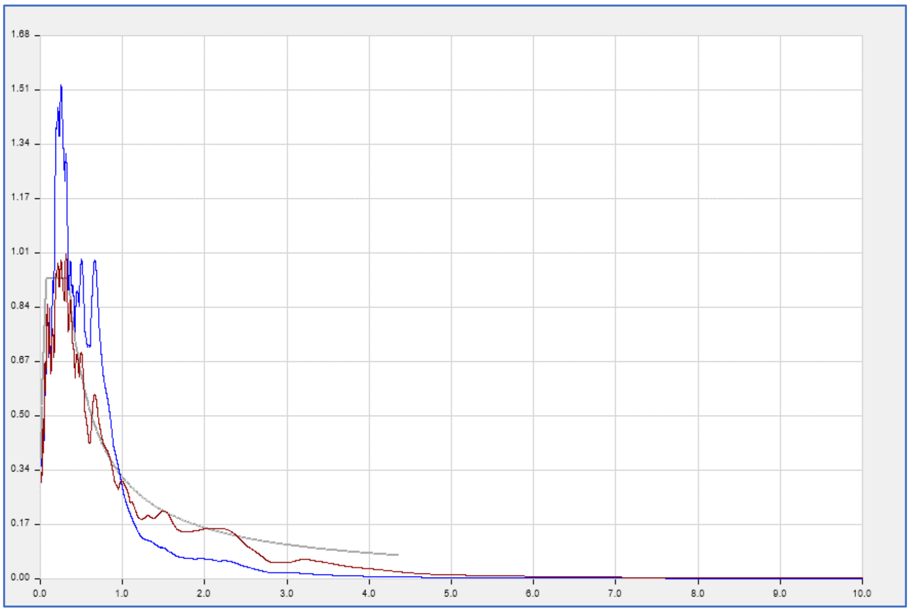


**Figure 52** 4455-00 Earthquake Matched Response Spectrum.

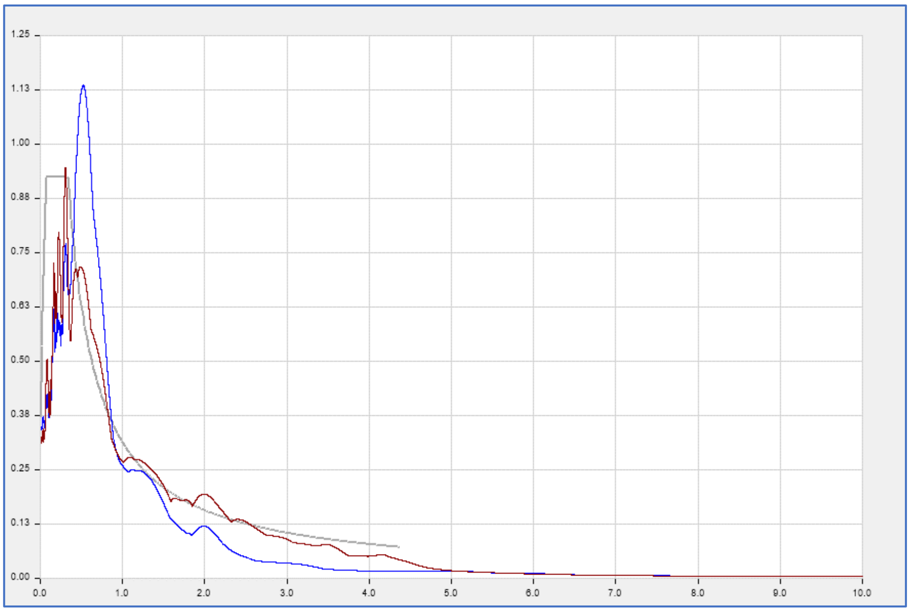


**Figure 53** 4889-00 Earthquake Matched Response Spectrum.

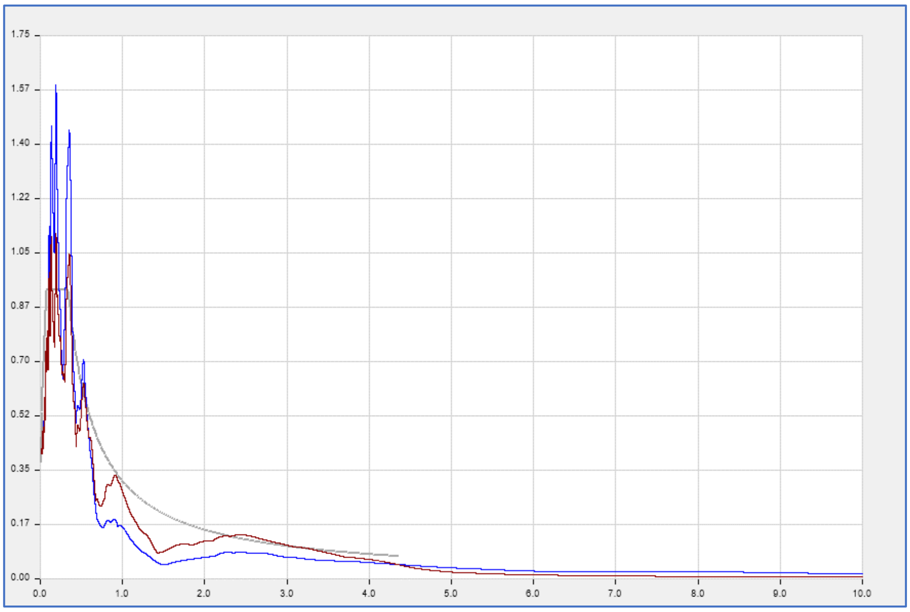


**Figure 54** 6915-00 Earthquake Matched Response Spectrum.

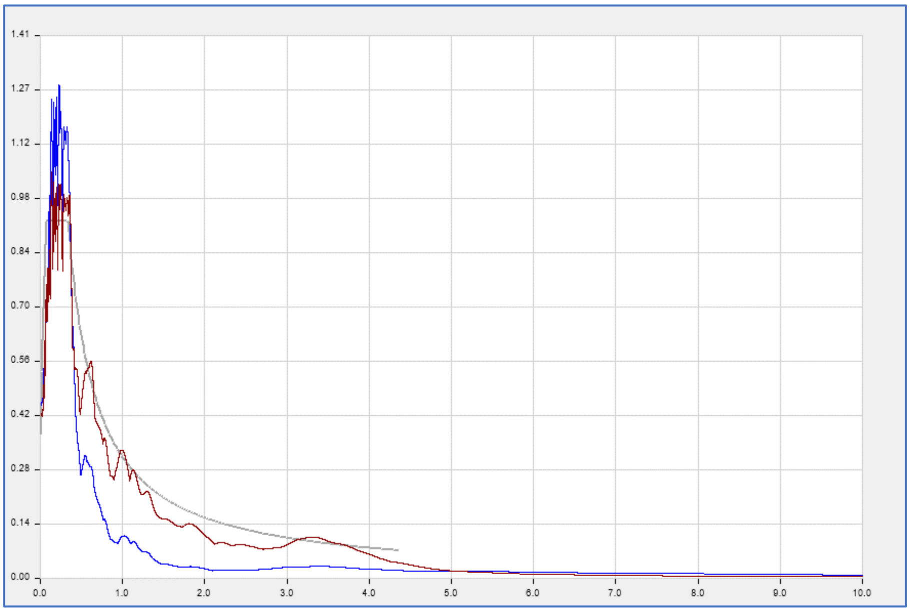


**Figure 55** 6915-90 Earthquake Matched Response Spectrum.

## Appendix B Structure 1 Story Displacement

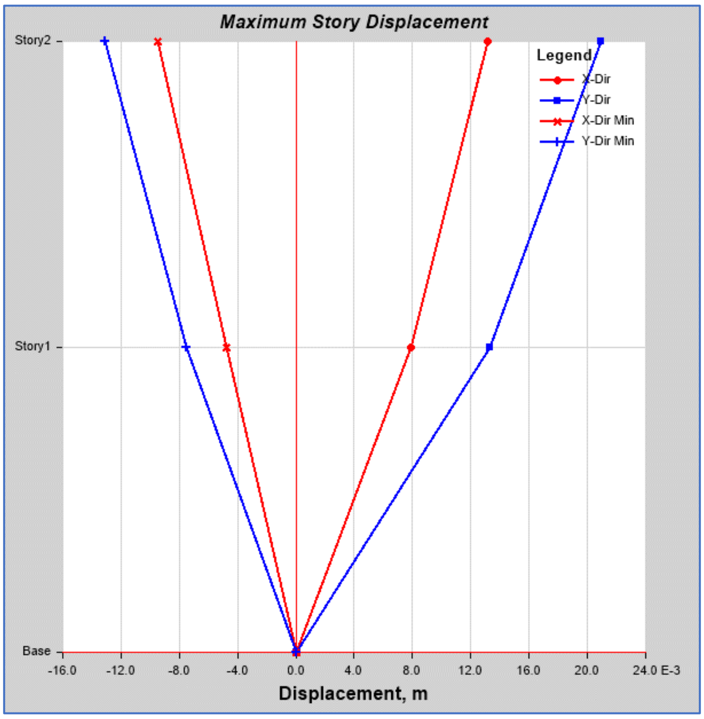


**Figure 56** Earthquake Record 288 Story Displacement of Structure 1.

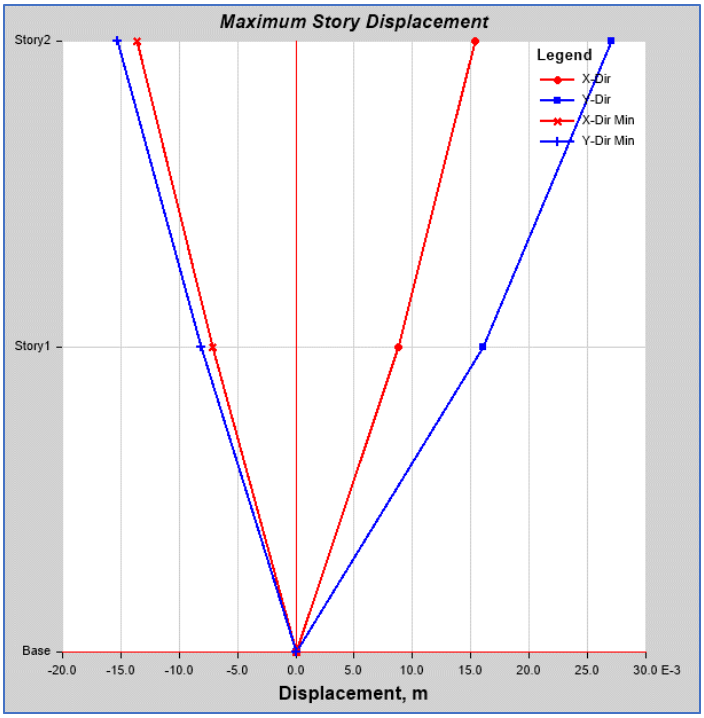


**Figure 57** Earthquake Record 534 Story Displacement of Structure 1.

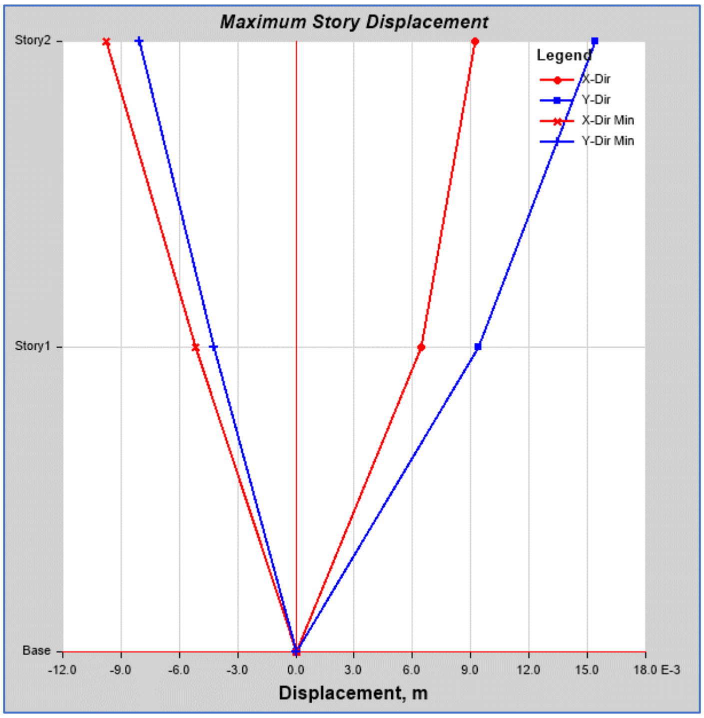


**Figure 58** Earthquake Record 963 Story Displacement of Structure 1.


**Figure 59** Earthquake Record 1006 Story Displacement of Structure 1.

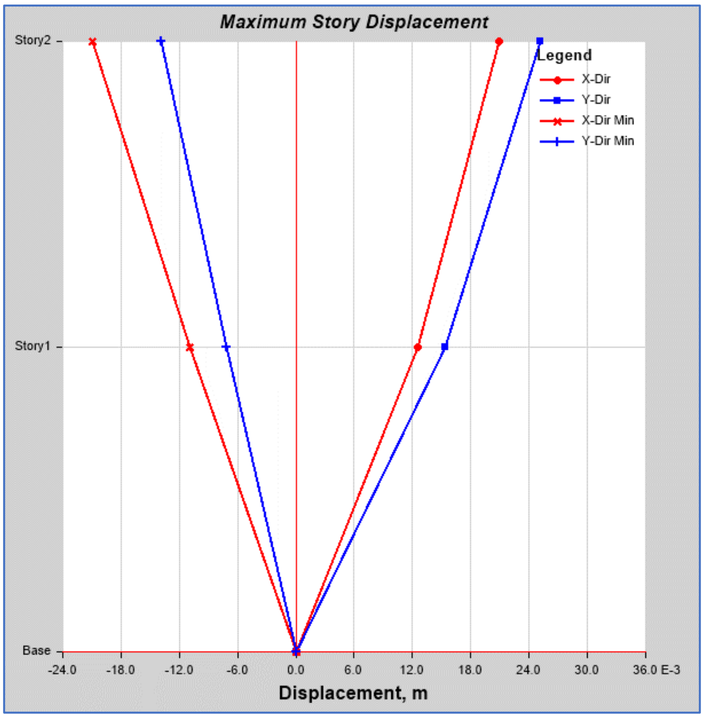


**Figure 60** Earthquake Record 1144 Story Displacement of Structure 1.

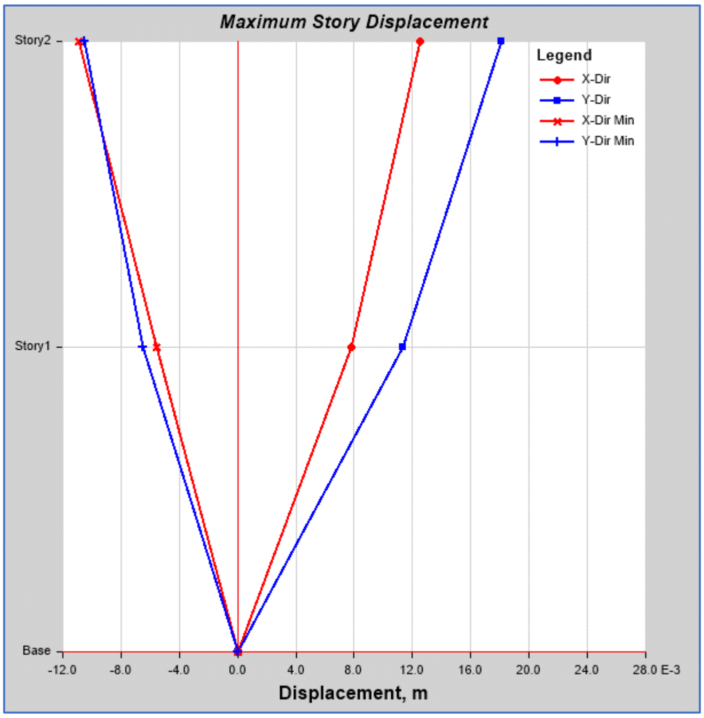


**Figure 61** Earthquake Record 1487 Story Displacement of Structure 1.

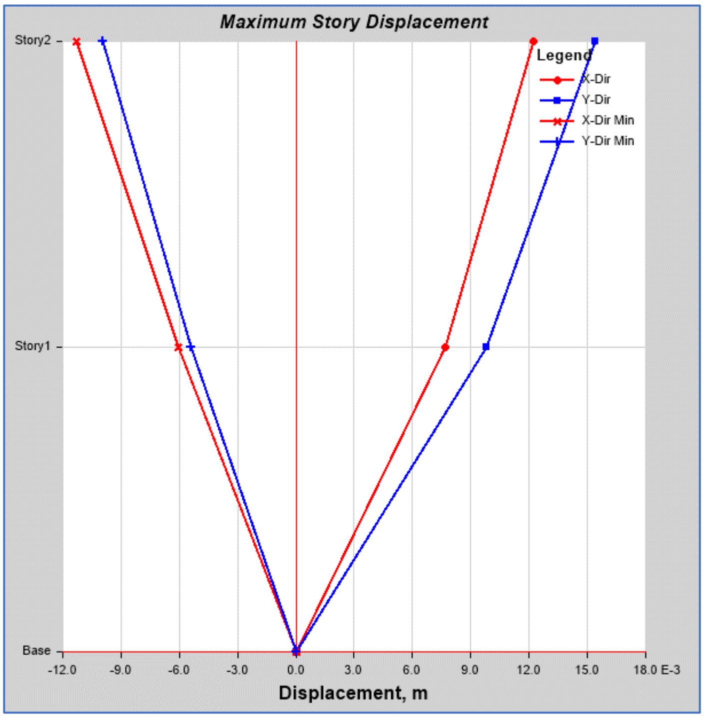


**Figure 62** Earthquake Record 1524 Story Displacement of Structure 1.

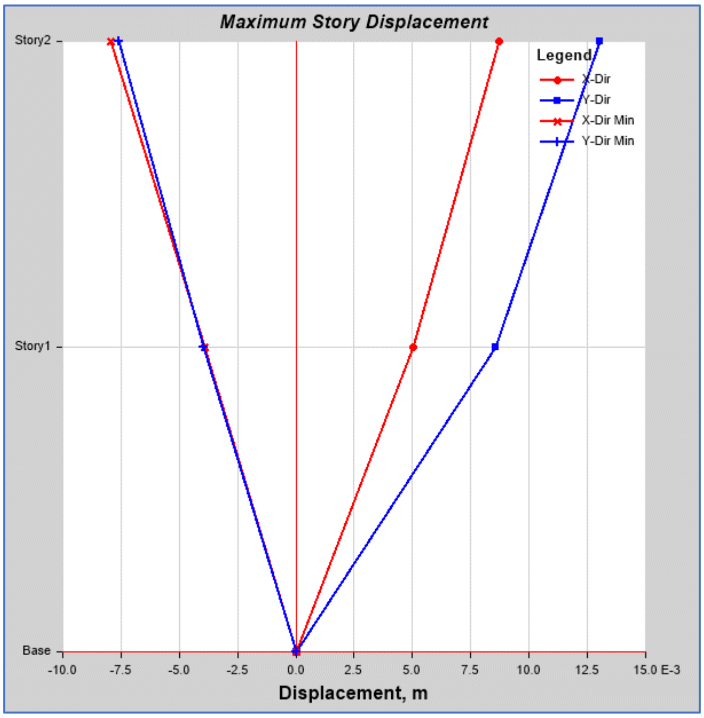


**Figure 63** Earthquake Record 4226 Story Displacement of Structure 1.

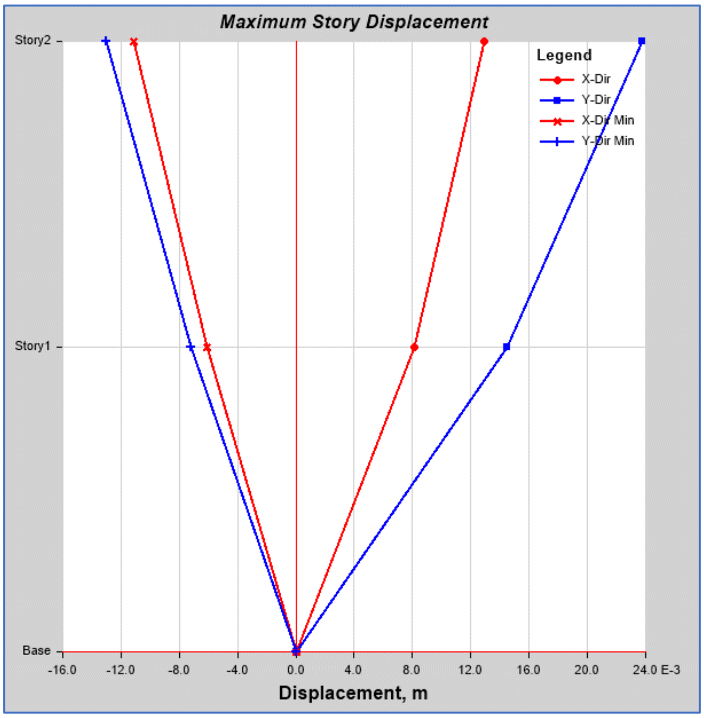


**Figure 64** Earthquake Record 4455 Story Displacement of Structure 1.

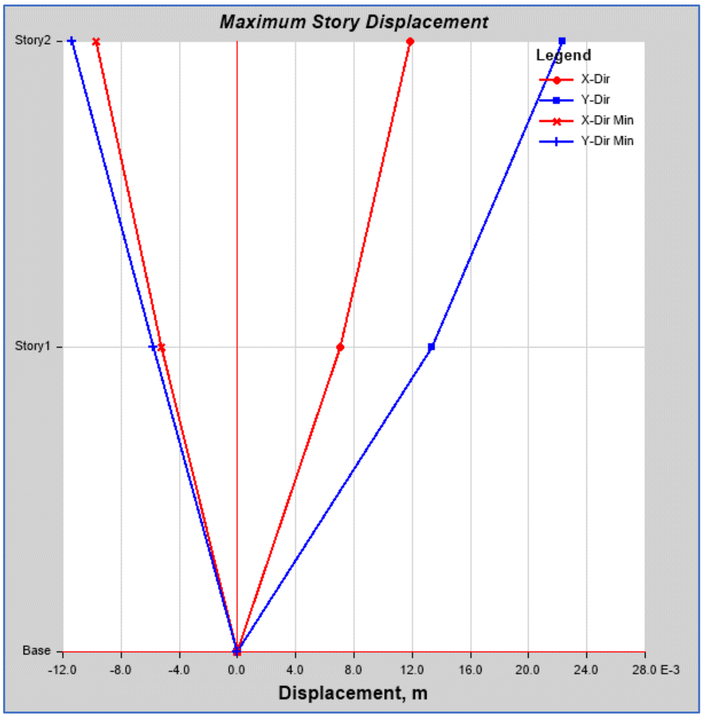


**Figure 65** Earthquake Record 4889 Story Displacement of Structure 1.

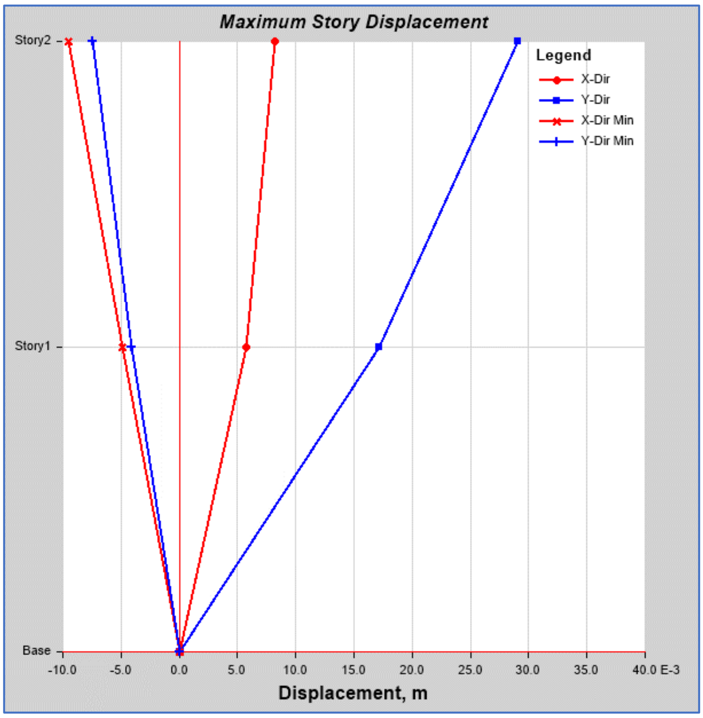


**Figure 66** Earthquake Record 6915 Story Displacement of Structure 1.

# Appendix C Structure 2 Story Displacement

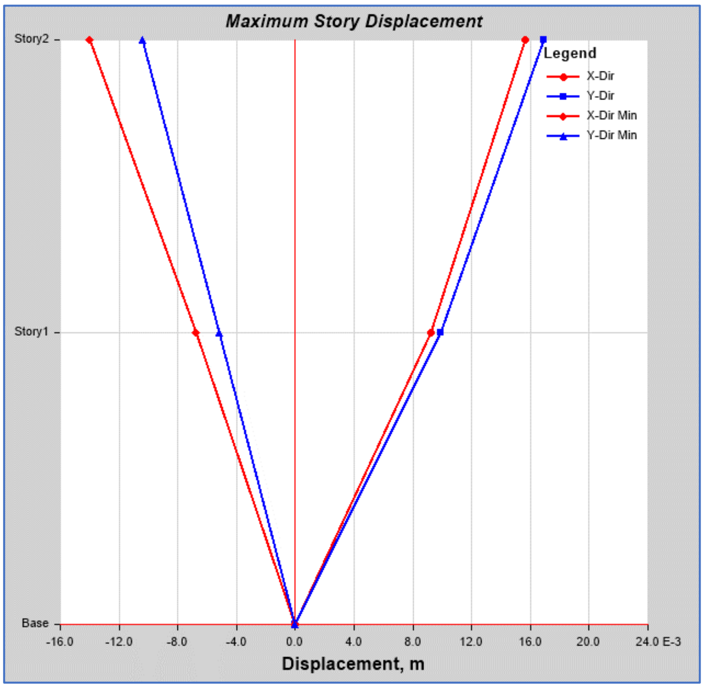


**Figure 67** Earthquake Record 288 Story Displacement of Structure 2.

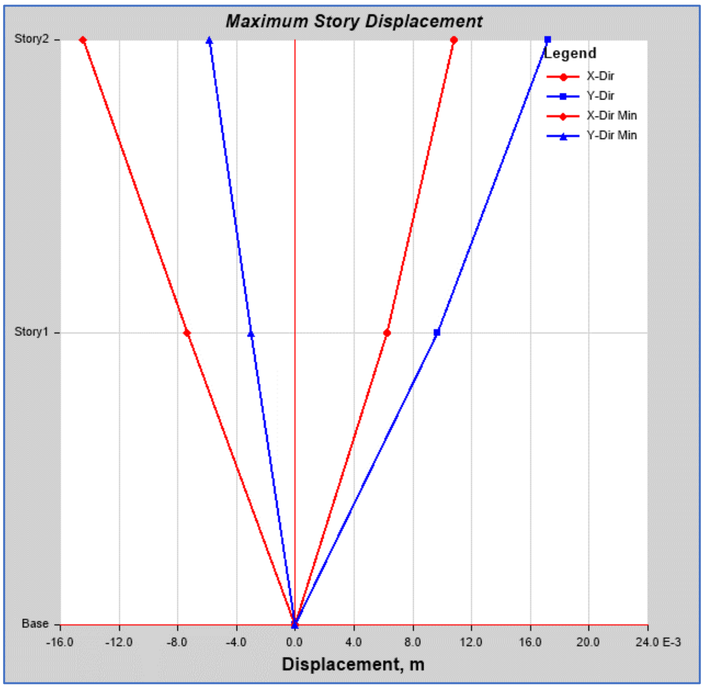


**Figure 68** Earthquake Record 534 Story Displacement of Structure 2.

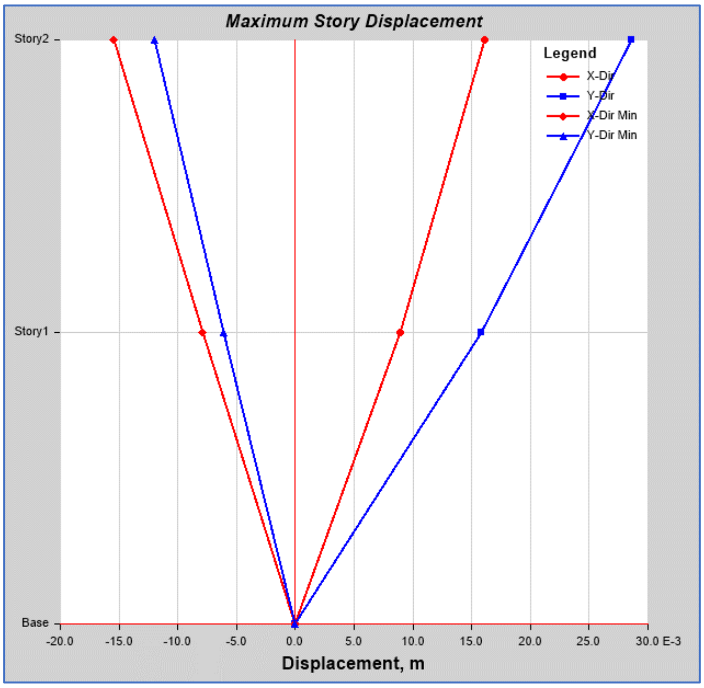


**Figure 69** Earthquake Record 963 Story Displacement of Structure 2.


**Figure 70** Earthquake Record 1006 Story Displacement of Structure 2.

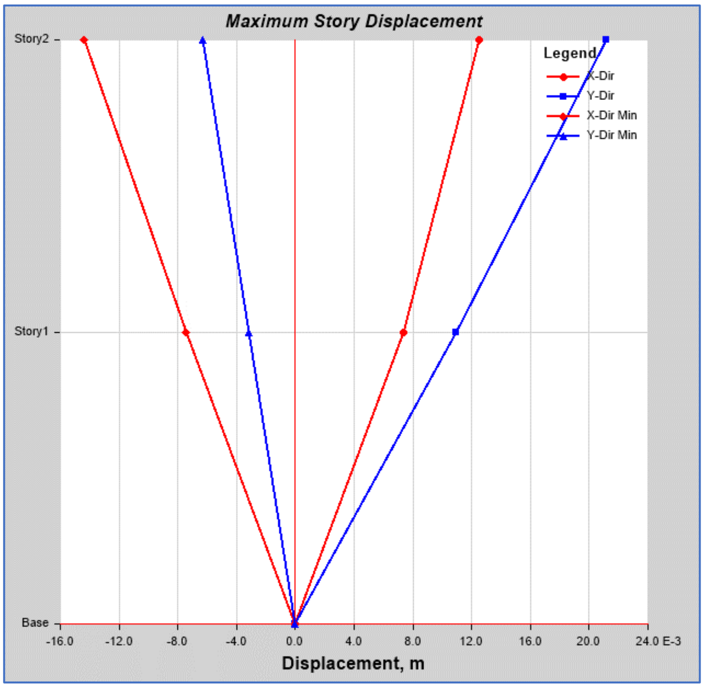


**Figure 71** Earthquake Record 1144 Story Displacement of Structure 2.

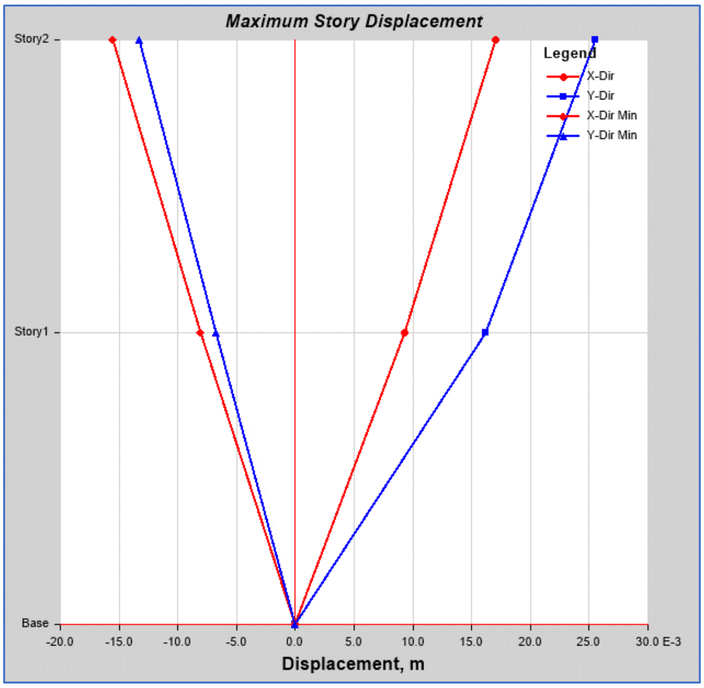


**Figure 72** Earthquake Record 1487 Story Displacement of Structure 2.

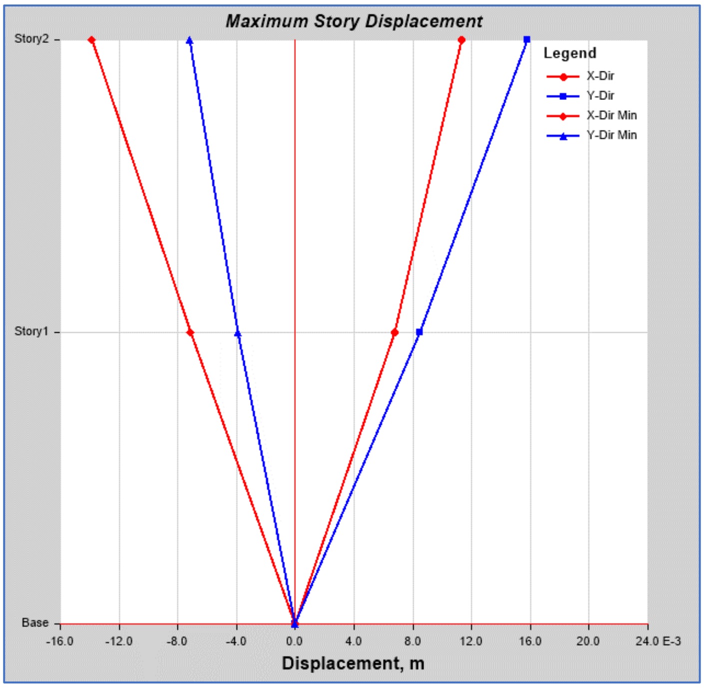


**Figure 73** Earthquake Record 1524 Story Displacement of Structure 2.

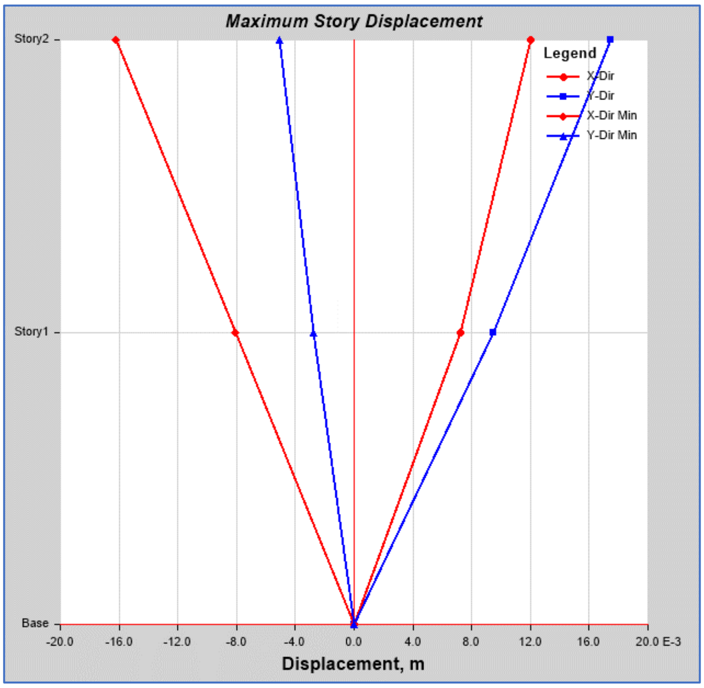


**Figure 74** Earthquake Record 4226 Story Displacement of Structure 2.

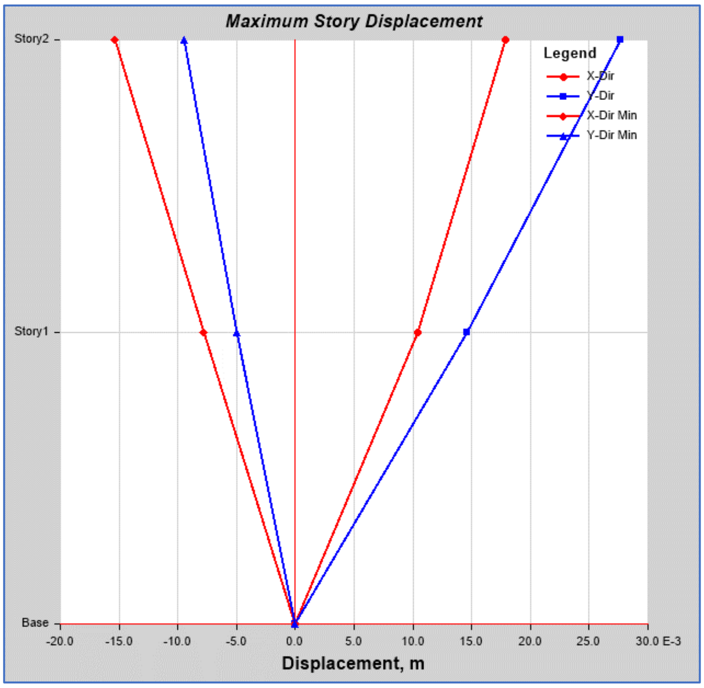


**Figure 75** Earthquake Record 4455 Story Displacement of Structure 2.

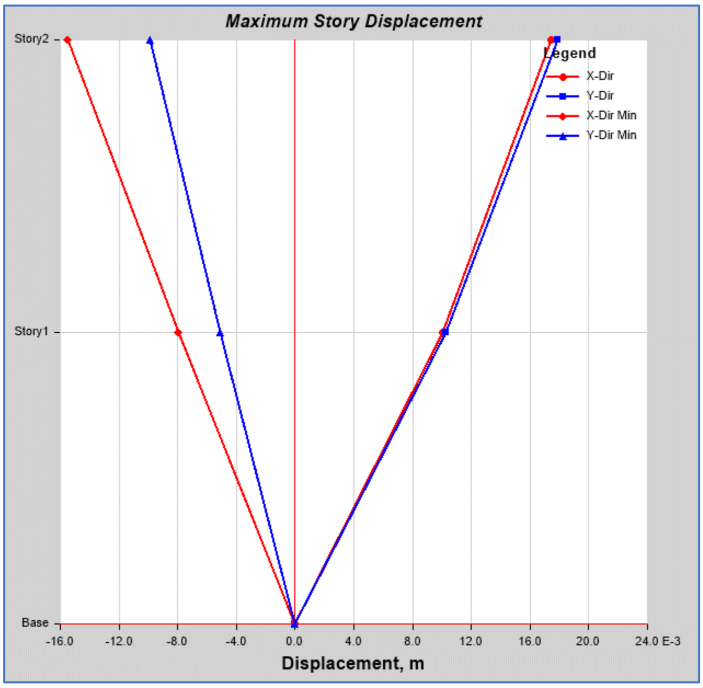


**Figure 76** Earthquake Record 4889 Story Displacement of Structure 2.

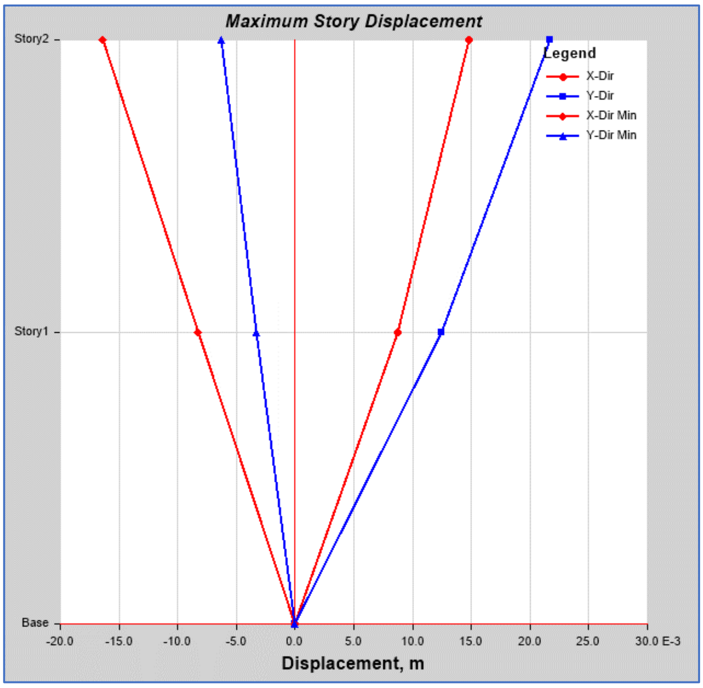


**Figure 77** Earthquake Record 6915 Story Displacement of Structure 2.

## Appendix D Base Shear Results of Structure 1:

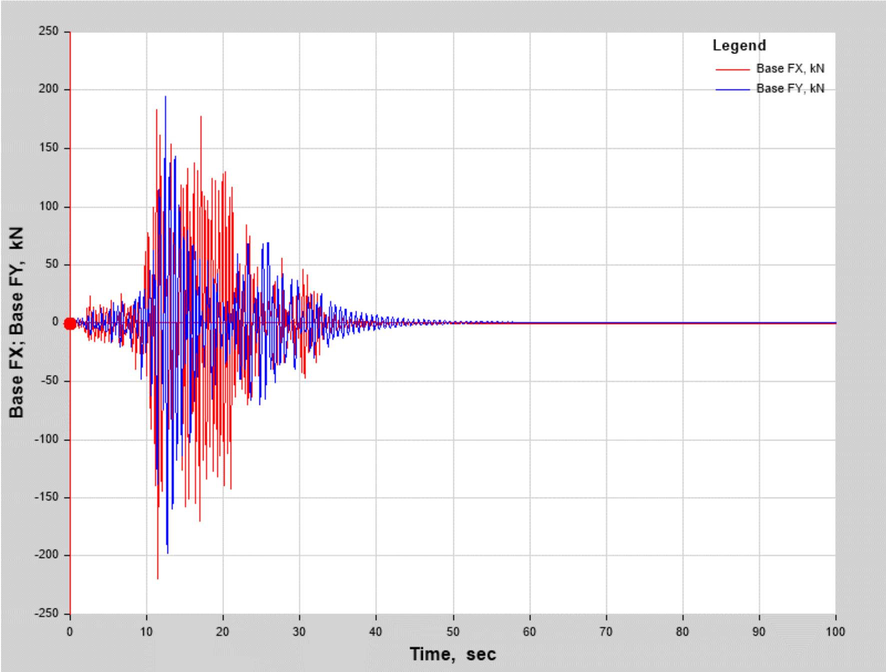


**Figure 78** Irpinia Earthquake Record 288 Base Shear in Structure 1

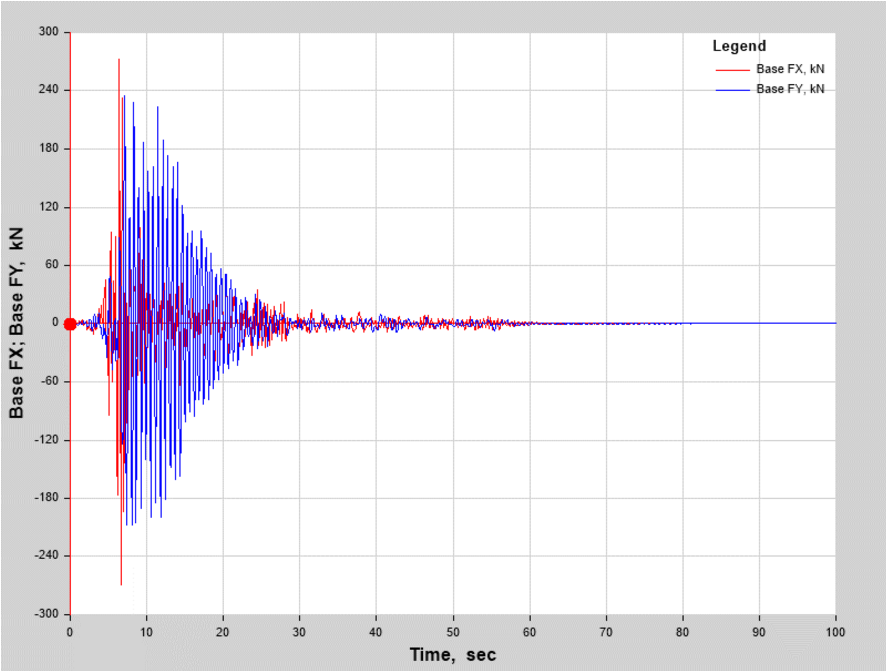


**Figure 79** N. Palm Spring Earthquake Record 534 Base Shear in Structure 1

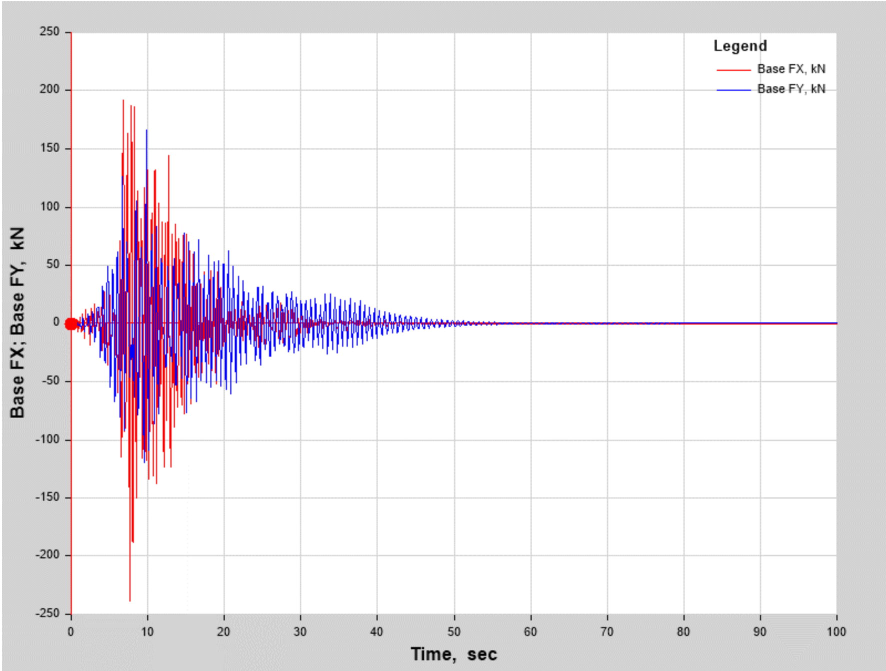


**Figure 80** Northridge-01 Earthquake Record 963 Base Shear in Structure 1

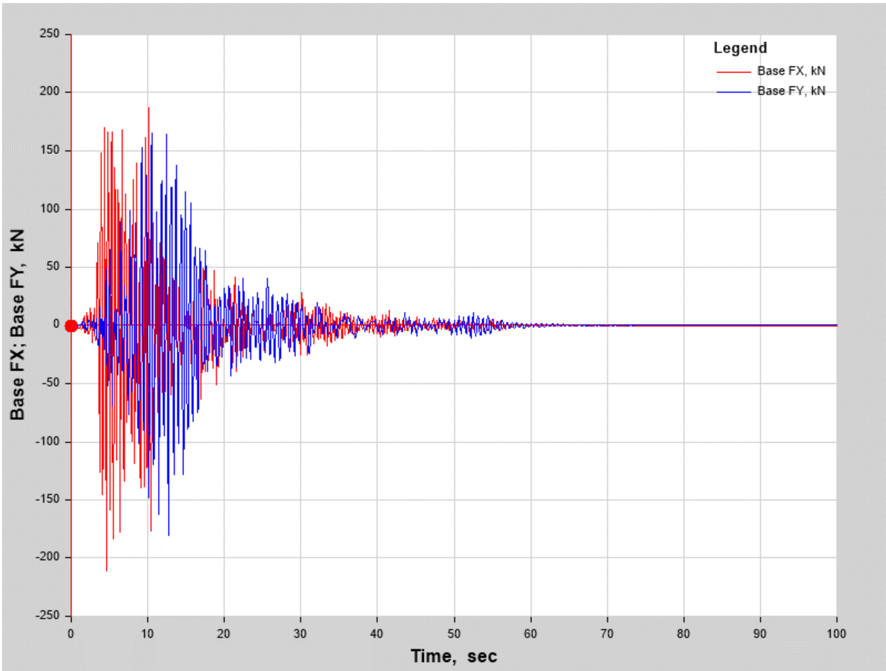


**Figure 81** Northridge-01 Earthquake Record 1006 Base Shear in Structure 1

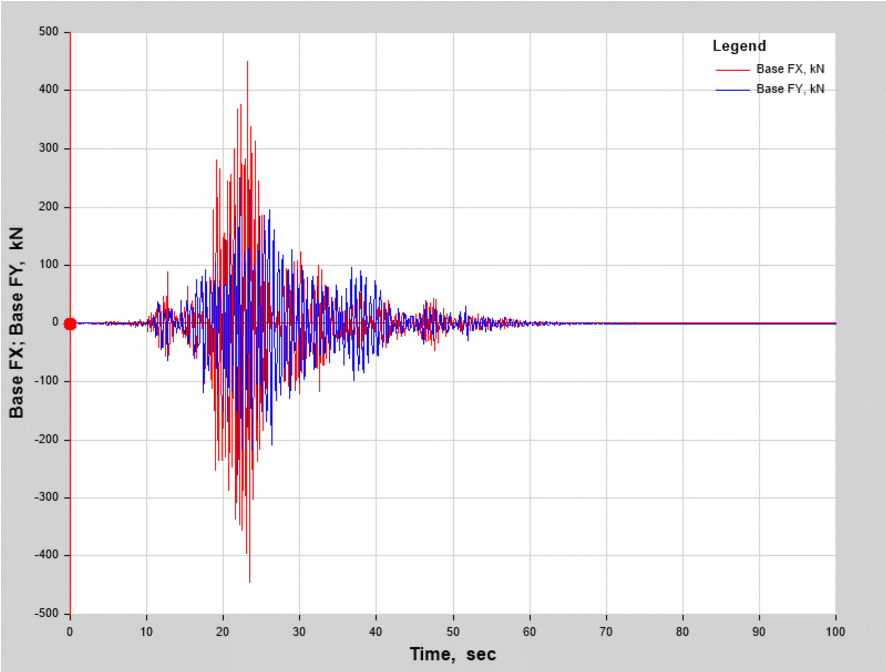


**Figure 82** Gulf of Aqaba Earthquake Record 1144 Base Shear in Structure 1

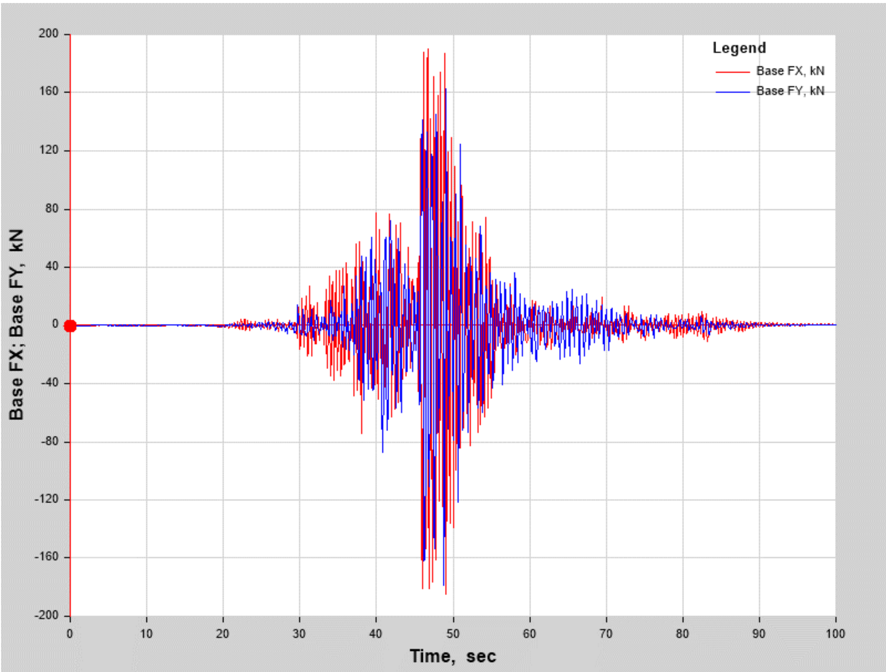


**Figure 83** Chi-Chi Taiwan Earthquake Record 1487 Base Shear in Structure 1

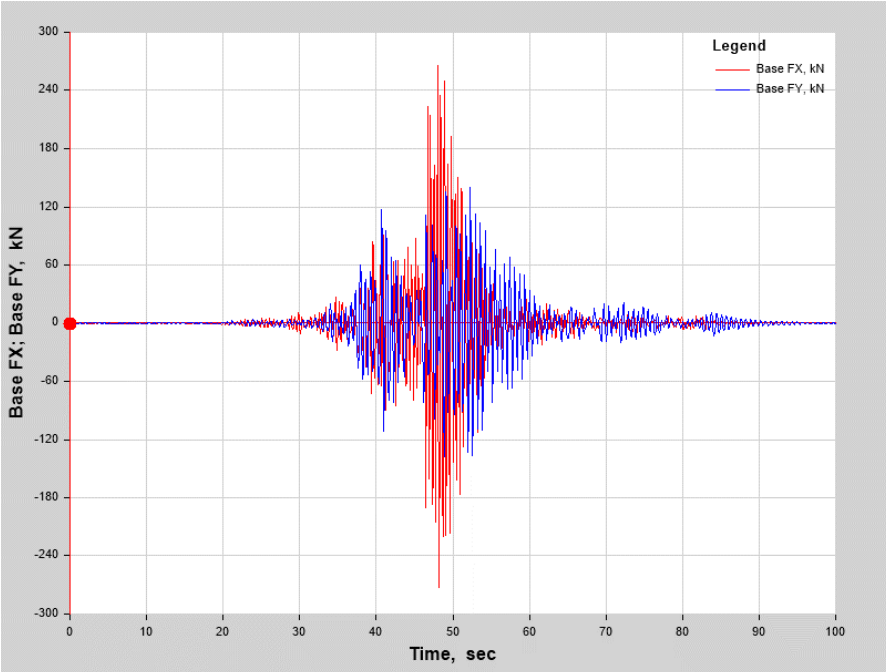


**Figure 84** Chi-Chi Taiwan Earthquake Record 1524 Base Shear in Structure 1

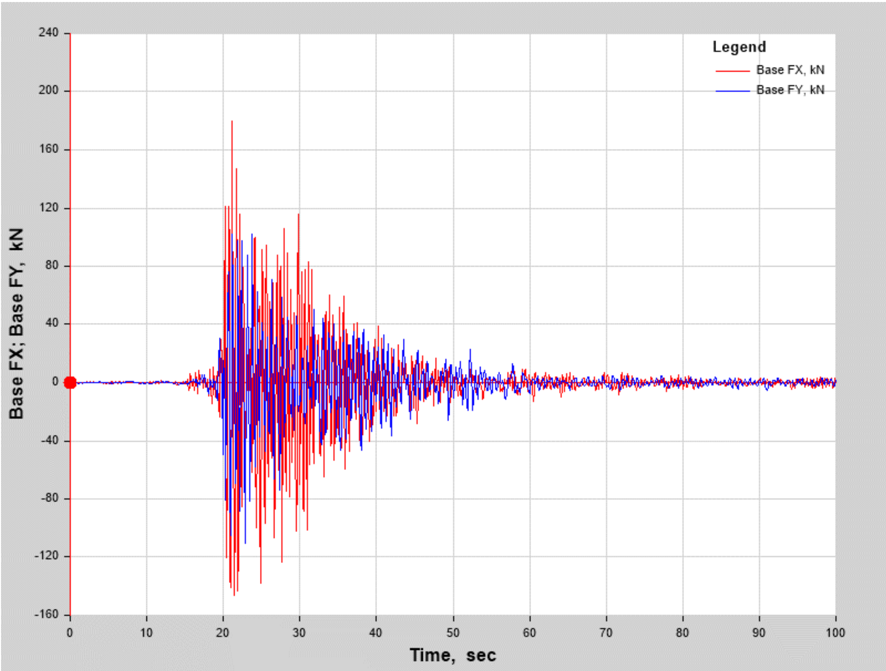


**Figure 85** Niigata Japan Earthquake Record 4226 Base Shear in Structure 1

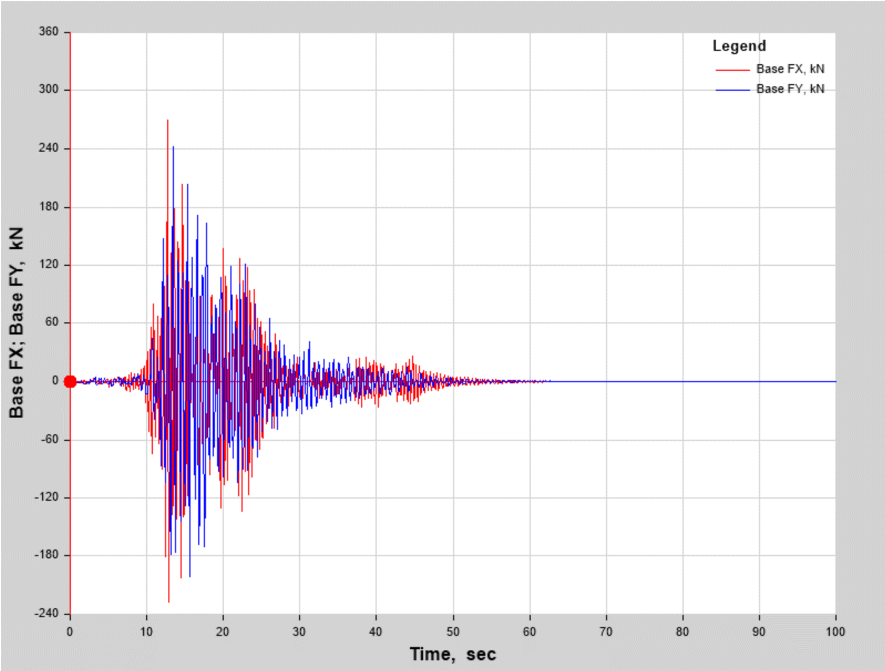


**Figure 86** Montenegro Yugosla Earthquake Record 4455 Base Shear in Structure 1

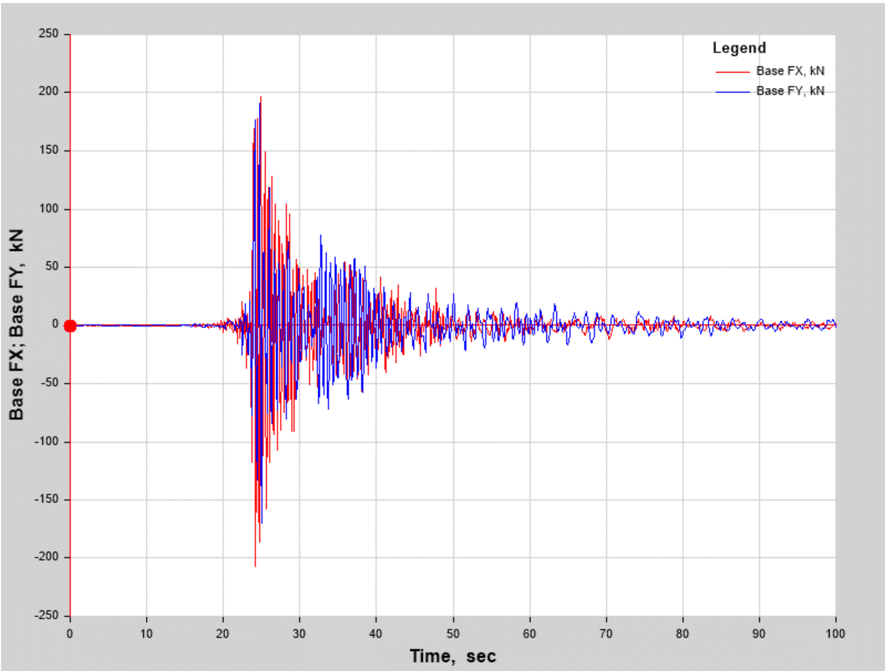


**Figure 87** Chuetsu-Oki Japan Earthquake Record 4889 Base Shear in Structure 1

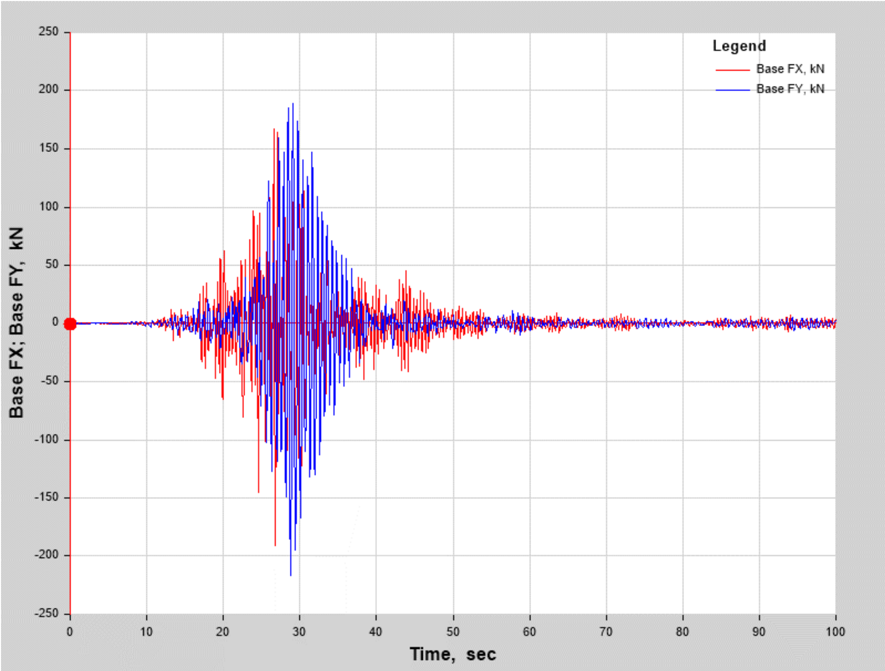


**Figure 88** Darfield New Zealand Earthquake Record 6915 Base Shear in Structure 1

## Appendix E Base Shear Results of Structure 2:

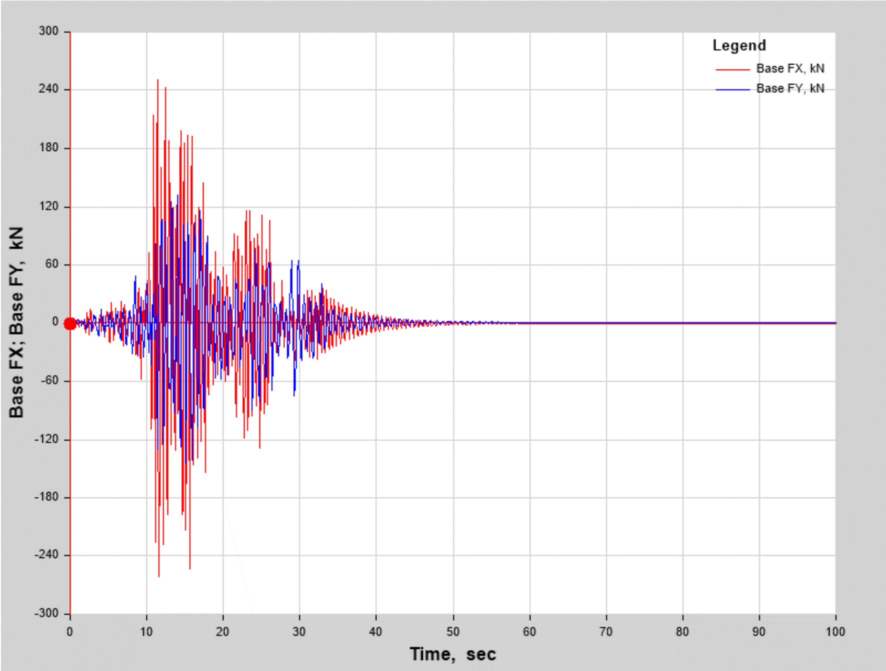


**Figure 89** Irpinia Earthquake Record 288 Base Shear in Structure 2

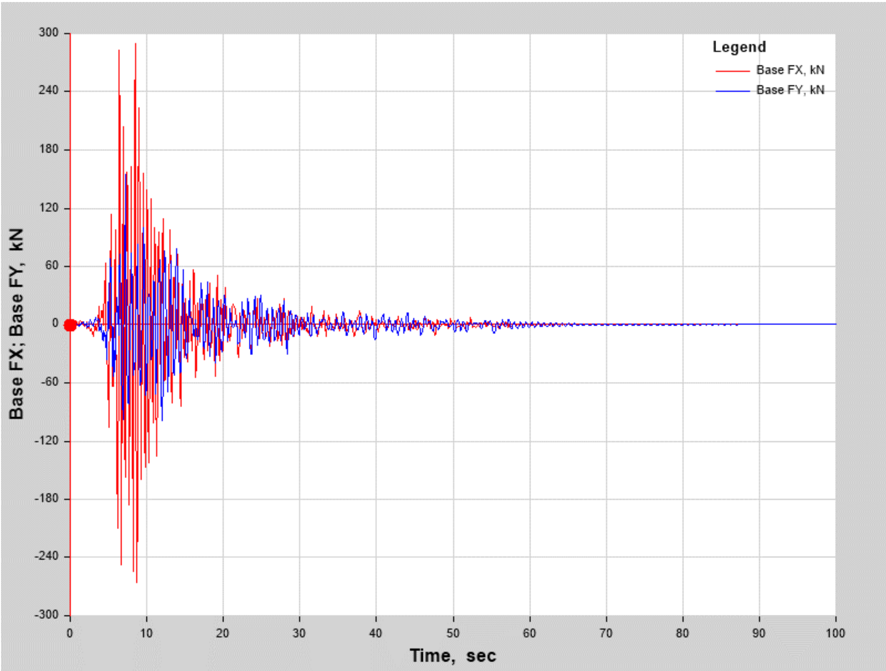


**Figure 90** N. Palm Spring Earthquake Record 534 Base Shear in Structure 2

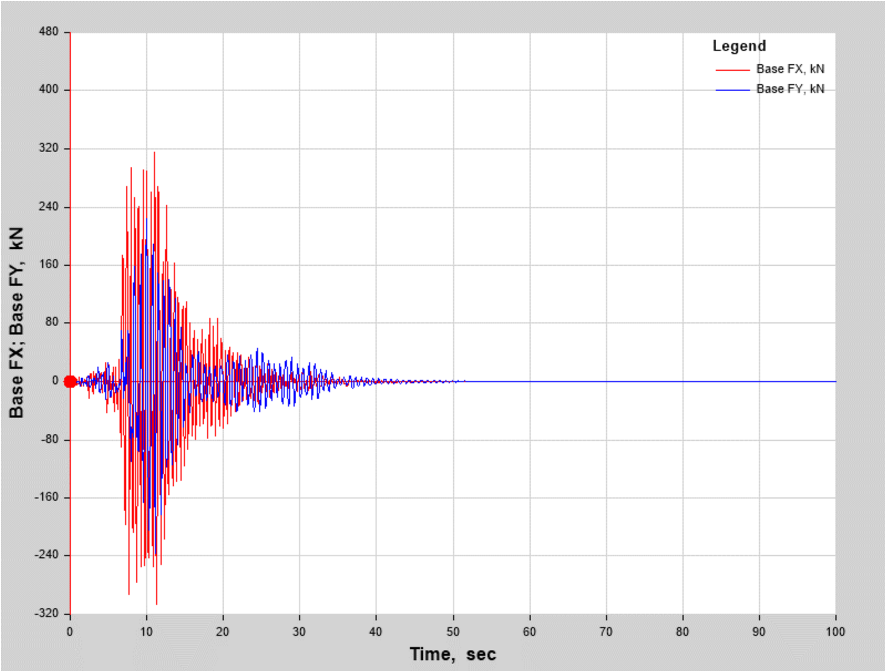


**Figure 91** Northridge-01 Earthquake Record 963 Base Shear in Structure 2

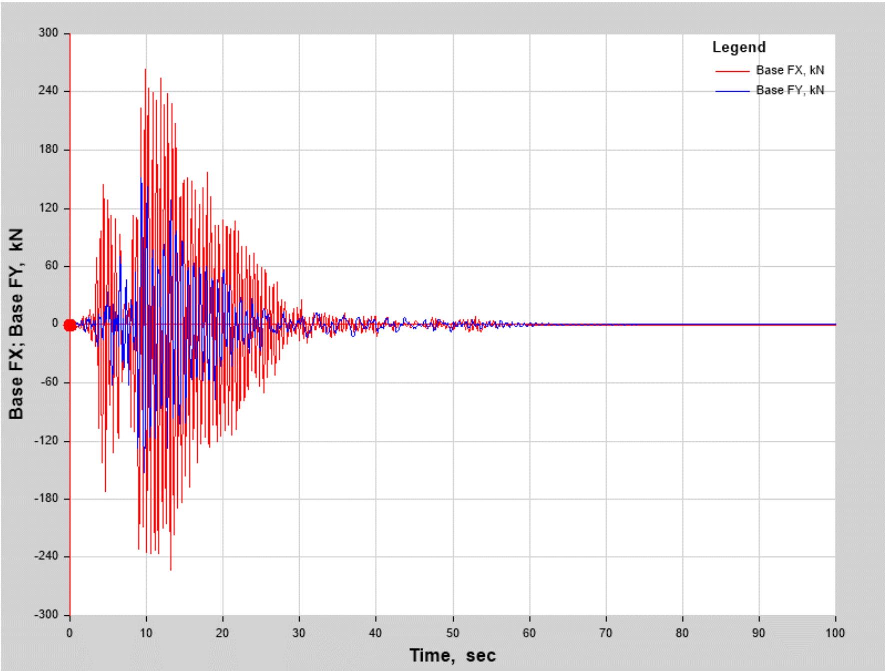


**Figure 92** Northridge-01 Earthquake Record 1006 Base Shear in Structure 2

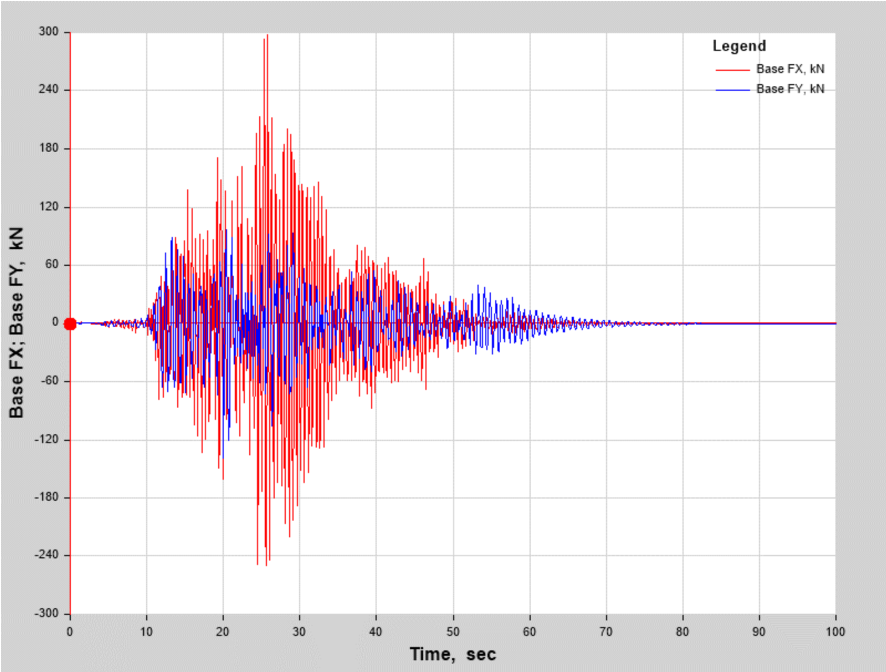


**Figure 93** Gulf of Aqaba Earthquake Record 1144 Base Shear in Structure 2

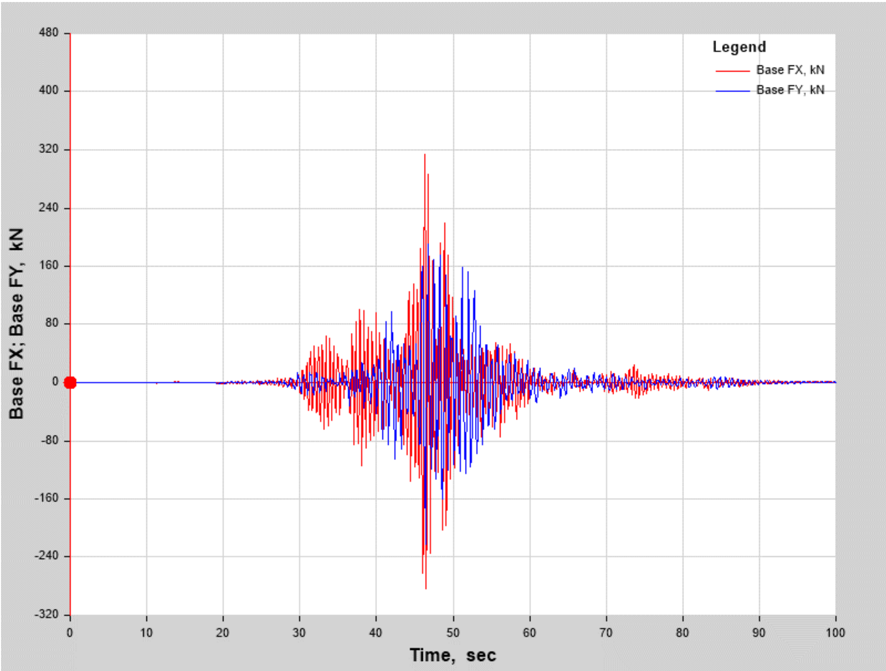


**Figure 94** Chi-Chi Taiwan Earthquake Record 1487 Base Shear in Structure 2

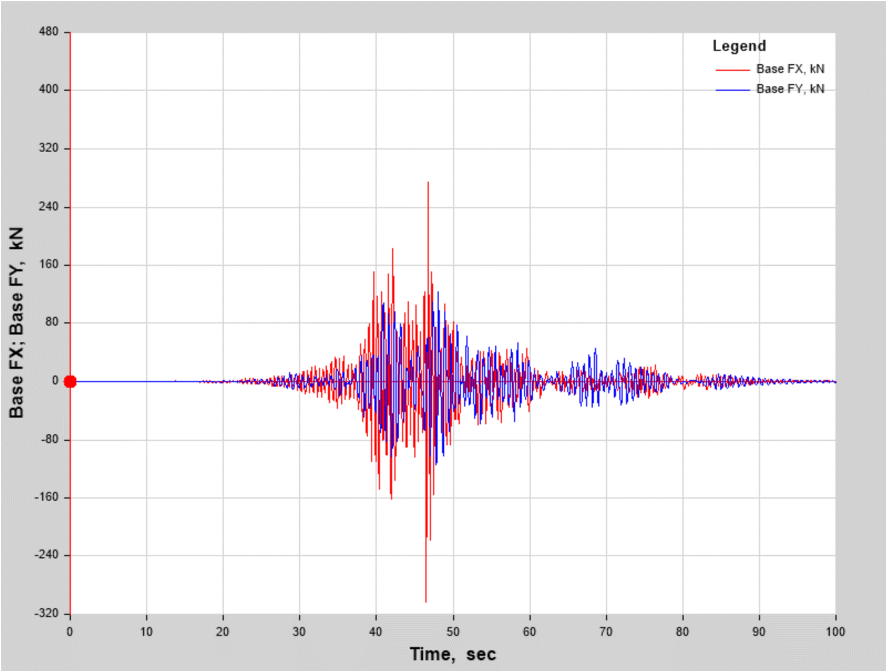


**Figure 95** Chi-Chi Taiwan Earthquake Record 1524 Base Shear in Structure 2

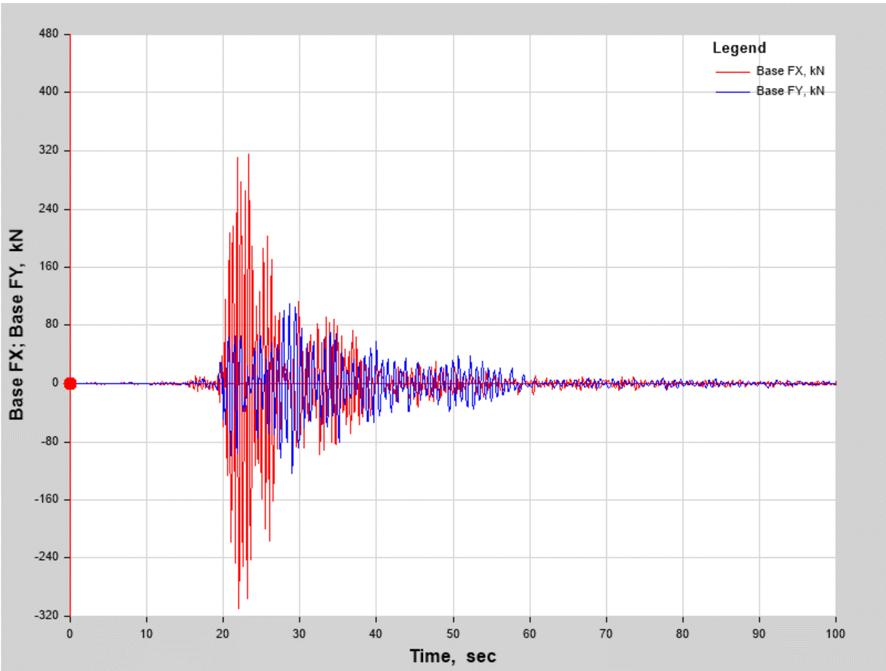


**Figure 96** Niigata Japan Earthquake Record 4226 Base Shear in Structure 2

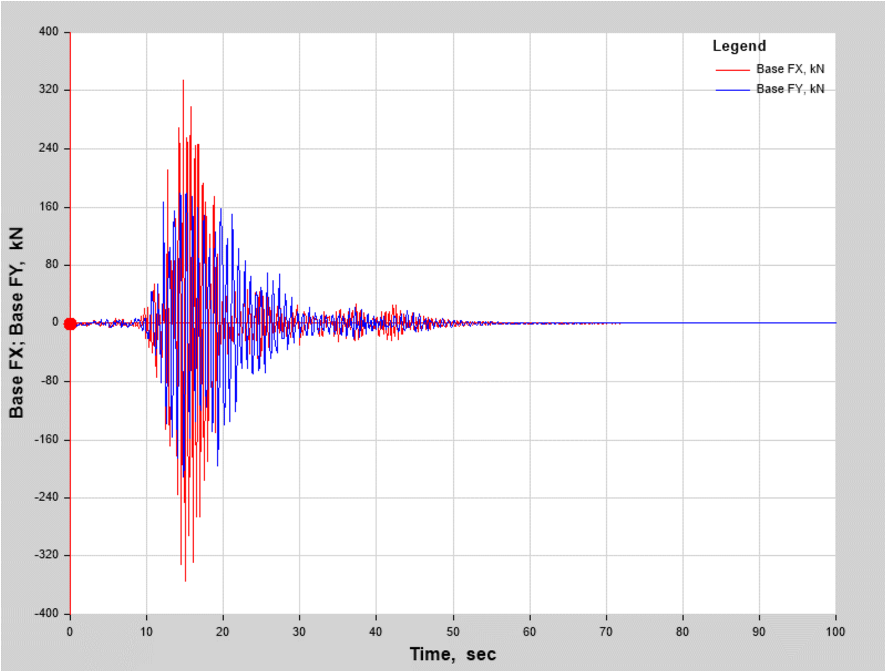


**Figure 97** Montenegro Yugosla Earthquake Record 4455 Base Shear in Structure 2

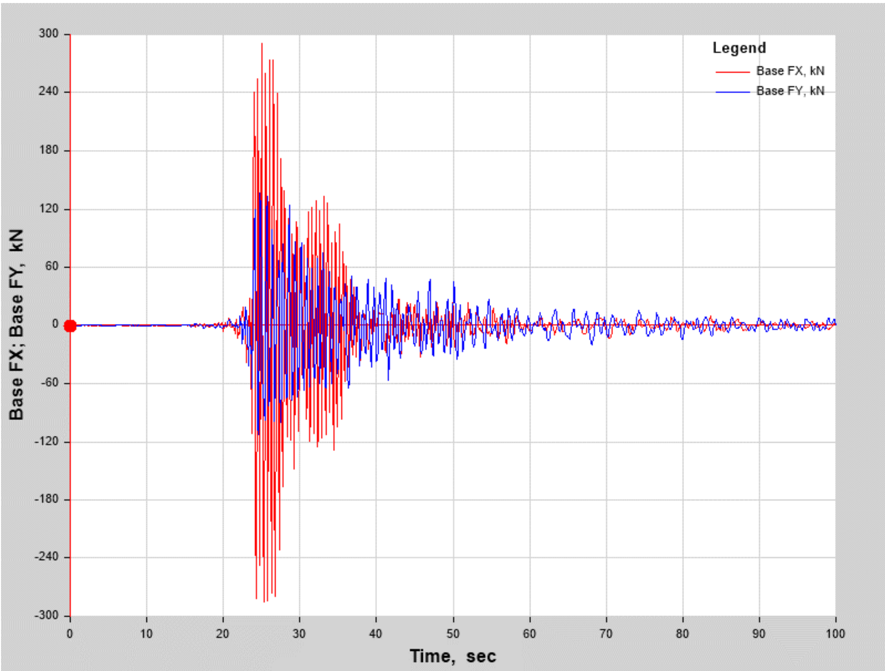


**Figure 98** Chuetsu-Oki Japan Earthquake Record 4889 Base Shear in Structure 2

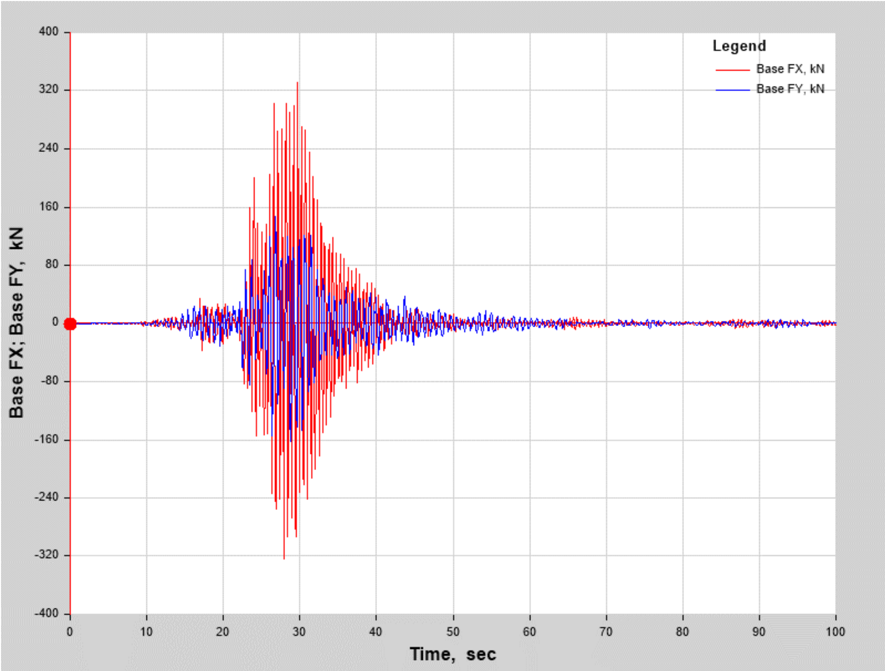


**Figure 99** Darfield New Zealand Earthquake Record 6915 Base Shear in Structure 2

## Appendix F Earthquake Acceleration, Velocity, Displacement, Graphs vs Time

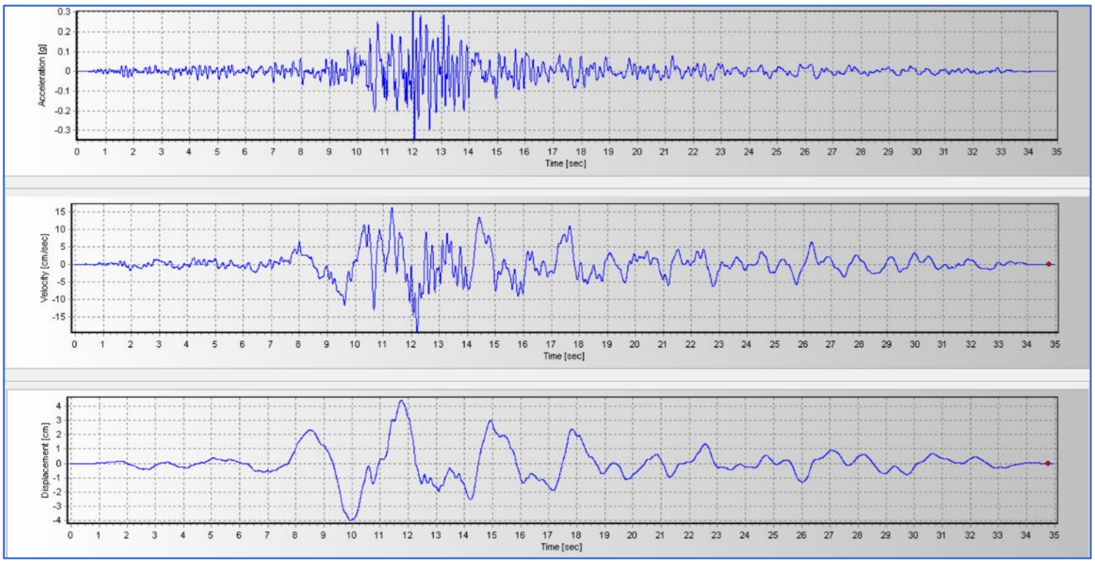


**Figure 100** Irpinia Earthquake Record 288, Acceleration, Velocity, and Displacement, vs Time.

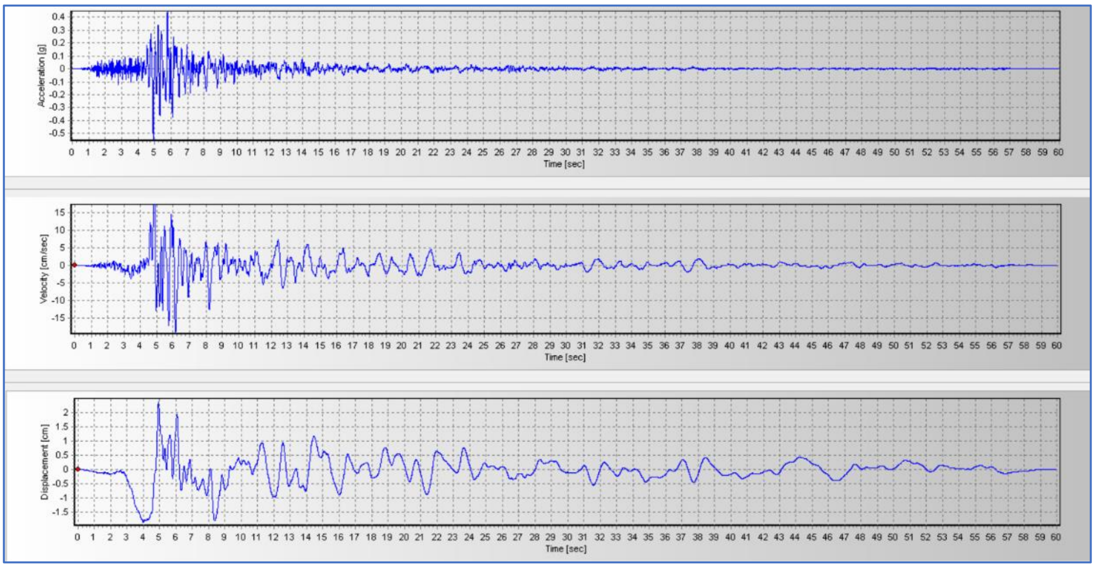


**Figure 101** N. Palm Springs Earthquake Record 534, Acceleration, Velocity, and Displacement, vs Time.

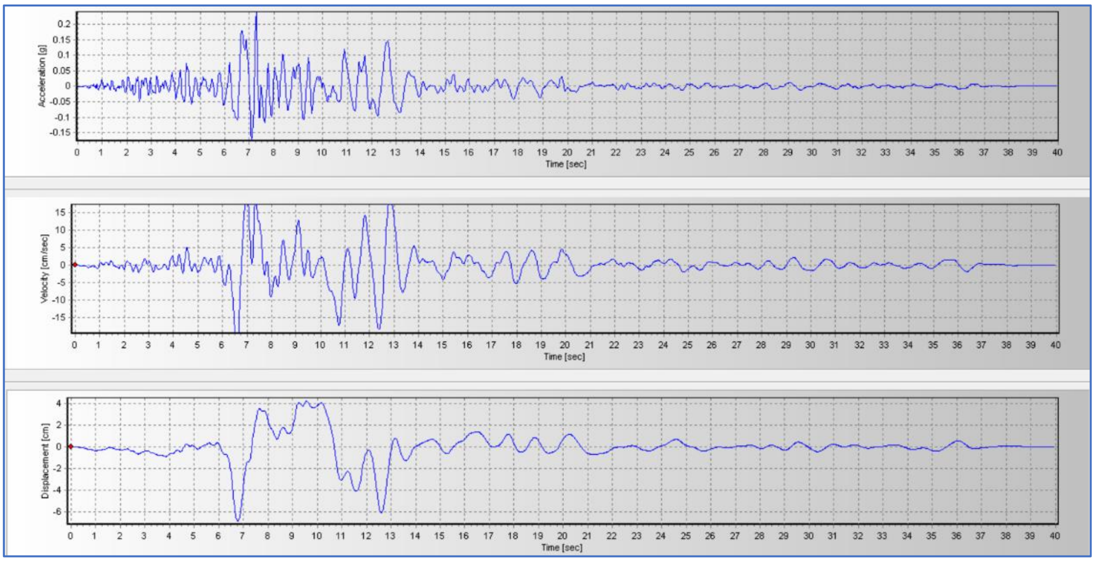


**Figure 102** Northridge-01 Earthquake Record 963, Acceleration, Velocity, and Displacement, vs Time.

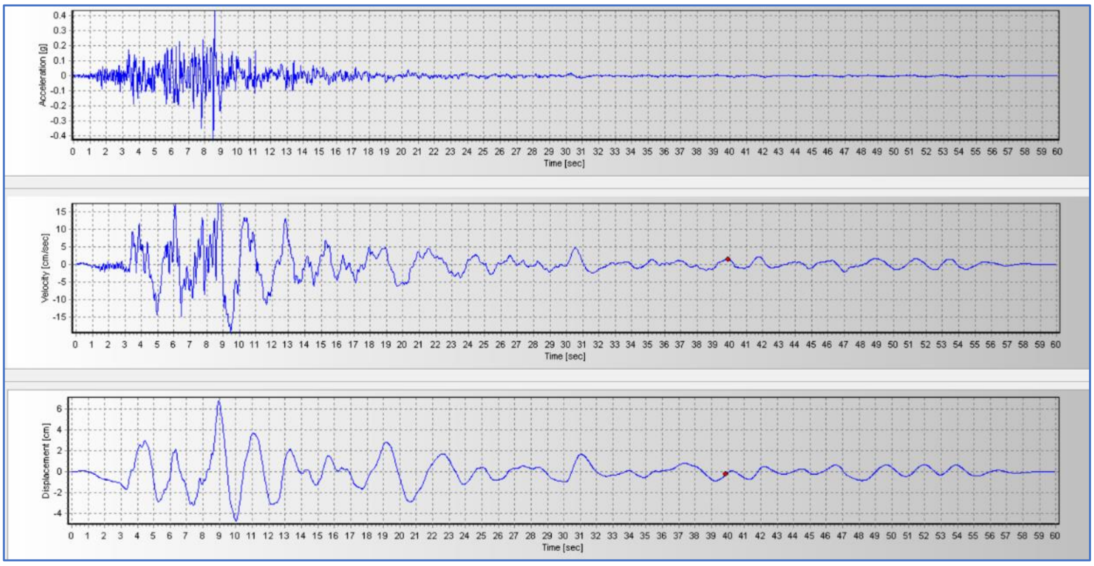


**Figure 103** Northridge-01 Earthquake Record 1006, Acceleration, Velocity, and Displacement, vs Time.

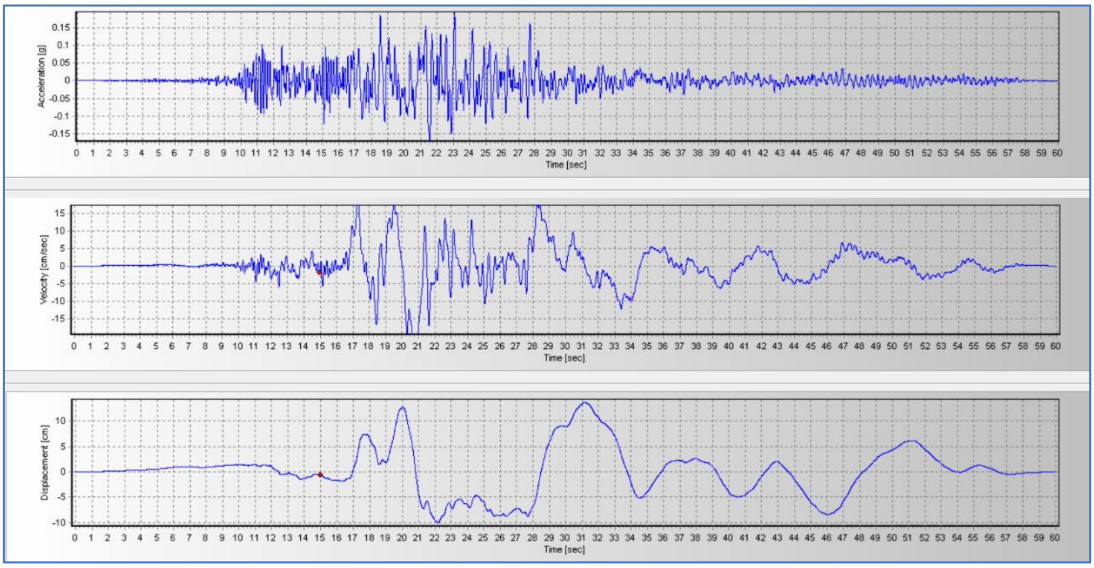


**Figure 104** Gulf of Aqaba Earthquake Record 1144, Acceleration, Velocity, and Displacement, vs Time.

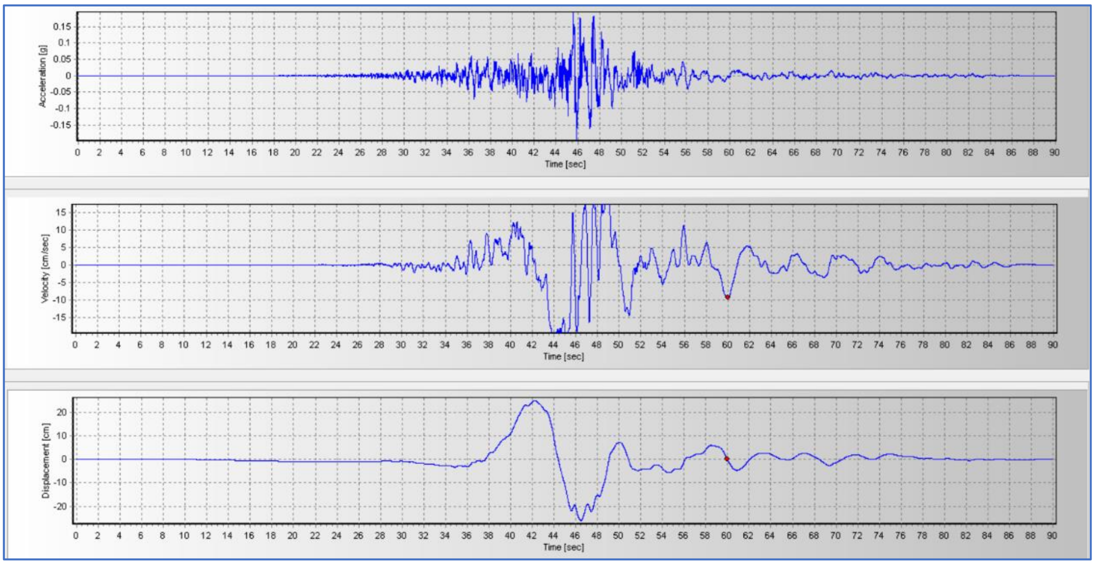


**Figure 105** Chi-Chi Earthquake Record 1487, Acceleration, Velocity, and Displacement, vs Time.

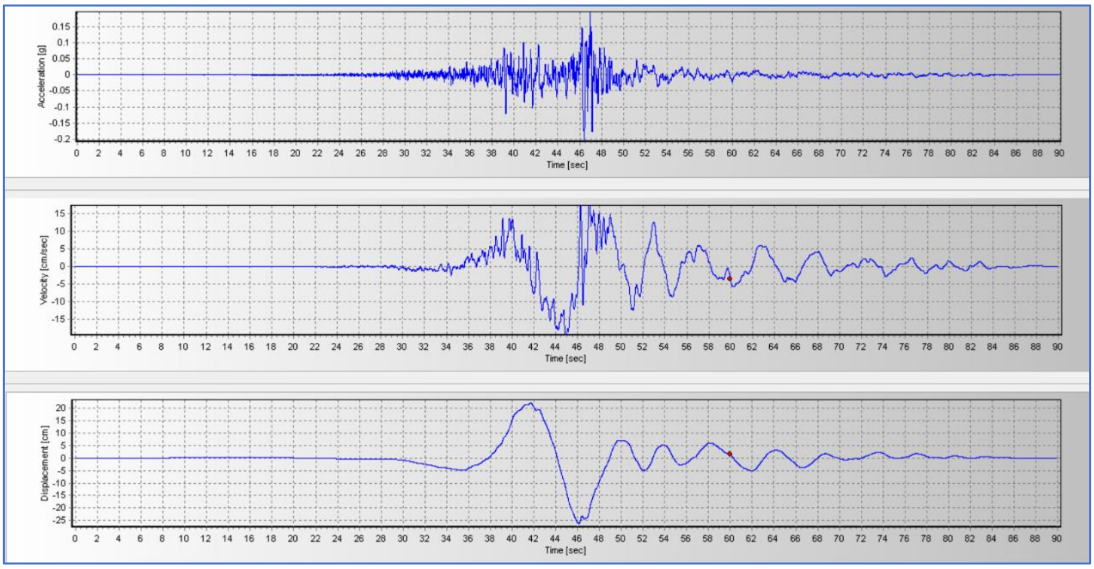


**Figure 106** Chi-Chi Earthquake Record 1524, Acceleration, Velocity, and Displacement, vs Time.

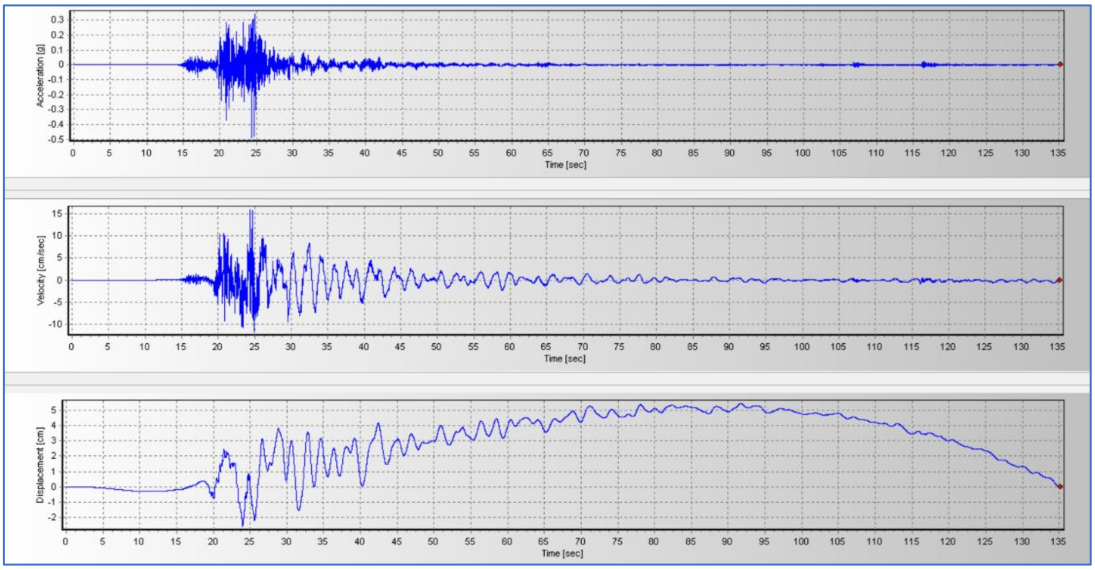


**Figure 107** Niigata Earthquake Record 4226, Acceleration, Velocity, and Displacement, vs Time.

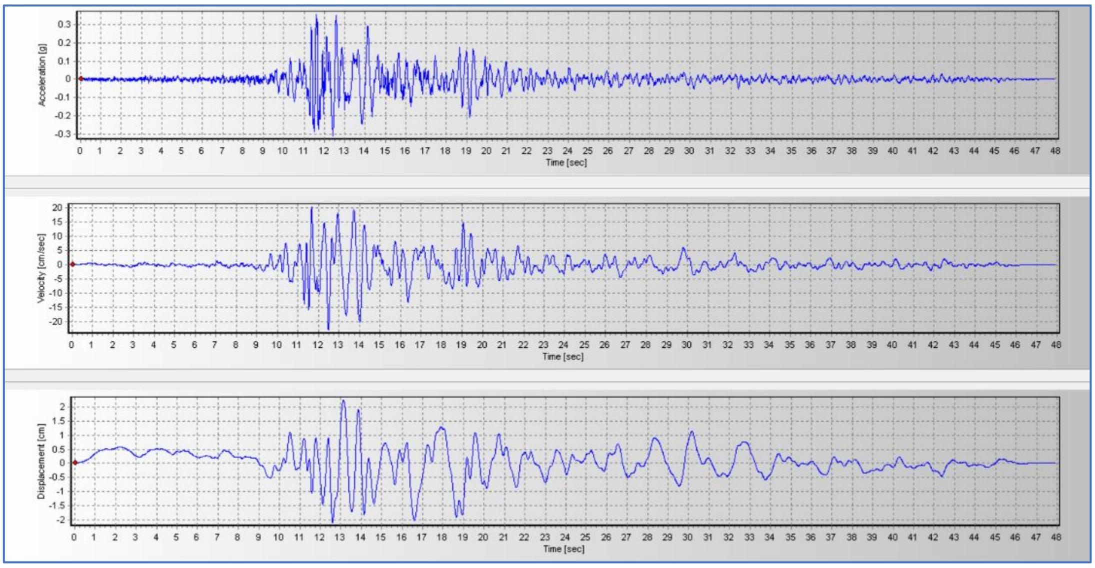


**Figure 108** Montenegro Earthquake Record 4455, Acceleration, Velocity, and Displacement, vs Time.

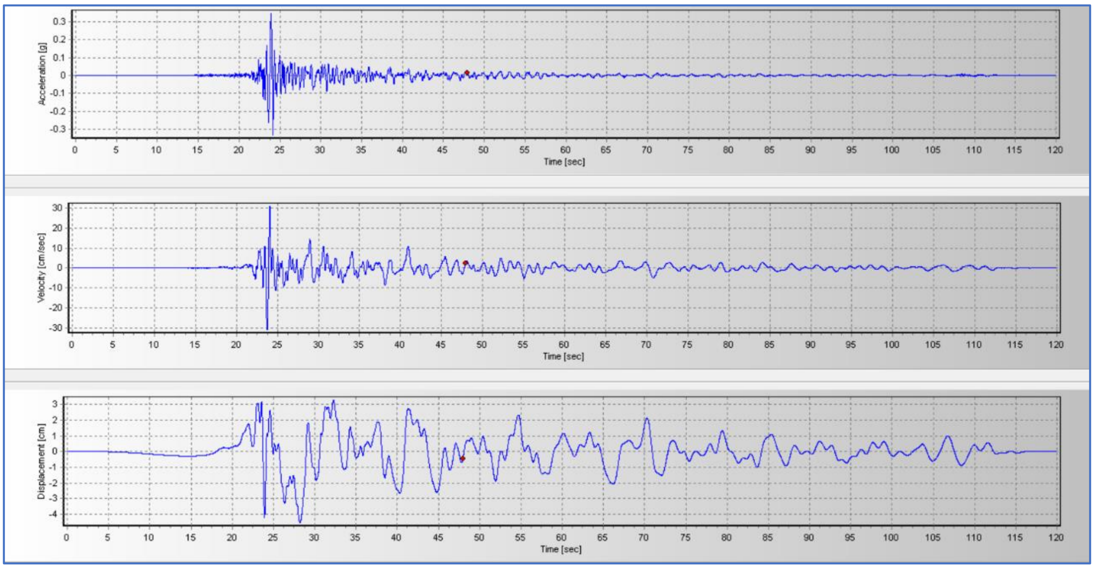


**Figure 109** Chuetsu Earthquake Record 4889, Acceleration, Velocity, and Displacement, vs Time.

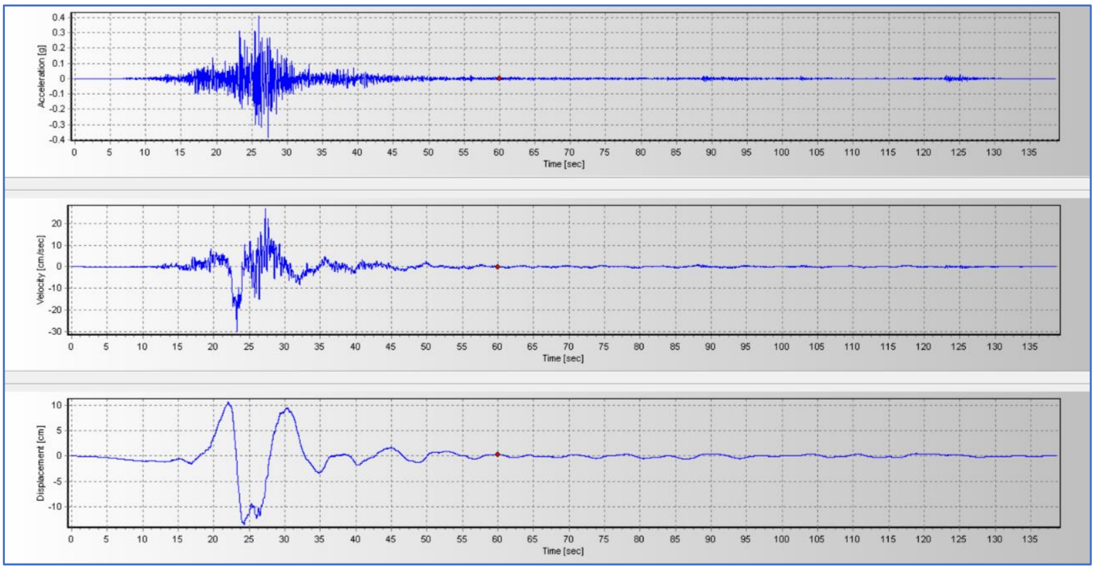


**Figure 110** Darfield Earthquake Record 6915, Acceleration, Velocity, and Displacement, vs Time.

# CURRICULUM VITAE